Final report

Topic

Advanced Electro Polishing Technologies – AdEPT

(Verbesserte Elektropoliertechnologien zur formtreuen Oberflächenbehandlung – AdEPT)

Reporting period

01.09.2017 - 30.11.2019

Research institutes:

CRM Group

Hahn-Schickard-Gesellschaft für angewandte Forschung e.V.

TU Chemnitz, Center for Micro Technologies

Université de Namur, CES laboratory

This CORNET Final report on hand counts at same time also as an AiF-iGF final report

1. Work package 1: Definition of reference cases

Task 1.1: Selection and characterization of samples with reproducible surface conditions

CRM:

Within this task, CRM was in charge of the selection and supply of stainless steel grades as substrate materials for the investigation of electropolishing technologies. The electropolishing processes for stainless steels are rather well established and these materials are therefore excellent reference materials for investigating possible improvements of the polishing technologies. For the AdEPT project, we selected three different grades, a ferritic one and two austenitic ones. AISI 430, the ferritic grade, contains only chromium as alloying element. AISI 304 is a chromium-nickel stainless steel, while AISI 316 contains also molybdenum. The composition of these three grades is summarized in Table 1. It should be noted that these three grades represent more than 90% of the overall stainless steel production. In order to achieve a reproducible surface condition in terms of roughness and surface morphology, the three grades were purchased with a grinded surface finish (320 grit). The resulting surface morphology is similar to that of a machined part i.e. representative for the starting condition of the 3D parts to be treated in the frame of AdEPT.

Composition (%)	Type	Cr	Ni	Mo	C	Mn	Si	P	S
EN 1.4016 / AISI 430	F	16-18	-	-	<0.12	<1	<1	<0.04	<0.03
EN 1.4301 / AISI 304	A	18-20	8-12	-	<0.08	<2	<0.75	<0.045	<0.03
EN1.4401 / AISI 316	A	16-18	10-14	2-3	<0.08	<2	<0.75	<0.045	<0.03

Table 1: Composition of the stainless steel substrates selected as substrate for *A*dEPT

The purchased base materials were fully characterized in order to have accurate definition of the reference state. Figure 1 compares the surface morphology of the three grinded surfaces. It can be observed that the morphology of the three grades are almost identical, consisting of parallel trenches and characteristic burrs. Hence, as expected, the grinding step therefore efficiently 'resets' the surface.

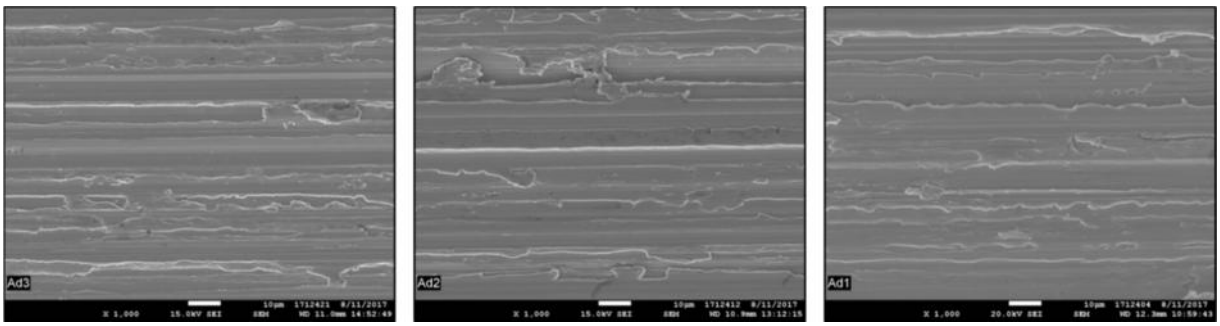

Figure 1: Comparison of the surface morphologies of, respectively, AISI430, AISI304 and AISI316, with 320 grit surface finish

Interferometry measurements were performed in order to describe more quantitatively the surface morphology of the samples. Roughness parameters for the three steel grades are

shown in Table 2. A roughness profile is included as well on Figure 2. It is observed that the roughness is quite low for all three grades but significant differences are observed between AISI 430 and AISI 316.

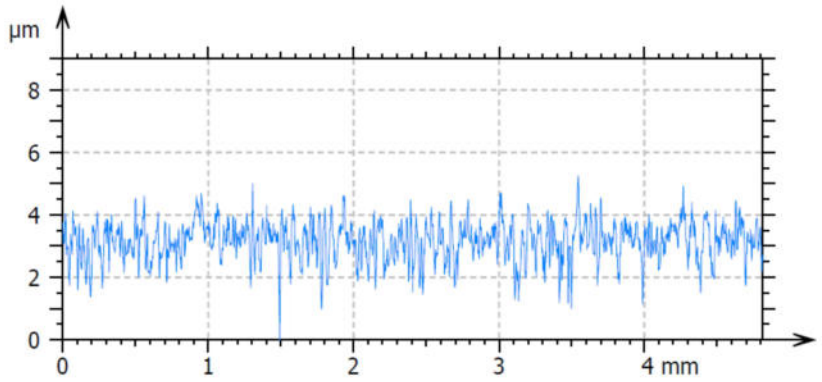

Figure 2: Surface profile of AISI 304 steel as measured by interferometry

Composition (%)	Ra	Rz	Rp	Rv	Rc	Rt	Rq	Rsk	Rku
EN 1.4016 / AISI 430	0.463	3.47	1.56	1.91	1.44	4.82	0.594	-0.313	3.39
EN 1.4301 / AISI 304	0.583	4.59	2.1	2.48	1.78	6.08	0.756	-0.169	3.94
EN1.4401 / AISI 316	0.776	5.46	2.61	2.85	2.5	6.94	0.984	-0.189	3.29

Table 2: Roughness parameters of the three stainless steel grades as measured by interferometry

The surface chemistry was also investigated by XPS. On all three grades, the native oxide film is very thin (< 2 nm) and consists essentially of ion and chromium oxides, with a Fe:Cr ratio identical to that of the bulk. No nickel is observed in the native oxide on both 304 and 316 stainless steels. The XPS depth profile measured on 316 steel is shown in Figure 3.

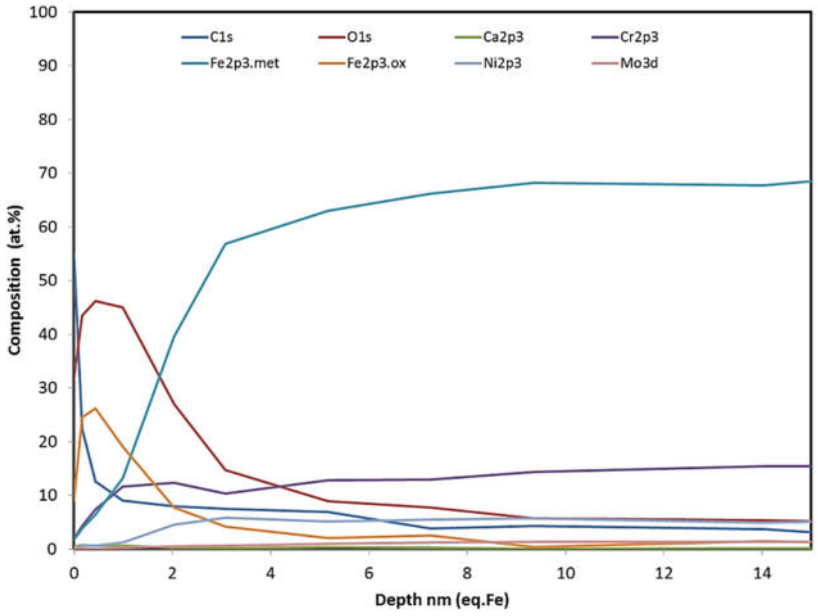

Figure 3: XPS depth profile of AISI316 steel

H-S:

For the EP trials, two steel grades were chosen. 1.2343 ESU and 1.2379. The composition of the two steel grades is shown in Table 3: Composition of the steel grades 1.2343 ESU and 1.2343. The most significant difference between the materials is the chromium content, which is significantly higher for 1.2379. Those two materials where chosen, since they are commonly used in the tool making industry and therefore of high interested for the companies in the user committee.

Table 3: Composition of the steel grades 1.2343 ESU and 1.2343

	C	Si	Mn	Cr	Mo	V
1.2343 ESU	0,38	1,1	0,4	5,0	1,3	0,4
1.2379	1,55	0,4	0,3	11,8	0,75	0,82

In consultation with the user committee, EP trials are also performed on hardened 1.2343 ESU and M333 steel by Böhler. To use hardened 1.2343 ESU steel was recommended by the user committee to see if the EP results are different, comparing hardened and non-hardened material. Furthermore, the hardened material is frequently used by the companies and therefore of high interest. Böhler M333 steel is known for very good surface qualities which can be achieved with this material. It is therefore used for direct ultra-precision machining with diamond tools to obtain optical surface qualities.

For the EP trials, the samples had a grinded surface finish. To compare evaluate the improvement in surface quality by electropolishing, the surface roughness was measured prior and after the EP process using white light interferometry.

ZFM:

The ZFM will focus on the electro polishing of electrodeposited aluminum films on silicon substrates. The reference samples were deposited on a 6 inch highly doped Si wafer with a layer thickness of approximately 25 µm. After deposition, the samples were characterized in wafer and chip size. During dicing of the first batch in smaller pieces (chip size approx. 3x4 cm²), the Al layer was peeled off. Thus, these samples could not be used for EP process because of low adhesion to the Si. In Figure 4, an as deposited wafer, the analyzation steps and the diced samples without adhesion are shown.

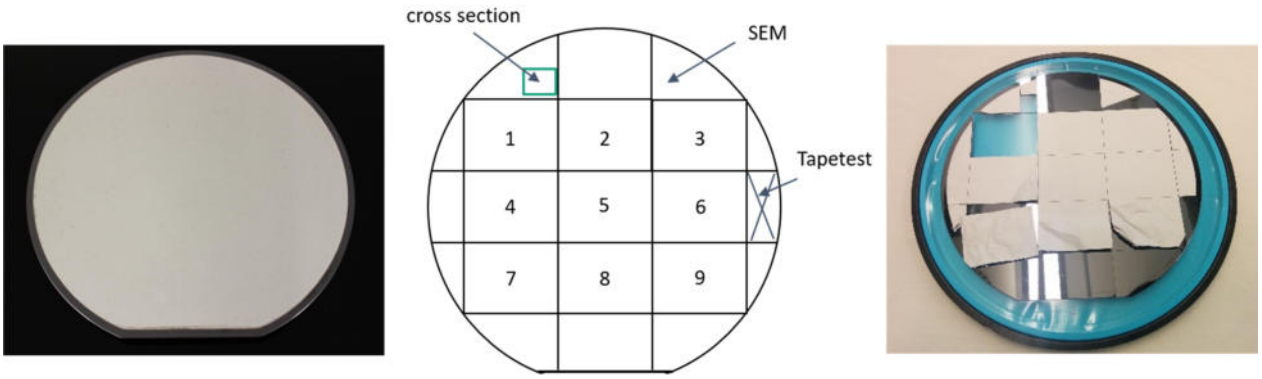

Figure 4: Left - as deposited Al film on highly doped SI wafer, middle- dicing grid and position of characterization, right - diced samples without adhesion to the substrate

Because of the low adhesion of the Al layer to the Si substrate, a heating step as post-treatment was introduced. The heating was carried out at 400 °C for 1 h in a nitrogen (N_2) atmosphere.

In Figure 5, SEM images of cross sections of three samples with Al deposition are shown. The cross sections were polished by using focused ion beam (FIB). The upper pictures with "without heating" show two different samples without post-treatment. There is no mechanical contact visible and the layer sticks on the substrate with very low adhesion. The two pictures below show one sample, left in overview and right the detailed interface. The introduced diffusion of Al into the Si is called silicidation. It is been used often in microelectronics to improve the contact resistance and adhesion between layer and substrate. The adhesion was significantly improved so that the samples can be used for the EP trials.

Furthermore, the Figure 5 shows the grain structure of the Al layer. The sample "with heating" was polished with lower FIB current. Thus, the grain structure is more detailed. It can be seen that the layer starts growing with smaller grains. The grains become bigger by increasing the layer thickness. Thus, the surface roughness increases with layer thickness due to additive free deposition. For bonding applications, this roughness has to be improved by EP. As long as the deposition parameters are the same, the surface conditions are comparable. Nevertheless, all coated chips were characterized before and after the EP experiments. The characterization was carried out via confocal microscopy.

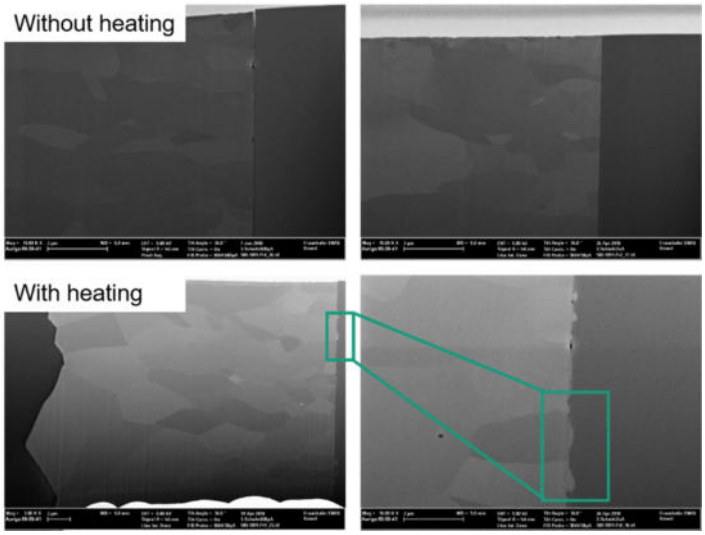

Figure 5: SEM images of cross sections of Al layers with and without post-treatment heating. The cross sections are polished by focused ion beam

Task 1.2: Preparation of samples with specific features + characterization

ZFM:

The goal of the EP technology is to integrate this process in micro system technology. Nowadays, the chemical mechanical polishing (CMP) is a well-established process to remove surface roughness and to flatten the layer structure. The EP was tested as alternative post-treatment method for electrodeposited layers.

In our case, Al bonding frames were used. Due to an additive-free deposition process, the roughness is too high to use the layer as deposited. The bonding frame width will be 60 µm or 80 µm. The Al deposition was carried out on wafer level using pattern plating process. As a seed layer sputtered Al was used. After deposition, the EP process took place. As a protection of the seed layer, we have to use the resist from the plating, but then the characterization before and after EP was not possible on the same sample. Therefore, we decided to use just similar deposited wafer with a bit thinner Al layers. The characterization was done using confocal microscope for roughness and layer thickness. The microstructure was characterized using SEM. The Al microstructure in a 60 µm bonding frame is shown in Figure 6.

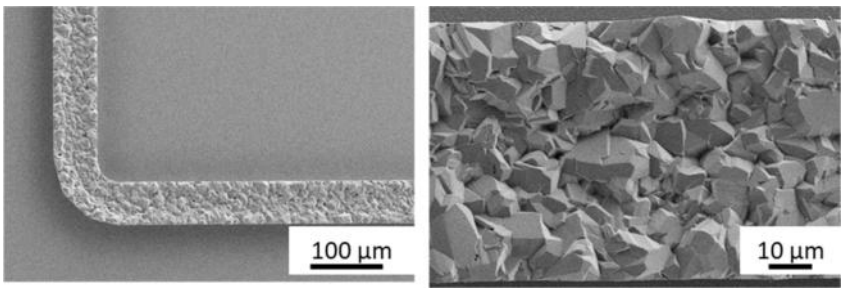

Figure 6: SEM pictures of the non-polished Al layer with a layer thickness of approximately 21 µm

H-S:

Beside flat samples for the initial EP trials, structured samples were designed and prepared, to evaluate the performance and limitations of the EP process. The design of the 3D test sample is shown in Figure 7. The sample consists of five different micro structures which can be used to evaluate the EP performance.

- Micro-channels with a channel width from 200 µm to 800 µm to evaluate if the EP process also works in very small channels;
- Steps with varying step height from 2 µm to 10 µm to evaluate which step height can be removed by the EP process;
- Drillings with varying diameters from 300 µm to 900 µm and varying depth from 100 µm to 500 µm;
- Slopes and a flat area to evaluate the influences of the EP process on the slopes as well as on a milled surface;
- Constriction to investigate the removal on existing burrs as well as milling marks which result when the milling tools need to be changed due to the small features.

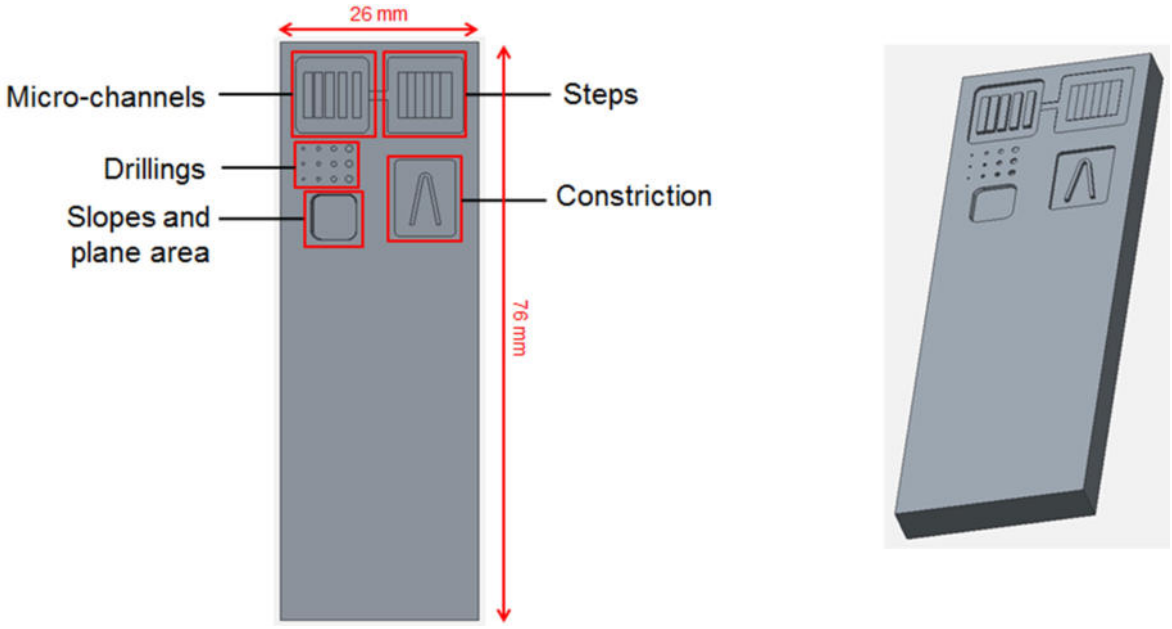

Figure 7: Design of the 3D test sample

The 3D test samples are prepared using regular CNC milling. For the characterization the samples are measured prior to the EP process using white light interferometry and laser autofocus probing. In Figure 8 a milled test sample is shown.

Figure 8: Milled 3D test sample before EP process

Task 1.3: Implementation of Electropolishing cells and procedures

CRM:

Within the AdEPT project, CRM was in charge of designing, constructing and supplying to all consortium members an electropolishing cell that would be used throughout the project by all participants. This is illustrated on Figure 9. It was chosen to machine the cell entirely from a block of PTFE to ensure the widest possible chemical compatibility.

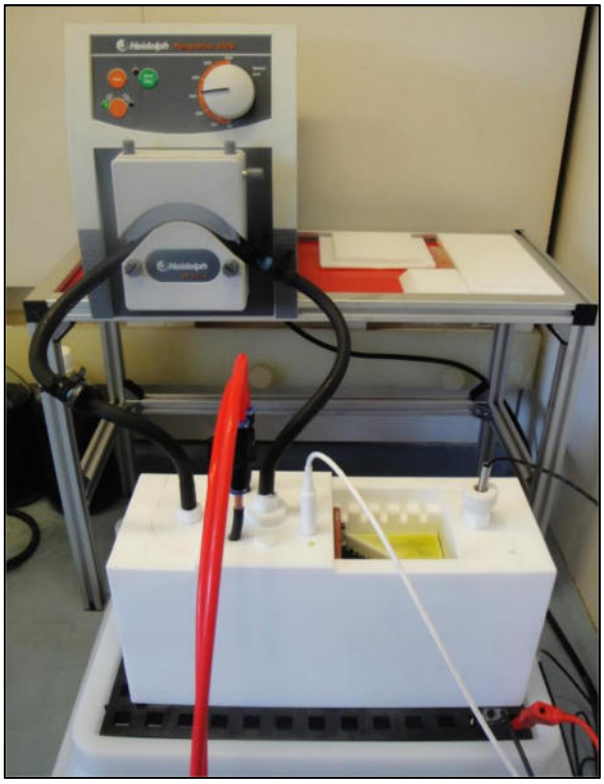

Figure 9: Picture of the electropolishing cell supplied to all the members of the consortium

The cell features the possibility to work either in a parallel electrodes configuration or in a Hull cell configuration. Hull cell is a classical cell design used in electroplating. In contrast, it is rarely used for electropolishing studies. However, it has proven very useful for the fast screening of bath compositions as well as defectology studies. The principle behind Hull cell is illustrated on Figure 10. Due to the inhomogeneous distance between the electrodes, a current density gradient is observed along the width of the sample. In addition, the hydrodynamics are different from the bottom to top of the sample. This allows probing a wide range of electropolishing conditions performing only a few trials. It is also possible to correlate different types of defects that are observed in electroplating to some specific conditions in terms of current density and hydrodynamics.

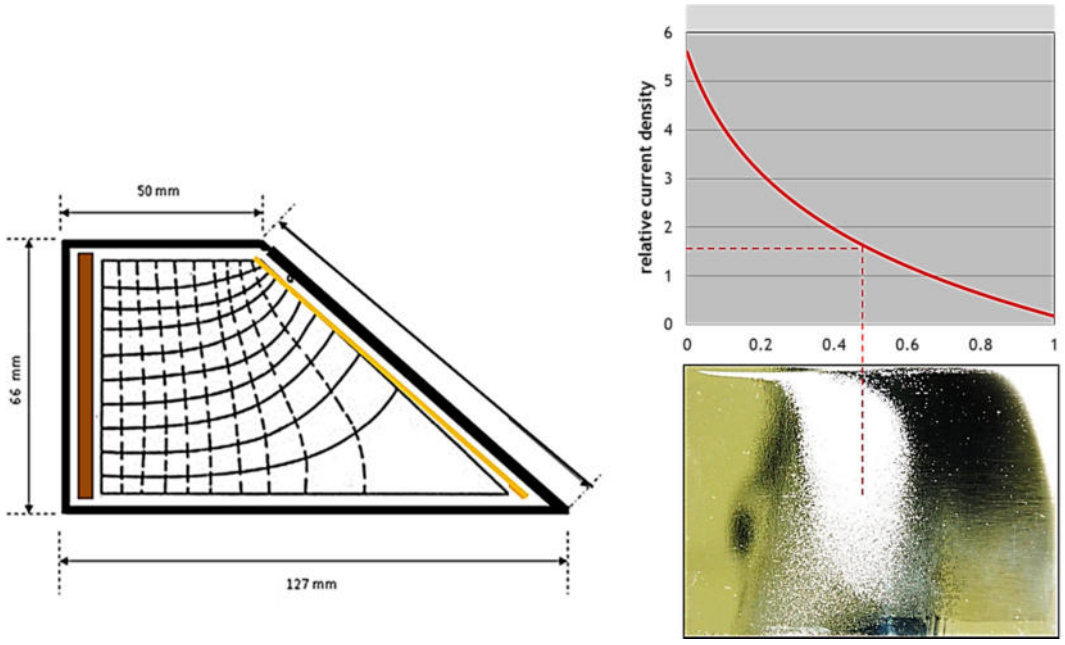

Figure 10: Illustration of the Hull Cell and its application to the electropolishing trials

H-S:

The EP cell is setup in a laminar flow chamber within the laboratories of Hahn-Schickard. For the EP trials a DC rectifier (TN65-650, Heinzinger GmbH, Germany), a cryo-thermostat (AD15R-40, VWR International GmbH, Germany) and a peristaltic pump (Pumpdrive 5206, Heidolph Instruments GmbH & CO. KG, Germany) are used. A picture of the setup is shown in Figure 11.

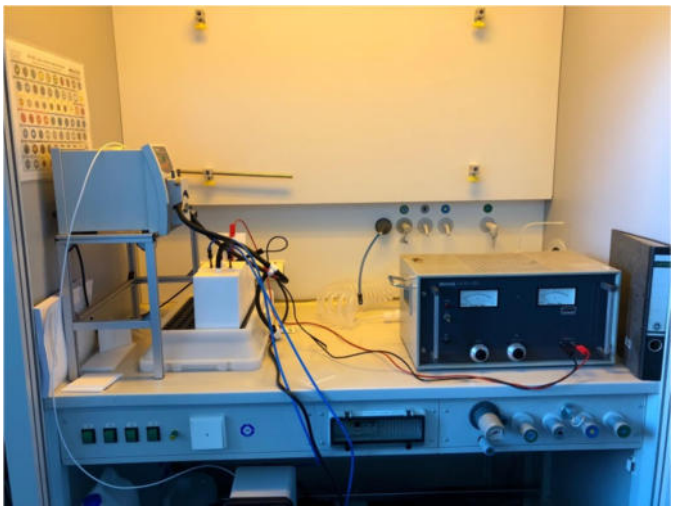

Figure 11: Setup of the EP cell at HS

ZFM:

The EP cell is set up in a fume hood within the laboratories of Fraunhofer ENAS but used from the ZFM. The cell is connected to a peristaltic pump (MCP Standard, Cole Parmer). The temperature of the electrolyte is controlled by a cryo-thermostat (AD15R-40, VWR International GmbH, Germany). The setup is shown in Figure 12a. Because this set up was not working well for the EP of electroplated Al layers, an easier beaker set up was used, shown in Figure 12b. During the experiments, it was found that small gas bubbles instead of

magnetic stirring were sufficient for good EP results. The nitrogen bubbling was realized using different methods but a porous stone from aquarium supplies has shown the best results in the end.

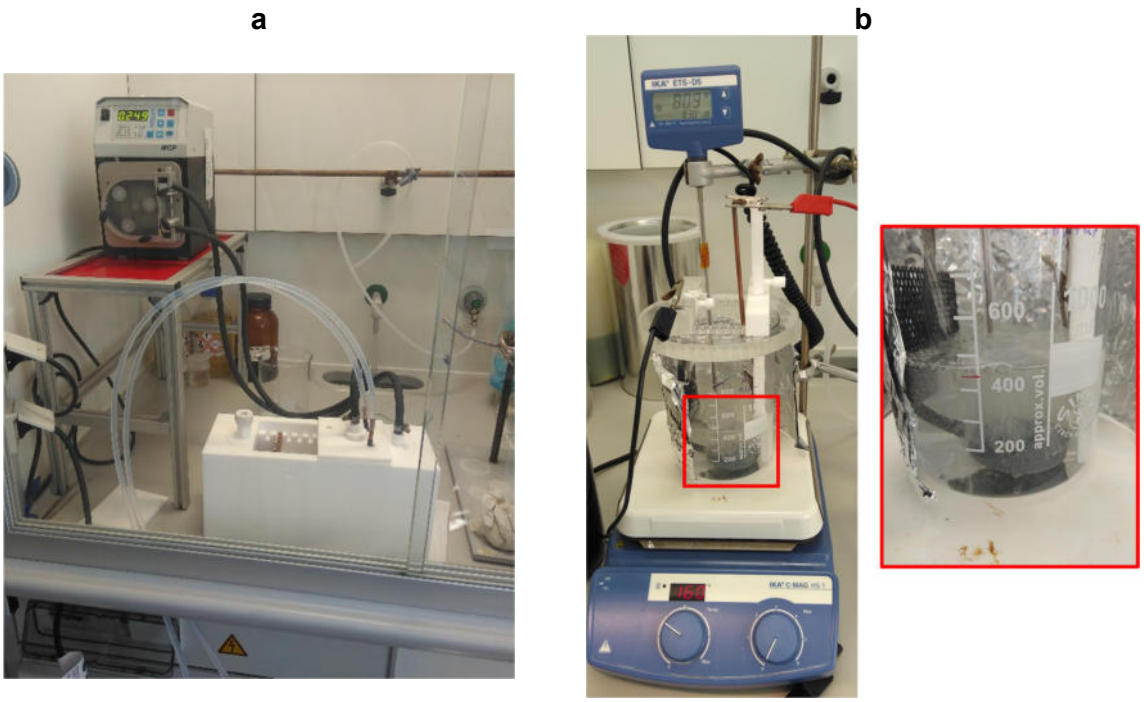

Figure 12: Experimental set up for the electropolishing experiments

Task 1.4: EP trials on selected samples under reference conditions and characterization of the processed samples

CRM:

In order to validate the cell constructed at CRM and establish polishing and characterization procedures, the electropolishing of three different steel grades was investigated using different bath temperatures, stirring rates and current densities. Stainless steel was selected as a reference material since it is relatively easy to electropolish and most of electropolishing activities industrially are on stainless steel parts. Figure 13 shows the evolution of the surface average roughness (Ra) of stainless steel plates during electropolishing in a classical sulfuric-phosphoric bath, as a function of the amount of material dissolved. This representation allows comparing quite easily the efficiency of trials performed at different current densities. Two conclusions can be drawn from these experiments. On one hand, it is observed that, at 40 and 55 °C, too low current densities are inappropriate for electropolishing and result in an increase of the surface roughness. Secondly, provided that the current density is in the appropriate range, the minimum roughness that can be achieved is almost independent of the bath temperature and current value. Plotting the same data as a function of polishing time shows that, as expected, increasing the current density leads to a reduction of the time needed to achieve the same roughness improvement.

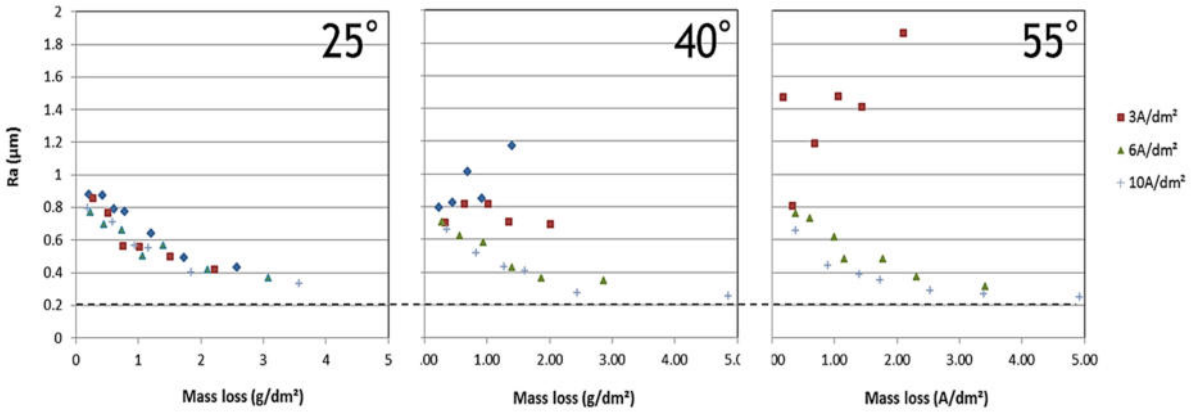

Figure 13: Influence of the bath temperature and the current density of the evolution of the roughness for electropolishing trials carried out on AISI316 stainless steel

While 'Ra' is the most usual parameter to describe the roughness, it is too restrictive to give a representative image of the real surface condition. In order to describe the surface of the samples in a more comprehensive manner, a methodology based on Fourier transform PSDF (power spectral density functions) was developed.

Figure 14 illustrates how PSDF can help interpret the results from electropolishing trials. As shown on Figure 14, from the Ra evolution, the samples electropolished at low current density are characterized by an increase of Ra, while those electropolished at high current density exhibit an Ra decrease. By looking at the corresponding PSDF, one can see that the roughness components of large wave numbers (*i.e.* short wavelengths) are efficiently removed by the electropolishing process, even at low current density. In contrast, the peak on the far left, corresponding to large wavelengths is increasing due to the appearance of orange-peel defects, which is the reason for the Ra increase. As for the high current density trials, all wavelengths are progressively eliminated, thus leading to an Ra decrease. PSD-based descriptions of the surface morphology provide a better description of the surface condition.

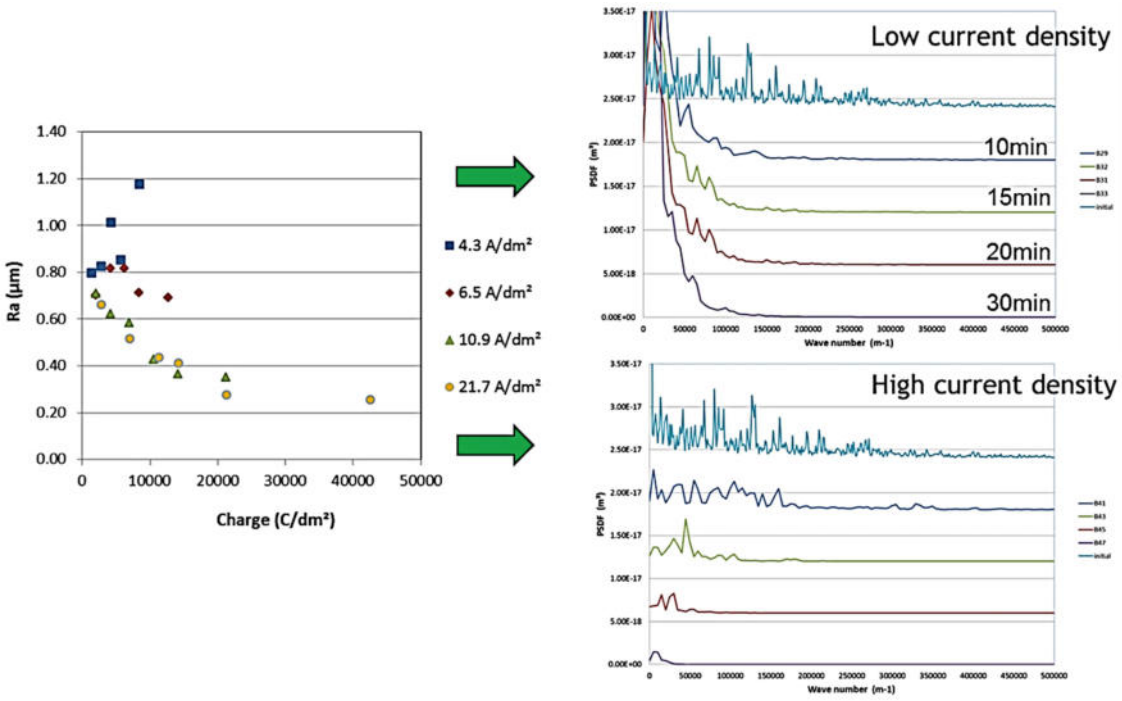

Figure 14: Illustration of the analysis of surface morphology data using power spectral density functions

A glossmeter was purchased by CRM with a view to expand the number of routine characterizations. The device is used to quantify the light reflection on a surface and the technology allows the apparatus to calculate four parameters: the gloss, haze, distinctness of image and reflected image quality:

- The gloss Is a measure of specular reflection, *e.g.* how well the surface reflects light in a mirror-like direction;
- The haze is caused by a microscopic surface finish that diffuses light adjacent to the main reflected light component;
- The distinctness of image (DOI) is the quantification of the deviation of the direction of light propagation from the regular direction by scattering during reflection;
- The reflected image quality (RIQ) has more proportionate response to orange peel on a wider range of surface finishes.

Gloss measurements were performed on AISI 316 samples electropolished in the classic acid bath at 2 currents densities during different times, the plot of the four parameters *vs.* the charge are presented in Figure 15. In addition to these plots, glosses of samples electropolished in the same bath with pulsed currents are also displayed.

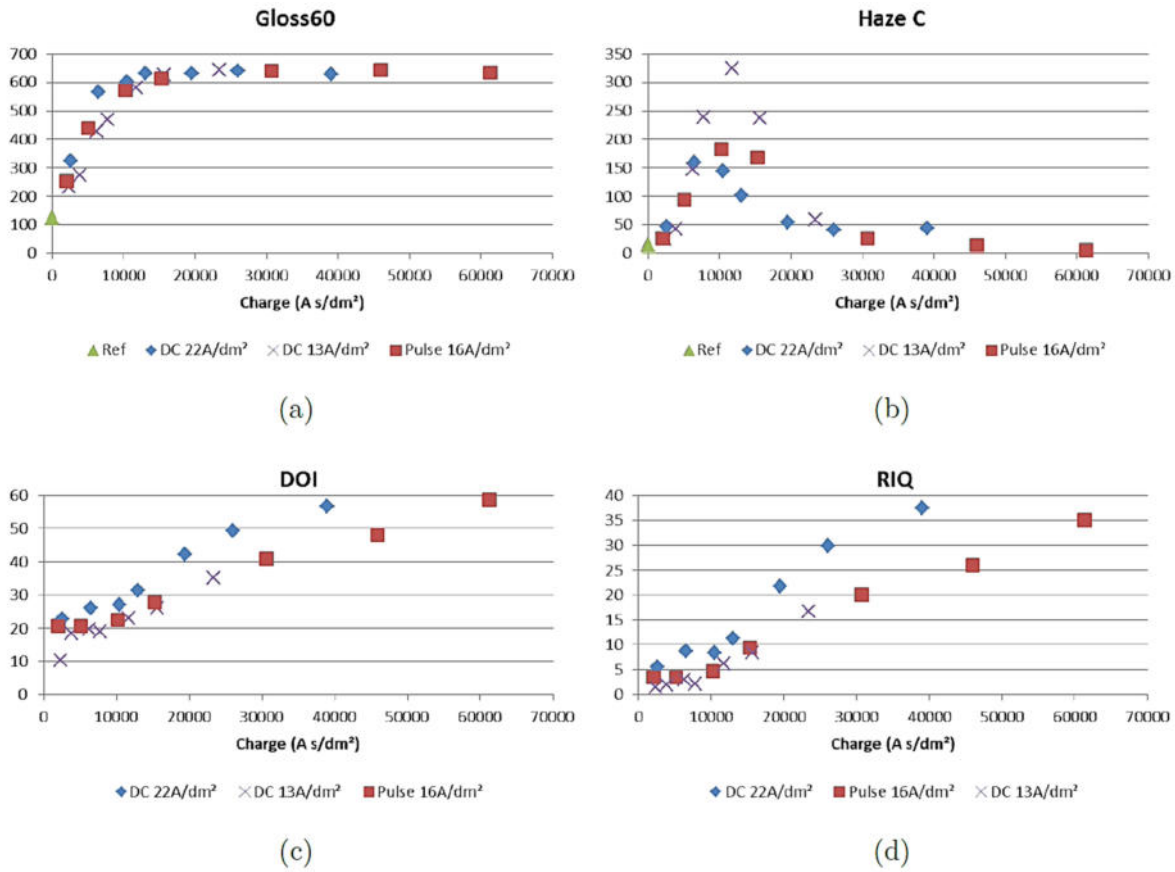

Figure 15: Gloss at 60° (a), haze c (b), distinctness of image (c) and reflected image quality (d) versus charge of electropolished 316 stainless steel in acidic medium

Different observations can be made. First, the gloss values increase rapidly in the same manner for the 3 series regardless of the current density, before reaching a plateau and stagnating around the same value.

The haze plot is more complicated to interpret. For short electropolishing times, the process levels the highest peaks of the sample (which causes the roughness to decrease rapidly) and affects the smaller parts to a lesser extent, this leads to an increase of light scattering (due to the difference in diffused light phases - see Figure 16b). Up to a certain roughness value, the sample tends to flatten and the reflected light becomes more in phase (Figure 16a), thus leading to a sudden drop in haze values. As in for the gloss, the plot of the haze *vs.* charge tends to a minimum plateau (near zero) as the surface becomes mirror-like.

The DOI and RIQ show similar trends, namely a small increase after short electropolishing times followed by a larger increase after longer times, this correlates with the decrease of roughness. It is also worthy to notice that the series of higher current density gives higher DOI and RIQ for the same amount of charge.

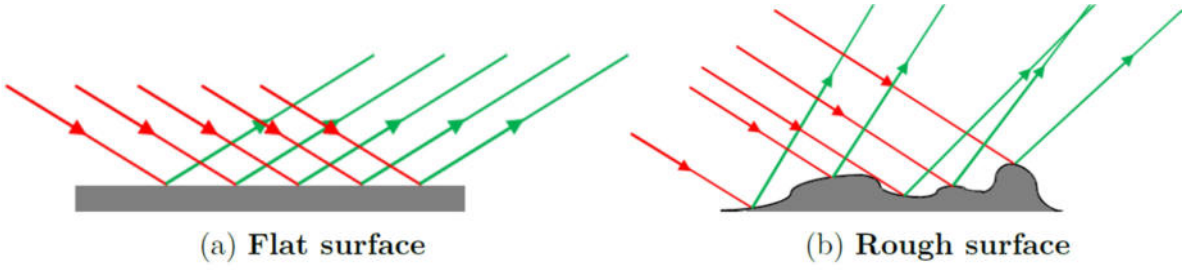

Figure 16: Schematic representation of the incident light reflection on a flat (a) and rough (b) surface

Figure 17 shows an example of a Hull cell experiment carried out on AISI 316 steel. The polished sample shows different areas with very distinct morphologies (shiny, matte, orange-peel) and degrees of polishing. The SEM micrographs show the corresponding defects at the micro-scale. As compared to the surface before polishing, the surface morphology was deeply modified and most of the machining burrs have been removed. On the other hand, on some areas, new defects have appeared.

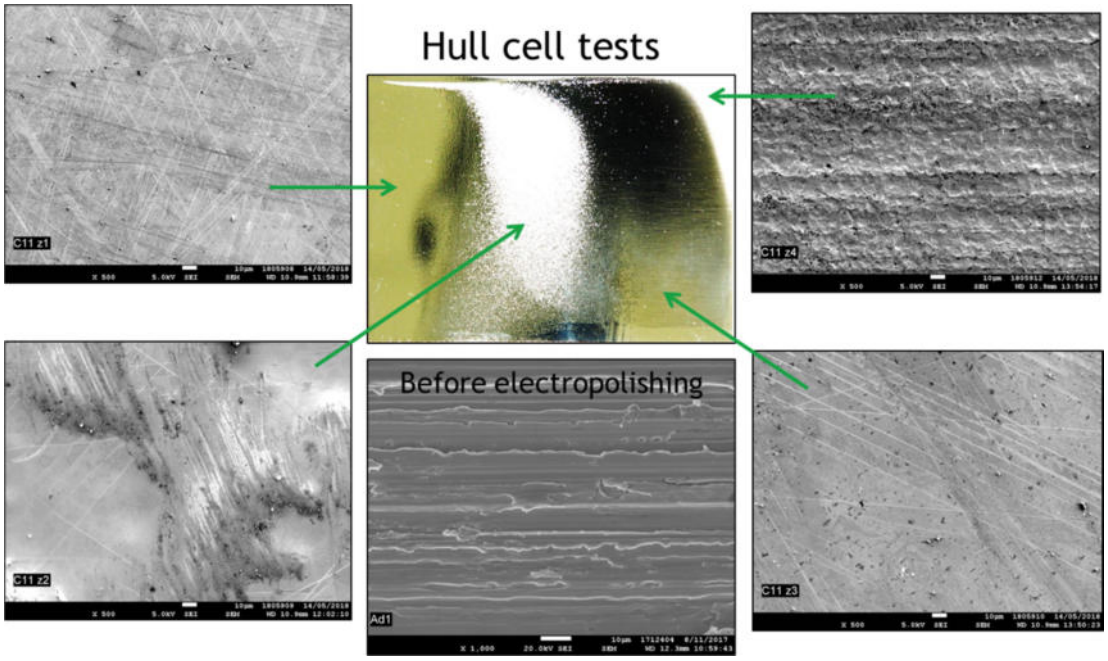

Figure 17: Illustration of Hull cell electropolishing trial and the surface morphologies corresponding to each region

Polishing of tool steel samples

Polishing trials have been performed on 1.2343 and 1.2379 steels, two grades that are typically used for the manufacturing of injection molds. Although such grades are very seldom eletropolished, a polishing electrolyte from Poligrat which is compatible with this chemistry was identified. The electrolyte is based on methanesulfonic acid in organic medium. It is highly viscous and resistive as compared to the classical phosphoric-sulfuric bath used for stainless steel. Therefore, the polishing voltage is much higher and longer polishing times are needed to remove the same amount of material. Figure 18 presents the evolution of Ra roughness as a function of mass loss at different current densities and temperatures. The evolution of the surface morphology during electropolishing is illustrated as well on Figure 19.

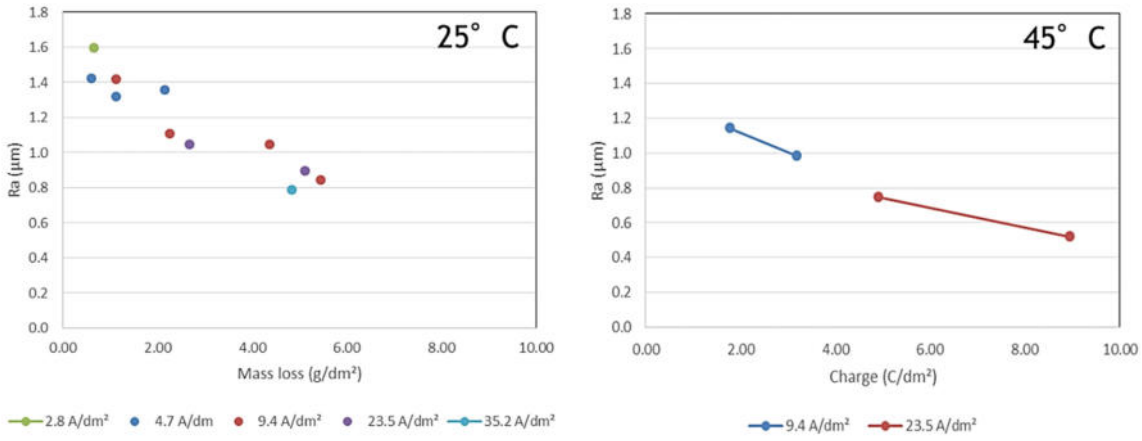

Figure 18: Evolution of the surface roughness (Ra) of 1.2343 steel parts as a function of mass loss in Poligrat electrolyte

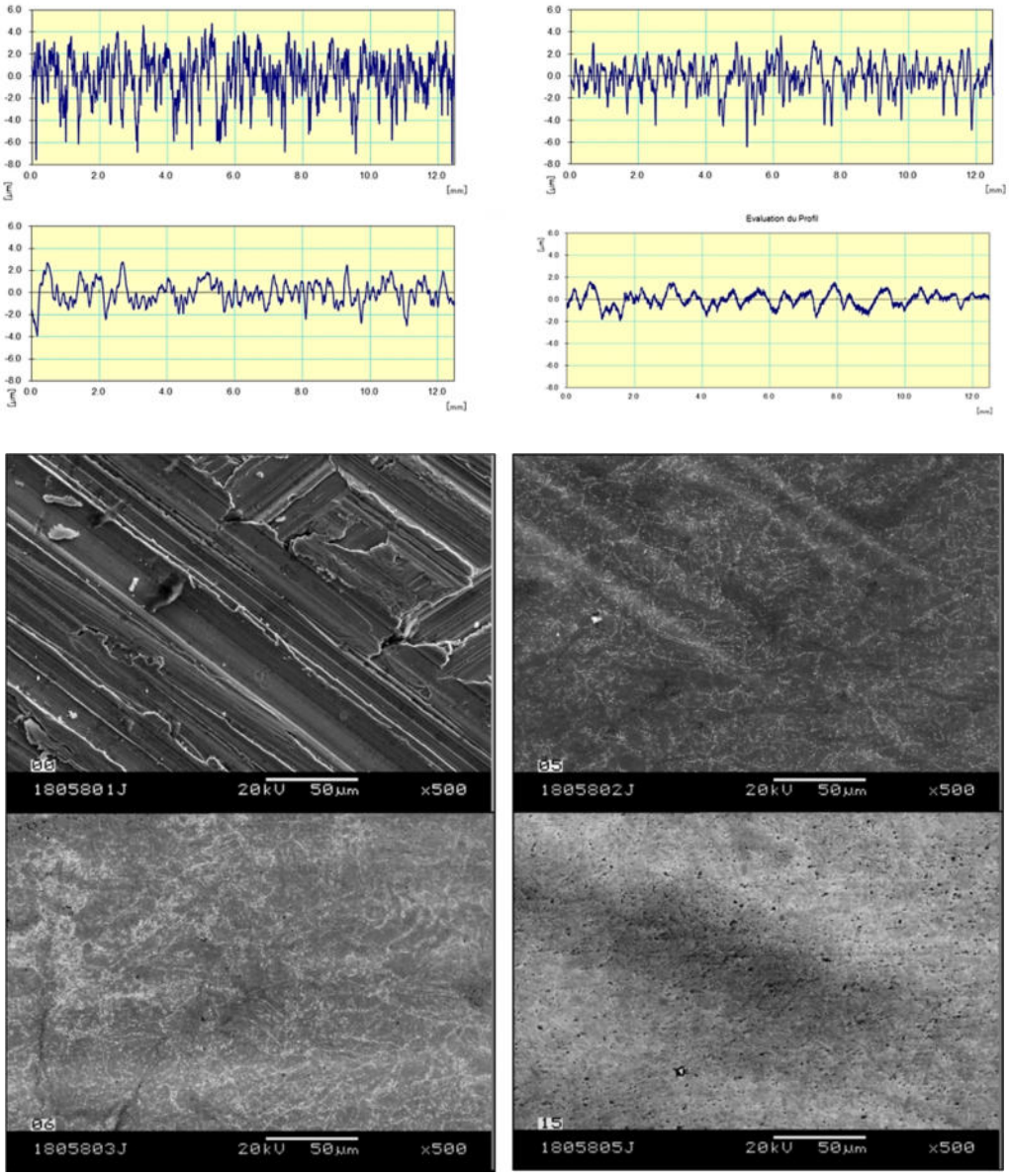

Figure 19: Evolution of the surface morphology of 1.2343 steel parts electropolished in Poligrat electrolyte for (from left to right and top to bottom) 0, 15, 60 and 90 min. The images on the top are surface profiles recorded using a Mitutoyo stylus profiler and the images on the bottom are the corresponding SEM micrographs.

ZFM:

For the EP process, a commercial electrolyte from Electronic Thingks was used. Smart Membranes GmbH, a member of the user committee, supplied it. The electrolyte contains sodium phosphate (Na_3PO_4). The electrolyte manufacturer recommends testing some samples to find the appropriate parameters. It is also recommended to move only the sample during EP process and to do not stir the electrolyte. However, without stirring it was not possible to remove the bubbles at the electrodes surface and an electrode movement was not applicable.

In summary, a real reference condition could not be applied due to a lack of standard procedures or too aggressive chemicals (highly concentrated acids). Therefore, the experimental part for EP was a study on how should the process be performed and which options can be considered for EP. Table 4: Parameter variations for setting up the EP process shows the different set ups as well as the options.

Table 4: Parameter variations for setting up the EP process

Stirring method	Potential /current range	EP time	Electrolyte temperature
Magnetic stirring	4 V	300 s	80 °C
N_2- bubbling through glass capillary	~400 mA	600 s	75 °C
N_2- bubbling through porous stone	Stepwise increase	900 s	70 °C
N_2- bubbling through porous tube	22.5 V	1200 s	65 °C

The following part of the report is a summary of some steps of development during the experiments without showing all results of all experiments.

The first EP trials were based on the linear scan voltammetry (LSV) in the electrolyte to find a sufficient parameter set. The scan was performed with a VersaSTAT 3 potentiostat (Princeton Applied Research) in the range of 0 to 10 V with a scan rate of 100 mV/s. The scans showed a typical behavior of EP with a current plateau starting at 3 V and 360-390 mA to the end of the scan. Because of that, 4 V and 380 mA at 80 ± 3 °C were used for EP in the first development step. It was found that the polishing works for the parameters but without reproducibility even on the same day. The removal and flattening of the typical ECD-Al microstructure was sufficient for 600 s. However, the optical appearance was covered with brownish shadows sometimes. Another problem was that there was a gas bubble formation at the electrode surface, which were projected to the sample after EP. In the Figure 20: Overview of the polishing behavior for the same parameter set but different current flow. The diagrams show the S_a before (blue) and after (orange) EP process at five different points on the sample the microstructure before and after EP, the optical appearance and the degree of polishing (S_a-change) can be seen for two samples with the same parameter set but different

current flow. This figure is representative for the work with low potential and magnetic stirring only.
The next set up used a glass capillary with nitrogen connection. The capillary was placed on different parts of the beaker: before cathode, before sample and in the middle. The potential was constant at 4 V and the polishing time was set to 900 s. Because of the N_2-bubbling, it was not possible to hold the electrolyte temperature constant (66…75 °C). The results from the different capillary positions show also different results in removal rate but not in S_a-improvement. However, also the change in temperature can be the reason for the change. Additionally, it was found that the gas bubbles were to larger to remove the bubbles from the electrode surface. Nevertheless, the bath movement through the bubbles resulted in a shiny surface at the electrolyte-air interface on the sample. Thus, the bath movement was important for a good optical polishing result.

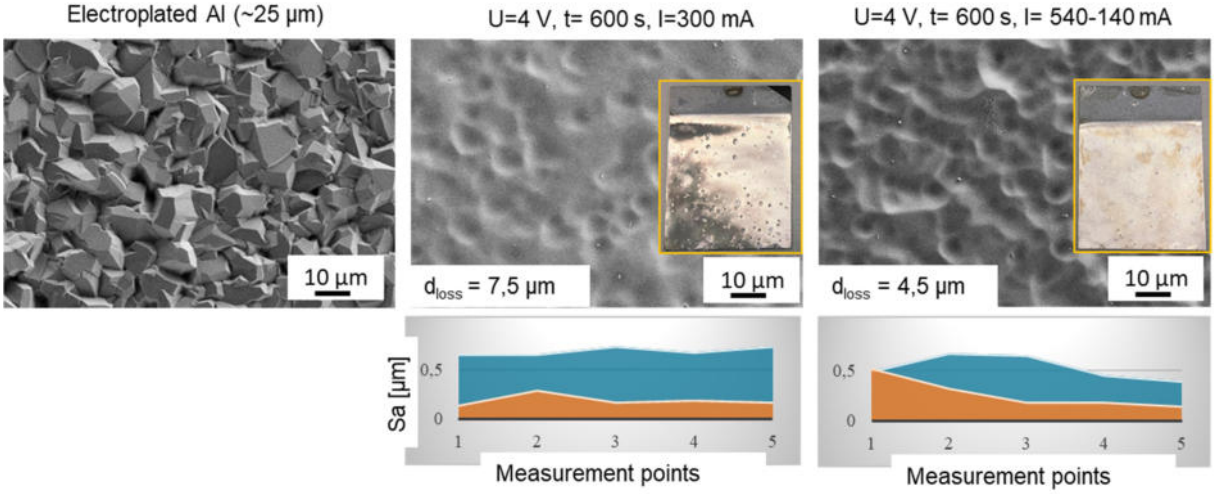

Figure 20: Overview of the polishing behavior for the same parameter set but different current flow. The diagrams show the S_a before (blue) and after (orange) EP process at five different points on the sample

From the previous studies, it was known that the low voltage is not controllable regarding the removal rate and the final polishing result. After discussion with Smart Membranes GmbH, a member of the user committee, a much higher potential of 22.5 V was used. The bath movement was realized with magnetic stirring and N_2-bubbling. The beaker set up was optimized to hold the temperature at 80 ± 2 °C. From Figure 21: Overview of the polishing behavior with increasing time at 22.5 V and 80 °C as photograph (top), SEM (middle) and surface roughness change S_a (bottom). The diagrams show the S_a before (blue) and after (orange) EP process at five different points on the sample it can be seen that the polishing of the samples was efficient. The photographs show that the brownish shadows still appear at some samples. The spotty surface of the samples was from the Al deposition itself. This could not be removed during the polishing. The SEM pictures for different polishing durations show a good evolution of the polishing degree. The reduction in the S_a is relatively comparable between all samples. In comparison to the previous S_a measurements, a higher magnification was used. Therefore, the S_a-values before polishing are also higher than from Figure 20: Overview of the polishing behavior for the same parameter set but different current flow. The diagrams show the S_a before (blue) and after (orange) EP process at five different points on the sample. The results show that higher polishing potential is sufficient for the EP of electroplated Al. However, the optic of the samples was not sufficient.

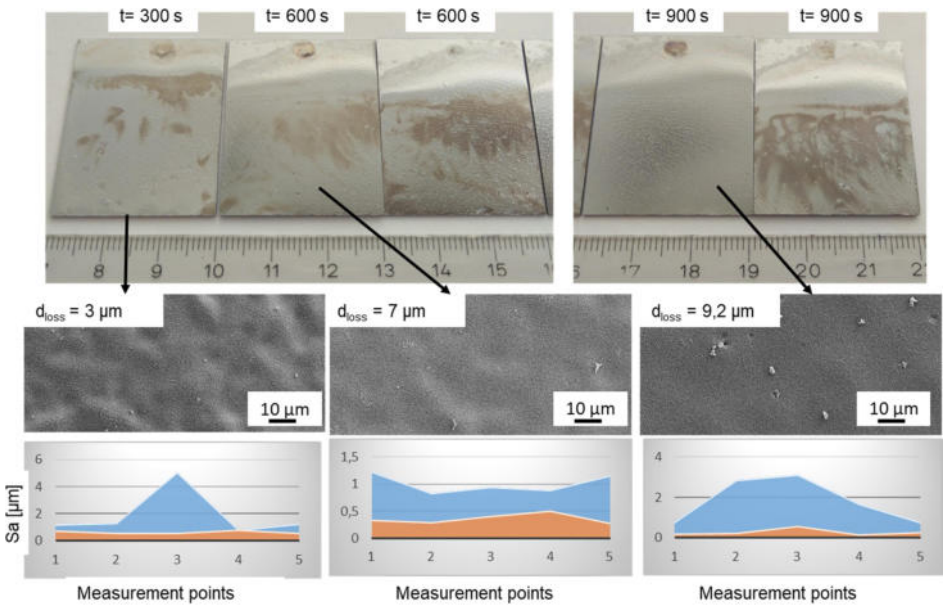

Figure 21: Overview of the polishing behavior with increasing time at 22.5 V and 80 °C as photograph (top), SEM (middle) and surface roughness change S_a (bottom). The diagrams show the S_a before (blue) and after (orange) EP process at five different points on the sample

Thus, a research on a better bath convection was performed. The solution was found in a porous stone, which is usually used for oxygen enrichment in aquariums, and a porous tube, which is used in some wet chemical etching processes. The homogeneity of bubbles from the tube and the stone were tested in water, firstly. The bubble formation of both systems was different. Thus, both were used for EP. The results were completely different. The EP-samples with the tube showed the same behavior than before: brownish shadows on the surface. In comparison, the porous stone showed nicely polished Al layers. Hence, the temperature influence was investigated for 900 and 1200 s. The Figure 22: Overview of the polishing behavior with temperature dependence at 22.5 V as photograph (top), SEM (middle) and surface roughness change S_a (bottom). The diagrams show the S_a before (blue) and after (orange) EP process at five different points on the sample shows some of the samples polished with the porous stone. The optical appearance looks homogenous for all samples without brownish shadow. The sample with 80 °C and 1200 s was strongly attacked at the interface electrolyte-air. In general, the removal rate decreases with temperature. From the photographs it cannot be seen clearly that the layer of 70 °C and 65 °C is matt and not shiny than the others. All samples show a huge reduction in roughness. The sample at 75 °C and 1200 s shows the best polishing result. Nevertheless, it was found that 1200 s of process time attacks the layer more at the interface electrolyte-air. Therefore, a reproducibility study was performed at 75 °C and 900 s polishing time. Within this study, a general influence of the optical appearance was detected: the position of the porous stone. If the stone and thus the gas bubbles were not very close in front of the sample, the polished surface was covered with the brownish shadows as before. Hence, the bath movement should be right in front of the sample with a consistent distance each time. For the used beaker set up, it was not easy to fix this problem without a new tooling. Hereafter, the set up and the defined parameters can be used as reference conditions for the demonstrator level.

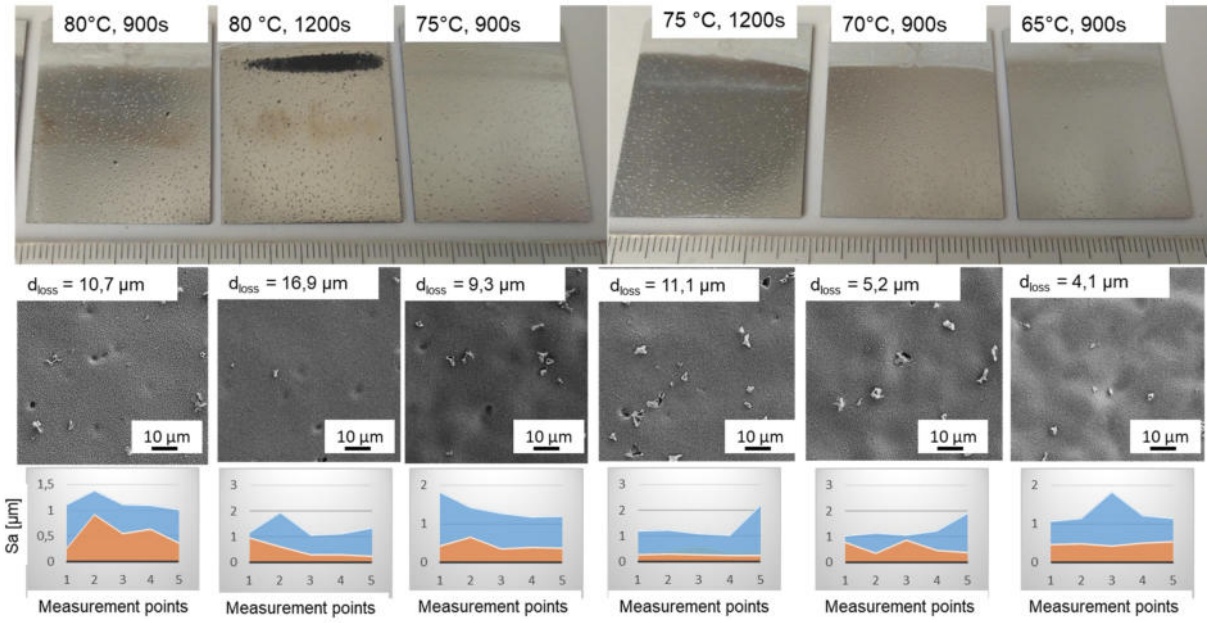

Figure 22: Overview of the polishing behavior with temperature dependence at 22.5 V as photograph (top), SEM (middle) and surface roughness change S_a (bottom). The diagrams show the S_a before (blue) and after (orange) EP process at five different points on the sample

HS:

For the EP trials, the electrolyte E520 by Poligrat was used. It is a commercial electrolyte specialized for the polishing of metal surfaces. Four parameters were investigated with two values for every parameter. The parameters were:

- Temperature
- Time
- Voltage
- Configuration

In initial trials performed by CRM, those parameters were found to be the most important. Temperature was set to 40 and 45 °C. Higher Temperatures were not possible, since the electrolyte can only be used until 50 °C. When the temperature was set to 50 °C, difficulties occurred when the temperature exceeded 50 °C due to inaccurate temperature control. In this case, the current flow was intermitted. Therefore, the maximum value was reduced to 45 °C. Polishing time was varied from 30 to 60 minutes and the voltage between 15 and 20 V. Every parameter setting was tested using a standard configuration, whereby the sample is parallel to the cathode and the Hull configuration in which the sample is placed in a 45° angle to the cathode. The experimental design is shown in Table 5: Experimental design for EP trials with flat samples (1.2343 ESU steel and 1.2379 steel). The procedure was performed using 1.2343 ESU and 1.2379 steel samples.

Table 5: Experimental design for EP trials with flat samples (1.2343 ESU steel and 1.2379 steel)

Number	Temperature	Time	Voltage	Configuration
1	40	60	20	Hull
2	45	60	20	Standard
3	45	30	15	Hull
4	40	30	15	Standard
5	40	30	20	Hull
6	45	30	20	Standard
7	45	60	20	Hull
8	40	30	15	Hull
9	40	60	15	Hull
10	45	60	15	Standard
11	40	60	20	Standard
12	45	30	20	Hull
13	40	30	20	Standard
14	45	60	15	Hull
15	40	60	15	Standard
16	45	30	15	Standard

1.2343 ESU steel

The roughness measurements before and after the EP trials are shown in Figure 23: Roughness measurements (RA and Rz) before and after EP on 1.2343 ESU steel. It can be seen, that the roughness improves significantly for both, Ra and Rz value. It is worth mentioning, that the initial roughness varies significantly although they are produced the same way and every sample was measured several times, using white light interferometry. With the right parameter setting, surface roughness can be improved to Ra < 0.2 µm from an initial roughness of about 1 µm.

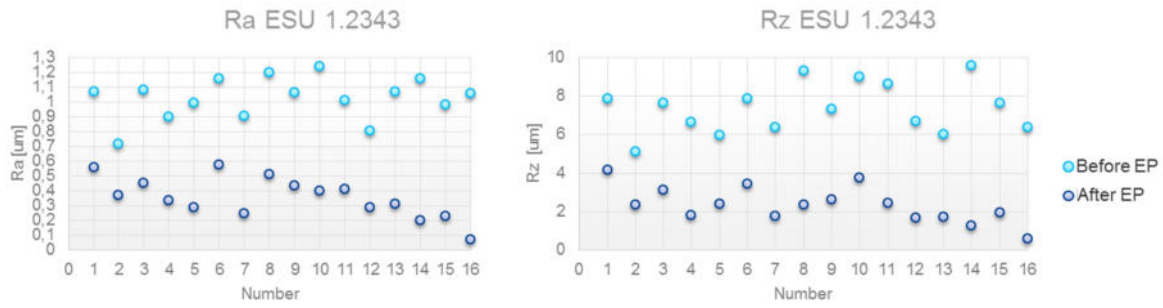

Figure 23: Roughness measurements (RA and Rz) before and after EP on 1.2343 ESU steel

Looking on a polished test sample, the difference between treated and non-treated area can clearly be seen. The improvement of the surface quality is shown in Figure 24: 1.2343 ESU steel sample after EP treatment. The left side is the untreated sample side, the treated area is on the right. It can be seen, that the surface looks smoother, however small white spots are visible which cannot be explained at the moment. The white areas can be found on every sample.

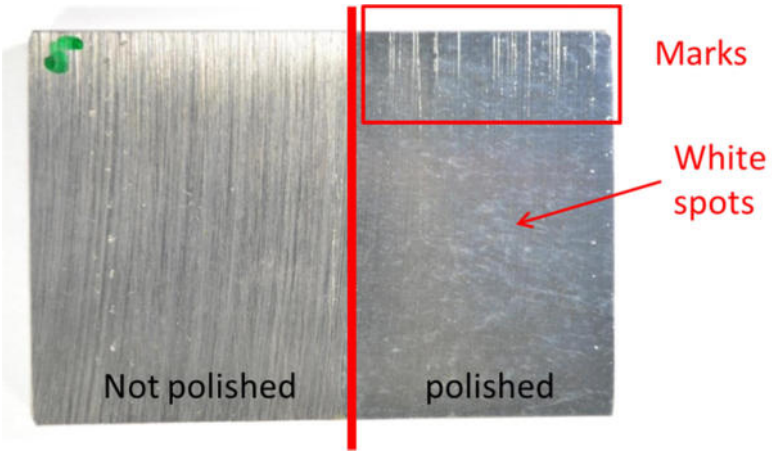

Figure 24: 1.2343 ESU steel sample after EP treatment

As an overall conclusion it can be said, that high voltage and long polishing time achieve the best surface qualities. However, especially long polishing time also results in marks, which can be seen in Figure 24: 1.2343 ESU steel sample after EP treatment. The marks occur at the edge of the sample. The temperature does not have a significant influence on the resulting surface quality which might be due to the fact, that the tested temperature difference was only 5 °C. To compare the configurations is not meaningful, since in the Hull configuration the current density changes throughout the area. The Hull configuration was only performed to see, if any effects occur at high current densities.

1.2343 ESU hardened steel

The same procedure which was performed with 1.2343 ESU steel was repeated with hardened samples. This was suggested by the user committee to see, if the EP process can also be used in hardened steel. In contrast to the previous trials, the EP process was only performed in the standard configuration and not in the Hull configuration.

Table 6: Experimental design for EP trials with hardened 1.2343 ESU samples

Number	Temperature (°C)	Time (min)	Voltage (V)	Configuration
1	40	30	15	Standard
2	40	60	15	Standard
3	40	30	20	Standard
4	40	60	20	Standard
5	45	30	15	Standard
6	45	60	15	Standard
7	45	30	20	Standard
8	45	60	20	Standard

The surface roughness of the test samples before and after the EP process are shown in Figure 25: Roughness measurements (RA and Rz) before and after EP on hardened 1.2343 ESU steel. Similar to the non-hardened substrates, the surface quality can be significantly

improved from Ra > 1.2 µm to almost Ra = 0.2 µm. This result is comparable to the non-hardened substrates.

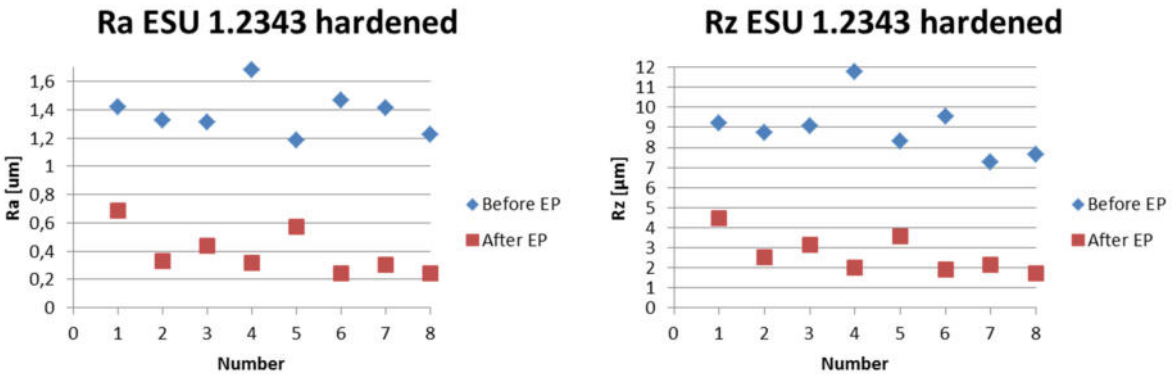

Figure 25: Roughness measurements (RA and Rz) before and after EP on hardened 1.2343 ESU steel

1.2379 steel

For the 1.2379 steel samples, the same procedure as described in Table 5: Experimental design for EP trials with flat samples (1.2343 ESU steel and 1.2379 steel) was used to get comparable results. The results show, that the initial roughness is smaller, compared to the ESU samples. Also the resulting surface roughness is slightly better than with the ESU Samples with several parameter settings resulting in Ra ~ 0.1 µm. The better surface quality is probably a result of the higher Chromium content in this steel grade and the lower initial roughness.

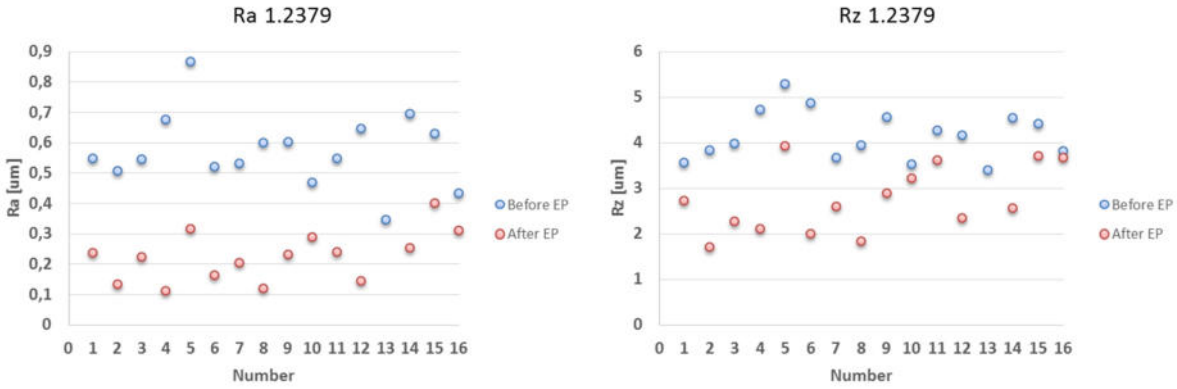

Compared to the ESU samples, the results of the Hull configuration showed large white areas, which didn't occur on the other samples. An example of a sample after the EP process is shown in Figure 26. The white area is formed on the side with lower current density.

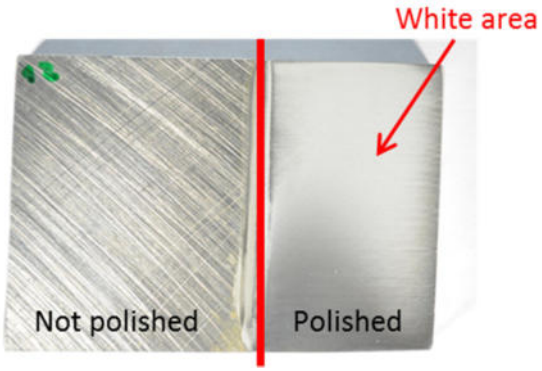

Figure 26: 1.2379 test sample after EP process with Hull configuration

In summary, the following conclusions can be drawn from the electropolishing trials:

- The electrolyte E520 (Poligrat) can only be used with temperatures < 50 °C;
- No significant influence of the temperature could be detected, comparing 40 and 45 °C;
- Using a higher voltage of 20 V leads to improved electropolishing quality compared to 15 V;
- For both investigated steel grades the surface roughness (Ra) could be decreased significantly;
- The polishing process also works on hardened steel and was able to reduce the surface roughness (Ra) of hardened 1.2343 ESU steel significantly.

Structured test samples

Since an improvement of the surface roughness is only useful for industrial applications if the dimensions of the features are not affected, further studies with microstructured test samples were performed. Therefore, test samples were milled using 1.2343 ESU steel and electropolishing. For the polishing trials, the previously identified process parameters were used:

Temperature	Voltage	Configuration	Time
40°C	20	Standard	varied

Since it is very important, that the dimensions of the micro features are not (badly) affected by the polishing process, the polishing time was varied using 30 s, 5 min and 50 min to identify the best polishing time. The goal was to reduce the surface roughness of the part without significantly affecting the feature dimensions and edges.

Measurements were taken at three different structures, as previously shown in Figure 25, before the electropolishing and after electropolishing with the respective duration. The results are described in the following:

Pictures of the electropolished samples are shown in Figure 27. The pictures already show that after 50 min of polishing, visible changes of the sample and the micro structures occur.

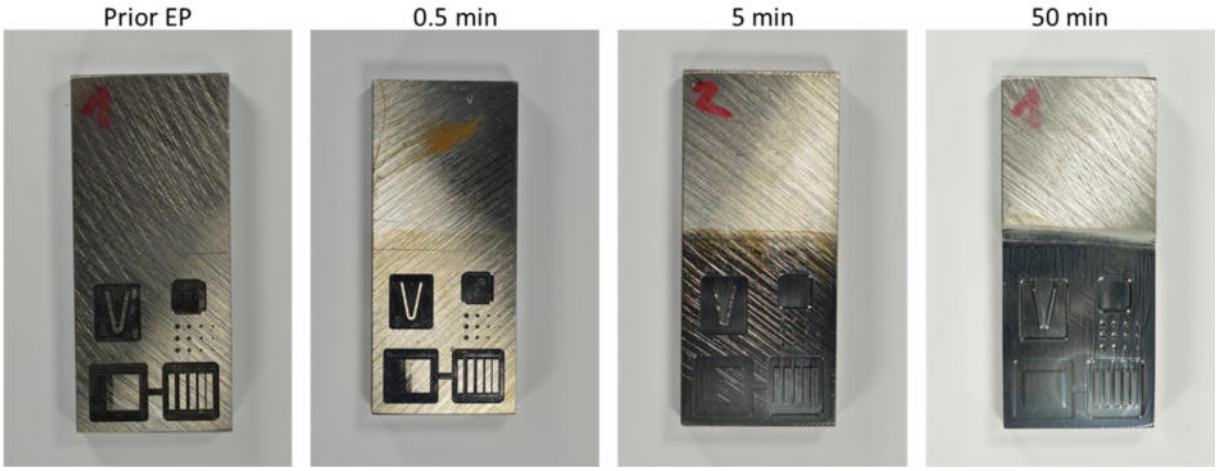

Figure 27: Pictures of the structured samples prior electropolishing and after different polishing durations

Micro channels:

Prior to the electropolishing process, sharp edges can be seen at the micro channels as a result of the milling process and a considerable roughness on the top surfaces. The measurements of the micro channels are shown in Figure 28. After 0.5 min of electropolishing, the edges remain sharp. The surface roughness could be slightly reduced from Ra = 0.25 µm to about Ra = 0.21 µm, however the Rz surface roughness could be reduces significantly from 2.4 µm to < 1 µm. Increasing the polishing time to 5 min significantly reduces the surface roughness to Ra = 0.15 µm. Also in the small 200 µm channel a reduction of the surface roughness could be measured, showing that the process also works in very small features. Compared to the unpolished sample, a small reduction of the edge sharpness can be identified; however this would still be a sufficient sharpness for most applications (e.g. microfluidics). After 50 min of electropolishing, the micro structures are significantly altered. The sharp edges are removed completely. Therefore, the polishing time is too long for most applications. Furthermore, the surface roughness is higher compared to the untreated samples. This leads to the conclusions, that excessive electropolishing significantly reduces the quality of the sample.

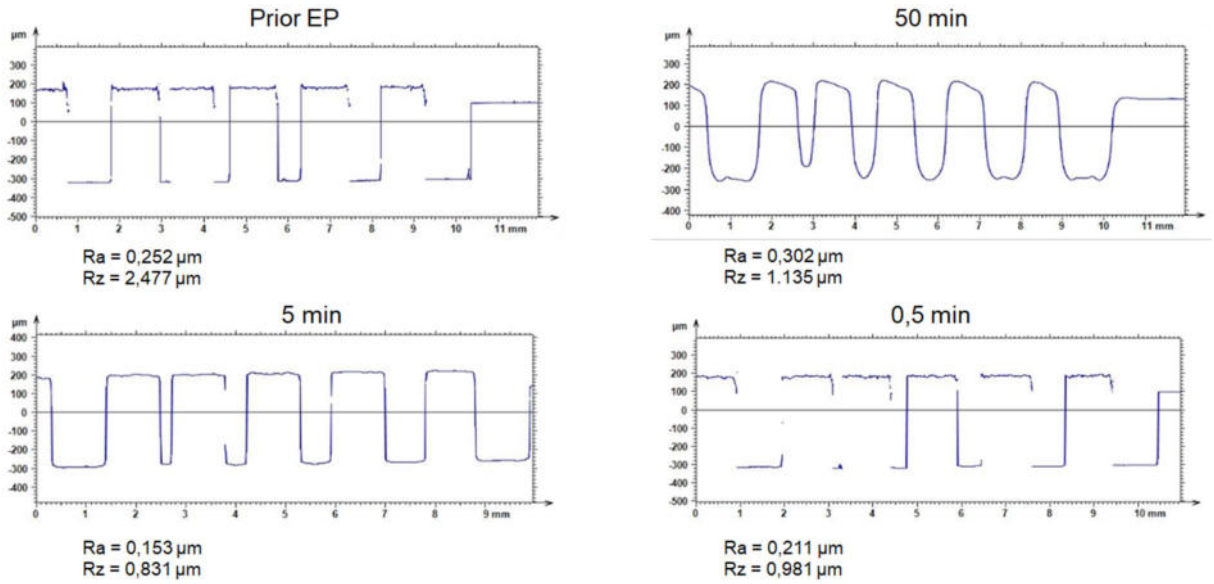

Figure 28: Profile measurements of the micro channels prior electropolishing and after different polishing times

Micro holes:

The micro holes are interesting structures to evaluate the effects of electropolishing on the edges. Furthermore, it can be investigated, if the polishing process also works in small holes. As shown in Figure 29, the quality of the micro holes is significantly altered by the electropolishing, when the duration is too long. After 0.5 min, only minor changes of the micro holes can be identified. After 5 min, the sharpness of the edges is reduced, however still in an appropriate extend. The rounding effect on the edges can be seen in every micro hole, showing that the process is working even in the smallest holes with a diameter of 300 µm. After 50 min, the structures are significantly altered. The results lead to the conclusion, that 5 min of polishing are a good duration, leading to acceptable changes in the features.

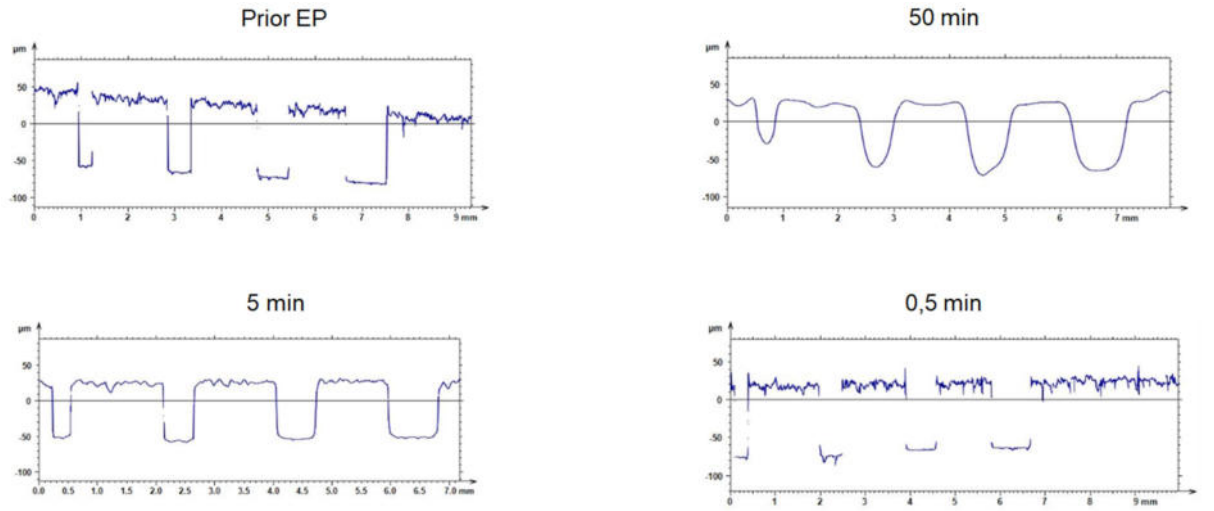

Figure 29: Profile measurements of the micro holes prior electropolishing and after different polishing times

Slopes:

For the structure with slopes, the four edge radii were defined as R1-R4 (see Figure 30) and measured using a laser autofocus system to analyze the change of the radii due to the polishing process. Furthermore, the structure was used to measure the change in the surface roughness (Ra and Rz) for different polishing durations. After 0.5 min and 5 min of electropolishing, only a minor change of the radii can be measured. However, after 50 min, the radii change significantly leading to round edges. However, the surface roughness further improves with increasing polishing time. This result contradicts the results that were gained at the micro channels, since the surface roughness increased at 50 min polishing time. This is probably due to the quality of the initial surface, which is better when the surface is milled compared to grinded. Therefore, it can be concluded, that the quality of the initial surface plays an important role on the achievable surface quality by means of electropolishing.

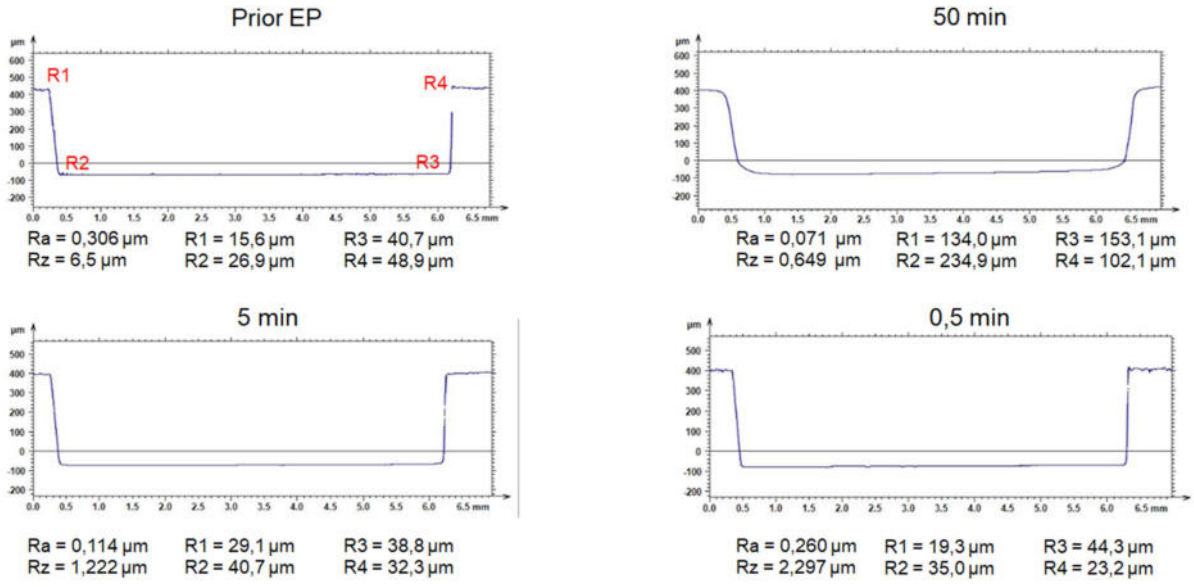

Figure 30: Profile measurements of the slopes prior electropolishing and after different polishing times

Task 1.5: setting up of the methodologies for the assessment of electropolishing mechanisms

The goal was, in a first time, to develop the tools needed to analyze the electropolishing results “in situ” and “ex situ”. Those tools will also be of use for tasks 1.1, 1.2 and 1.4 as characterization methods.

1) Ex-situ techniques

1.1) XPS (X-Ray Photoelectron Spectroscopy)

XPS is a technique commonly used for surface analysis. However, in its classical configuration, XPS will only provide information on the extreme surface of the samples (most of the photoelectrons came from the first 3 nm). As part of this project, it is needed to be able to analyze the structure of the oxide layer formed at the surface of the samples in order to be able to link this structure with the electropolishing conditions (applied potential, current density, bath, temperature…).

The use of depth profile by progressive etching using argon ions is a usual technique in that case. It is possible to obtain XPS spectra after each etching step and to treat those results in

order to extract the oxide layer structure. Some adjustments have been needed in order to adapt the depth profile technique to the case of stainless steel samples:

- to calibrate the etching speed in order to obtain an information in term of depth and not in term of etching duration
- to develop a methodology allowing to deconvolute the chromium and iron signals into components according to the environment and oxidation level
- to investigate and control the influence of environmental factor on the oxide layer structure between its formation and its analysis

Those various issues have been solved and will be published.

We are now able to characterize an oxide layer produced during electropolishing in terms of composition, structure and depth. The long-time stability of this oxide layer has also been proved.

Figure 31: K-alpha XPS used during this project

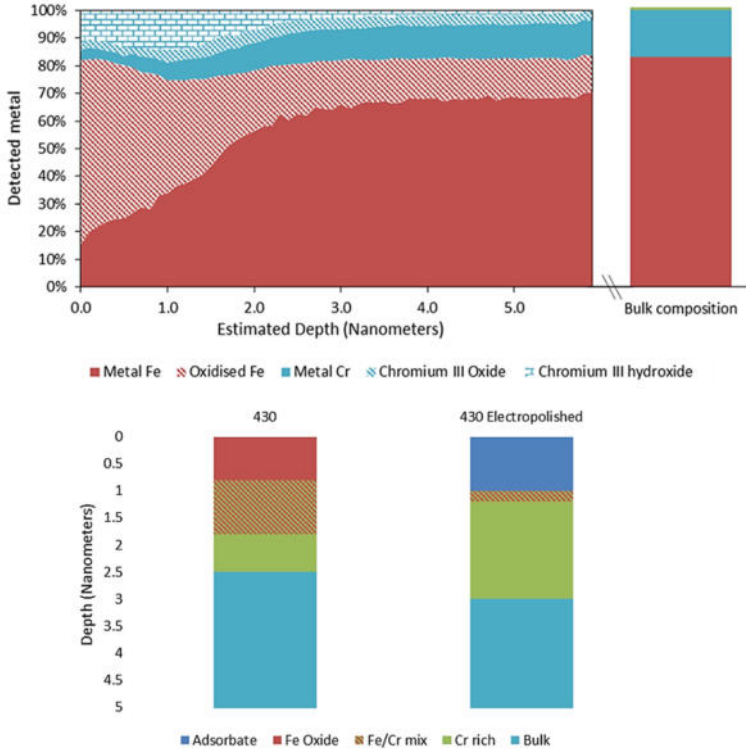

Figure 32: Data for the composition of the oxide layer as a function of the etching time (430 stainless steel, top) and illustration of the oxide layer structure before and after electropolishing (430 stainless steel, phosphoric acid/sulfuric acid bath, low)

1.2)Roughness measurement

During this project, roughness has been measured using a Mitutoyo SJ-210. This device is characterized by a resolution in length of ca. 0.5 micron. Usually, the roughness is expressed on the form of mean value like Ra (arithmetic average value of deviations from the mean value), Rp (maximum peak height…). Those parameters do not provide a full representation of the roughness complexity.

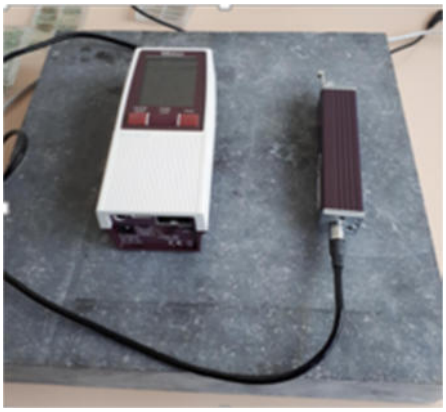

Figure 33: Mitutoyo SJ-210 used during this project

For this reason, a signal decomposition technique, also known as frequency analysis, has been applied to the electropolished samples. The goal of the frequency analysis is to decompose a given signal (here a roughness profile) as a sum of elementary signals (see Figure 34). This decomposition allows bringing to light some elementary components, something that Ra alone does not provide.

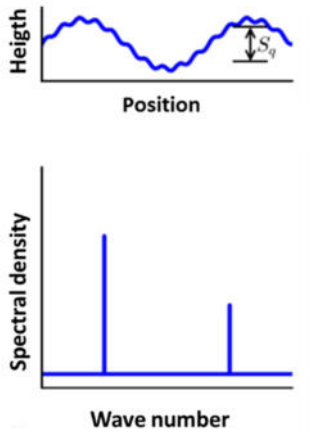

Figure 34: Illustration of the principle of frequency analysis

Figure 35 shows the use of frequency analysis on 316 stainless steel samples electropolished with two different current densities in the same bath. The electropolishing has been achieved during various times. It can be observed that for samples electropolished with a current density of 130 mA/cm², there is a strong decrease of the spectral density at wavelength lower than 100 µm. However, some signals still remain at wavelengths higher than 100 µm. On the contrary, when the electropolishing is performed at lower current density (50 mA/cm²), a signal decrease is noticed only at very low wavelength, below a few µm.

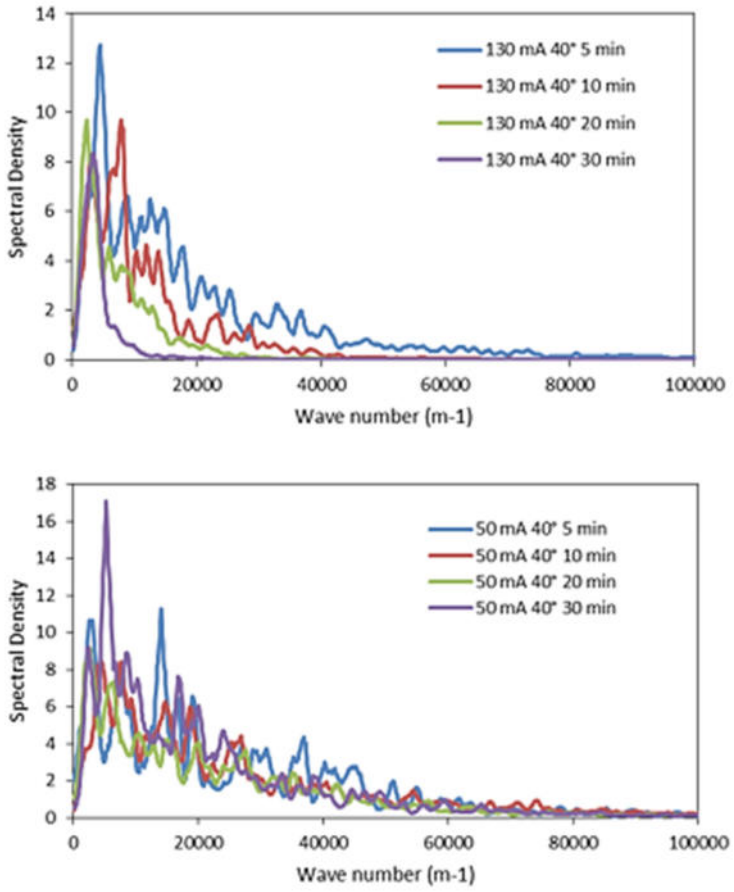

Figure 35: Application of the frequency analysis on 316 stainless steel samples electropolished with current densities of 130 mA/cm² (top) and 50 mA/cm² (low)

It should be noted that this technique is constrained by the intrinsic resolution of the used equipment. As a consequence, we are not able to observe roughness with wavelengths lower than one micron.

2) <u>In situ techniques</u>

2.1) <u>EIS (Electrochemical Impedance Spectroscopy)</u>

Electrochemical impedance spectroscopy consists in the study of the reaction of a system to an applied sinusoidal variation of potential (in the case of potentiostatic EIS). A constant potential (E_{ss}) is applied along with a sinusoidal variation of potential (δE). The system response is a constant current (i_{ss}) along with a sinusoidal variation of current (δi). Potential and intensity signals present a phase shift (Δt).

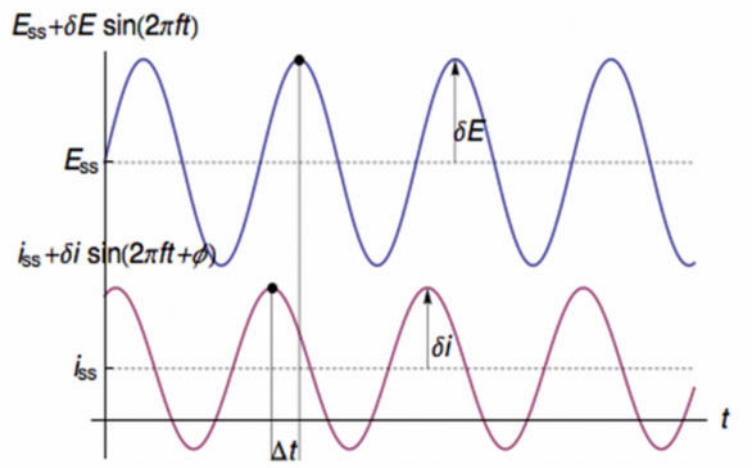

Figure 36: Illustration of the principle of electrochemical impedance spectroscopy (credits: Nicolas Murer)

The obtained results are expressed as intensity and phase shift as a function of frequency can be treated using two different and complementary approaches.

In a first approach, the experimental signal is fitted using an electrical equivalent circuit including a resistance, a capacitance and an inductance which can be linked to the composition of the system under study such as an oxide layer, an electrochemical double layer or the electrolyte resistance. An oxide layer, for example, can be expressed by a capacitor (if the oxide layer is complete) or by a capacitor and a resistor in parallel in the case of a porous oxide layer allowing a contact between the metal and the electrolyte. This approach can sometimes be problematic because an electrochemical system doesn't behave like a set of ideal electrical components. For example, the oxide layer thickness can vary, needing the use of a distribution of several capacitors to be properly represented. Another difficulty is the fact that different electrical circuits can be used to simulate the same set of impedance data. Thus, it is necessary to obtain additional information (for example using ex-situ techniques) to—establish the most appropriate electrical circuit representing the electrochemical system.

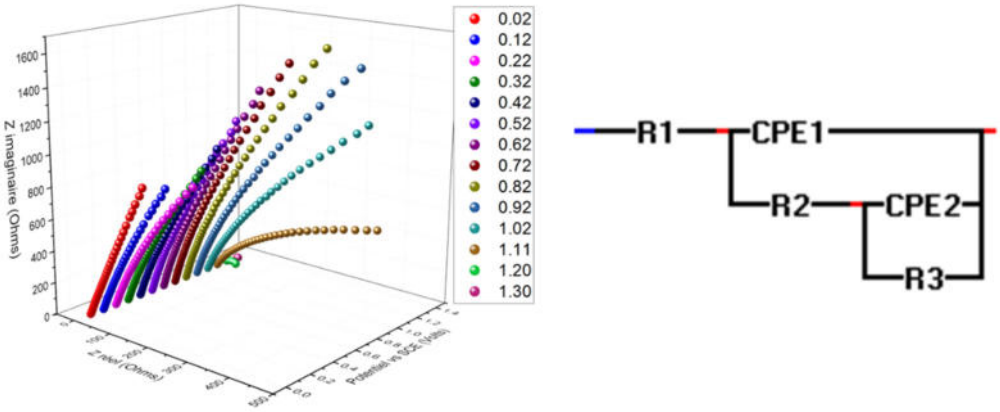

Figure 37: Example of an electrochemical impedance spectroscopy data set (316 stainless steel, sulfuric acid/phosphoric acid bath) and the equivalent electrical circuit which can be used to simulate these data. CPE stands for "constant phase element"

Second, it is possible to establish a model of the various reactions taking place at the electrode (oxidation, reduction, dissolution and complexation). It is possible to derive from those equations the impedance response. The matching between this impedance response and the one experimentally observed can be obtained by adjusting the constant values present in the various model reactions.

The combination of these two approaches allows the identification and the characterization of the mechanisms taking place at the electrode surface. Electrochemical impedance spectroscopy has been successfully applied to the various stainless steels (316, 304 and 430) in acid baths (phosphoric and sulfuric acids) as well as in the DES (deep eutectic solvents) baths. For those two types of baths, electrochemical impedance spectroscopy is a powerful tool to identify the mechanisms.

2.2) SECM (Scanning Electrochemical Microscopy)

This technique uses a microelectrode scanning a surface at a distance of a few microns in a solution containing a redox mediator. Following the conductivity of the surface (or the lack of conductivity), the current detected at the microelectrode will change (see Figure 38). If the surface is an electrical conductor, the approach of the microelectrode leads to an increase of the detected intensity due to the mediator regeneration at the surface. If the surface is non-conductive, the approach of the microelectrode leads to a decrease of the detected current as the access of the mediator to the electrode surface is increasingly difficult. The scanning electrochemical microscopy provides a two dimensional image of the surface conductivity.

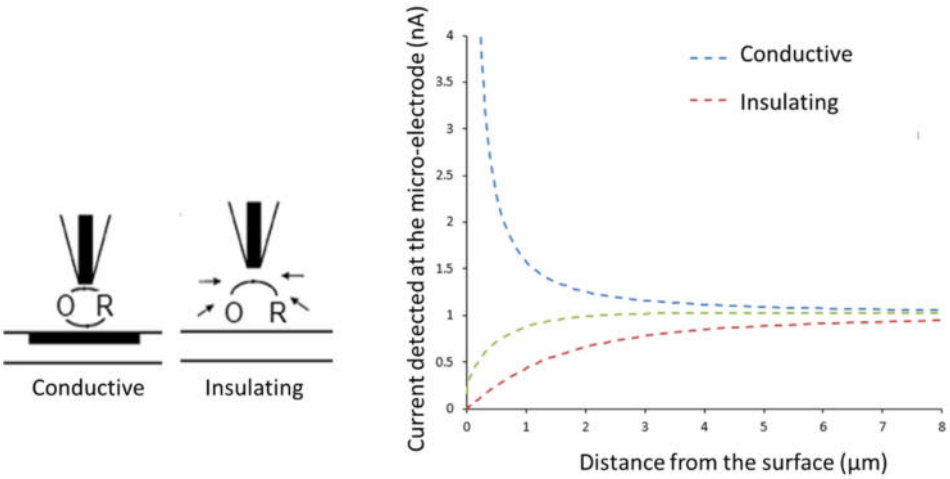

Figure 38: Illustration of the SECM principle

By substituting the redox mediator solution with an electropolishing bath, it is possible to make a cartography of the surface before and after the electropolishing. This possibility has been demonstrated using 316 stainless steel in a sulfuric acid/phosphoric acid bath.

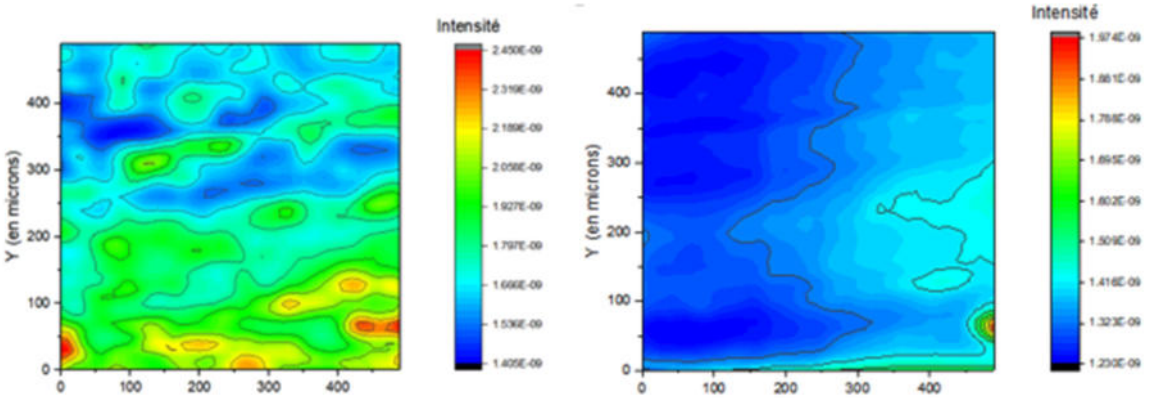

Figure 39: Change in the surface cartography following electropolishing

3) Methodology to establish the electropolishing mechanisms :

To establish the electropolishing mechanisms, a combination of the presented techniques is needed. A combination of XPS and electrochemical techniques allows us to establish the reaction leading to the formation of the oxide layer (at the microscopic level). Impedance spectroscopy, in combination with the previous information, allows the identification of the mechanism of formation (salt film, adsorbed acceptor…). Moreover, the electrochemical impedance spectroscopy allows the identification of the suitable conditions (applied potential or current density) for the electropolishing of a substrate in a particular bath. Finally, roughness measurement, but also SECM are useful to characterize the electropolishing efficiency.

At this point, it is important to present the status of our ability to identify and master the different aspects involved in the electropolishing.

- In the case of the formation of an oxide layer with a high resistance to corrosion, the methodology is available and under control for acid baths
- In the case of mechanisms taking place during the electropolishing and the way in which those mechanisms change with the bath and the applied potential, the existent literature is quite complete. The transposition of these literature data to our systems is also ready.
- Finally, we still have to establish the link between the roughness and the electropolishing conditions and mechanisms. This point is the object of task 2.2.

In all cases, the electrochemical impedance spectroscopy proved to be a powerful and polyvalent tool. Its use to identify the electropolishing mechanisms and the right polishing parameters will be developed during the project. The complementary characterization techniques, XPS and SECM, are now well mastered, as it is the case for the diagnostic techniques like roughness measurement and scanning electronic microscopy.

As described in the first annual report, an analysis method of the oxide layer structure using XPS depth profiling has been developed

This method allows:

- To know the elements distribution (Fe, Cr, Ni, Mo, C, O) on the depth of the oxide layer;
- To know, for iron and chromium, their chemical environment. This chemical environment allows the distinction between the metallic and oxidized from for iron and chromium and between the oxide and hydroxide for chromium;

- The whole analysis can be done in a short time. 40 To 80 minutes are needed for a complete depth profiling, depending on the steel complexity.

In the article in **Annex 1.5-1**, the development of the fast depth profiling is described. This method has been used with AISI 430, 304 and 4316 stainless steels.

The obtained results have been confirmed with independent technics such as HAXPES and AR-XPS (Angle-resolved XPS) and are consistent with the literature.

For the three stainless steels, it appears that:

- The structure of their oxide layer depends of their environment. This structure is strongly different between the as-received AISI 316 and the same stainless steel after mechanical polishing;
- For all the stainless steels, the oxide layer show an outermost part made of pure iron oxide. Beneath this iron oxide layer, chromium accumulate on the form of chromium oxide/hydroxide. This accumulation contains up to 150 % of chromium with respect to the bulk;
- For steels containing nickel, there is an accumulation of metallic nickel (up to 140 % with respect to the bulk) beneath the chromium layer;
- Molybdenum is present at the extreme surface on the form of molybdenum oxide. There is no accumulation of molybdenum but a depletion of all the other elements;
- The oxide layer structure slightly evolves (its thickness increases) during the first days after a mechanical polishing. It stabilizes after 9 days. This evolution seems to be related to the migration of chromium ions and nickel atoms. This behavior is reported in the literature for chromium;

The fast depth profiling method has been applied to several samples in the frame of AdEPT project:

1) In the case of Phynox special steel (a steel with a high content in cobalt). The **Annex 1.5-2** (which is a publication project for submission at short term) summarizes the obtained results. This study report on:

- The Phynox oxide layer structure after mechanical polishing;
- The evolution of the oxide layer after UV-Ozone pre-treatment;
- The evolution of the oxide layer structure after polarization in 10 mM KNO_3 electrolyte;
- The evolution of the oxide layer with time.

2) Some chemical or physico-chemical pre-treatments are commonly used prior to surface modification. The effect of those pre-treatment on the oxide layer of stainless steels have been studied. The effect of hydrothermal and UV-Ozone pre-treatment on AISI 430, 304 and 316 are detailed in **Annex 1.5-3**.

3) The oxide layer structure of stainless steels electropolished in acid electrolyte has been systematically studied. Figure 1 hereafter show the structure obtained for AISI 316 stainless steel polarized in a phosphoric/sulphuric acid electrolyte at various potentials.

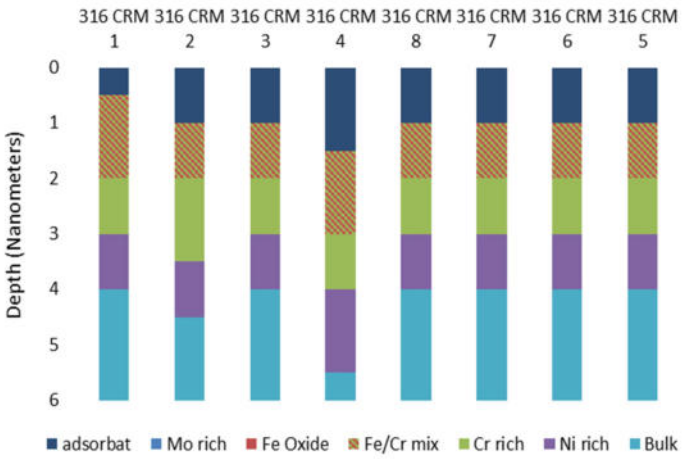

Figure 40: Structure of the oxide layer on AISI 316 stainless steel polarized at various potentials in phosphoric/sulfuric acid electrolyte

In opposition to stainless steel before electropolishing, the iron oxide surface layer is not present anymore. **The chromium (III) oxide/hydroxide rich layer forms the surface of the sample after electropolishing**. This surface rich in chromium oxide helps explain the increase in the corrosion resistance after electropolishing in acid baths.

It is worth noting that **a thin adsorbed layer made of iron and chromium phosphate covers the surface.** This layer is always present on the stainless steels after electropolishing and will be a strong argument in the discussion about the electropolishing mechanisms.

4) The analysis methodology has been used for AISI 430 samples polarized at various potentials between OCP and the electropolishing plateau. It appears that in the passivation domain, the increase in potential increases the oxide layer thickness without changes in the structure. The iron oxide surface layer disappears in the transpassive potentials domain. This led to the formation of the structure described in the previous point on the electropolishing plateau.

5) An AISI 430 stainless steel has been polarized at various potentials in a sodium sulphate electrolyte. The same relation between the applied potential and the oxide layer structure than the one reported for acid electrolytes has been observed. This work is part of an internship report (**Annex 1.5-4**).

6) The oxide layer structure of tool steels (1.2343 and 1.2379) has been investigated. There is no visible accumulation of iron or chromium. This is also the case after electropolishing in an acid electrolyte. It seems that the amount of chromium in the stainless steels composition is responsible of the oxide layer structure. This amount of chromium is also related to the oxide layer structure after electropolishing and to the high corrosion resistance. Without notable amount of chromium, the mechanism did not appear to be transposable to the case of tool steels.

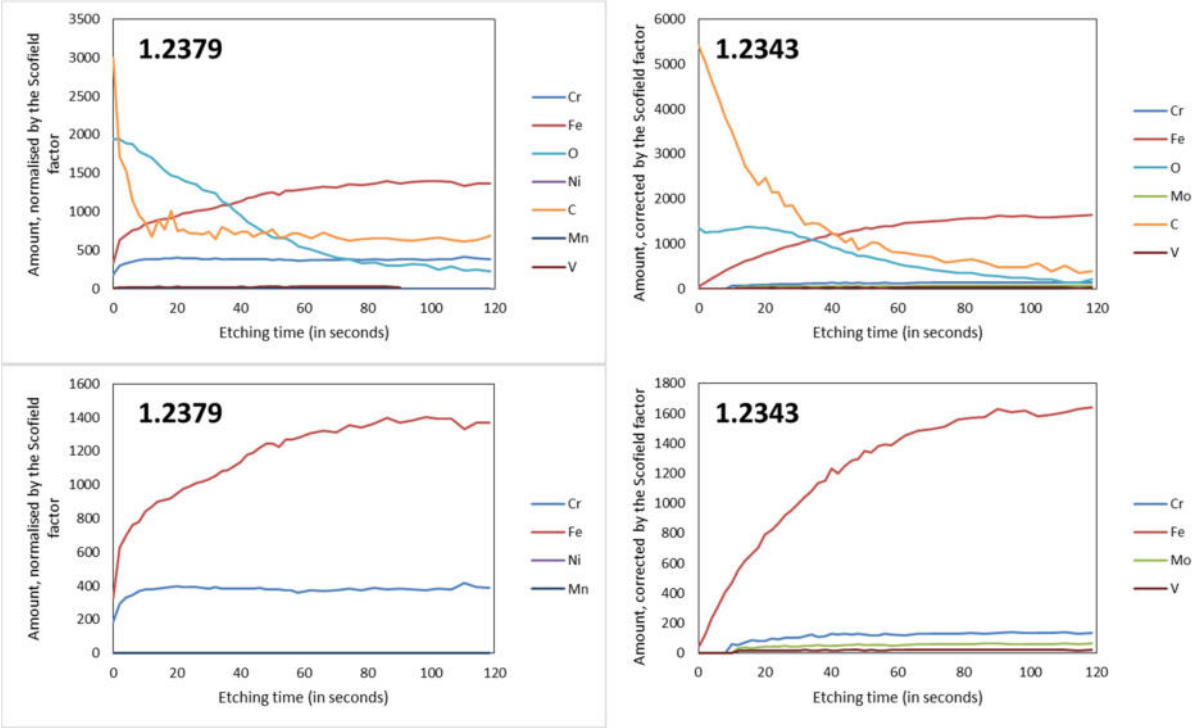

2. Work package 2: Investigation of advanced bath formulations

Task 2.1: Update of the literature review on advanced electropolishing bath chemistries

Literature about electropolishing date back to the patent of Madsen in 1925 (C. P. Madsen, U.S. Patent No. 1,562,711). It is possible to sort and organize this literature following the bath nature, the stainless steel type, the additive used or the used characterization method.

Electrolyte bath:

The electrolyte baths can be divided in two main families: the acid ones and the DES (deep eutectic solvents) ones.

Among the acid-based baths, the following can be encountered:

- Mixtures of phosphoric and sulfuric acid (in various proportions) [1]–[28].
- Phosphoric acid used alone [3], [4], [29], [30]
- Sulfuric acid used alone [3], or in combination with methanol [14], [24]
- Perchloric acid, mixed with acetic acid [4], [31]–[35] or with ethanol [34], [36], methanol [4], ethylene glycol [34] or monobutylether [37].
- Commercial mixtures [38]–[40]

DES are only used since a few years and are rarely encountered in the literature [41]–[44]. Those DES are based on choline chloride, in eutectic mixture with ethylene glycol, urea or malonic acid.

Stainless steel:

Most of the used stainless steels are from the AISI 300 family:

- AISI 316 [2], [6], [7], [12], [14]–[16], [18], [20], [22]–[25], [30], [32]–[34], [37], [38], [41]–[43], [45]
- AISI 304 [1], [4], [5], [8], [9], [13], [19], [26], [38], [40], [41]
- But also AISI 302 [41], AISI 308 [35], AISI 314 [46], AISI 321 [39] et AISI 347 [41]

Only a few studies deal with the AISI 400 family like AISI 410 [41] et AISI 420 [3], [47] or with duplex steels (Duplex 2205) [27] ou tool steels (O1) [48], [49].

Additives:

Some authors present baths containing various additives. Those baths are almost all based on the phosphoric acid/sulfuric acid mixture. The various additives encountered in the literature are:

- Chromium oxide (VI) [2], [12], [13], [21], [23], [46], [48], [49]
- Tartric acid [1]
- Lactic acid [1]
- Oxalic acid [43]
- Urotropine [1]
- Glycerol [8], [9], [15], [18], [29], [30], [47]
- Ethylene glycol [36]
- Monoethanolamine, diethanolamine, triethanolamine [5]

Characterisation techniques:

Various characterization techniques are used in the literature. Among the most used are those also used in the AdEPT project like:

- XPS [14], [15], [18], [20], [22], [25], [26], [29], [32], [33], [35], [41]
- SEM [1], [3], [8], [10], [13], [14], [16], [19], [20], [28], [30]–[32], [34], [36], [39], [41], [44], [46], [47]
- Roughness measurement [1]–[3], [6]–[9], [12], [14], [15], [18], [20]–[24], [28]–[30], [38], [39], [41], [44], [47]–[49]
- Electrochemical impedance spectroscopy [3,6,53,54,28,31,32,42,50,51,52]

Atomic force microscopy (AFM) is also widely used [8], [9], [14], [16], [18], [20], [24], [28], [29], [34], [35], [37], [41]. Some research groups also used more specific techniques depending of the goal of their research. Corrosion tests [6], [15], [16], [18], [40], [44], X-Ray Diffraction (XRD) [20], [28], [40], [44] and contact angle measurement [14], [29] are quite common.

It is worth noting that SECM has never been used on the stainless steel electropolishing literature.

Theoretical studies and review:

Theoretical studies on the electropolishing mechanisms are quite numerous [3], [13], [17], [48]–[51], [55]–[67]. However, no purely theoretical study on this subject has been published since 1998. This is of particular interest as all the aspects of electropolishing on stainless steel have not been treated. And no theoretical study has been realized on the electropolishing in DES.

Some review exist on the stainless steel electropolishing, sometimes about specific subjects like the use of DES [61], [62], [68]–[70].

Finally, the use of pulsed current is only cited twice [1], [38].

Conclusions:

The electropolishing of stainless steel (mostly of the AISI 300 series) in acid bath is a well-documented field. However, numerous side fields have not (or only sparsely) been the subject of researches. For example:

- Electropolishing of Duplex steels
- Electropolishing of the AISI 400 series
- Influence of additives on the mechanisms
- Electropolishing in DES baths
- More generally, electropolishing in a bath which is not made of a mixture of phosphoric acid and sulfuric acid.
- The use of pulsed currents.

Task 2.2: Investigation of electropolishing mechanisms in advanced acid-based baths

This work is based on the multi-technique approach described in task 1.5.

The electrochemical impedance spectroscopy led, in agreement with the literature, to the identification of conditions leading to a good electropolishing for “classical” sulfuric acid/phosphoric acid baths. The graphical representations of impedance data, shown below, corresponds to signals characteristics of electropolishing by an acceptor mediated mechanism. This mechanism takes place when the reaction limiting step is not the metal oxidation but the migration of an acceptor species needed to solvate cations produced by the oxidation.

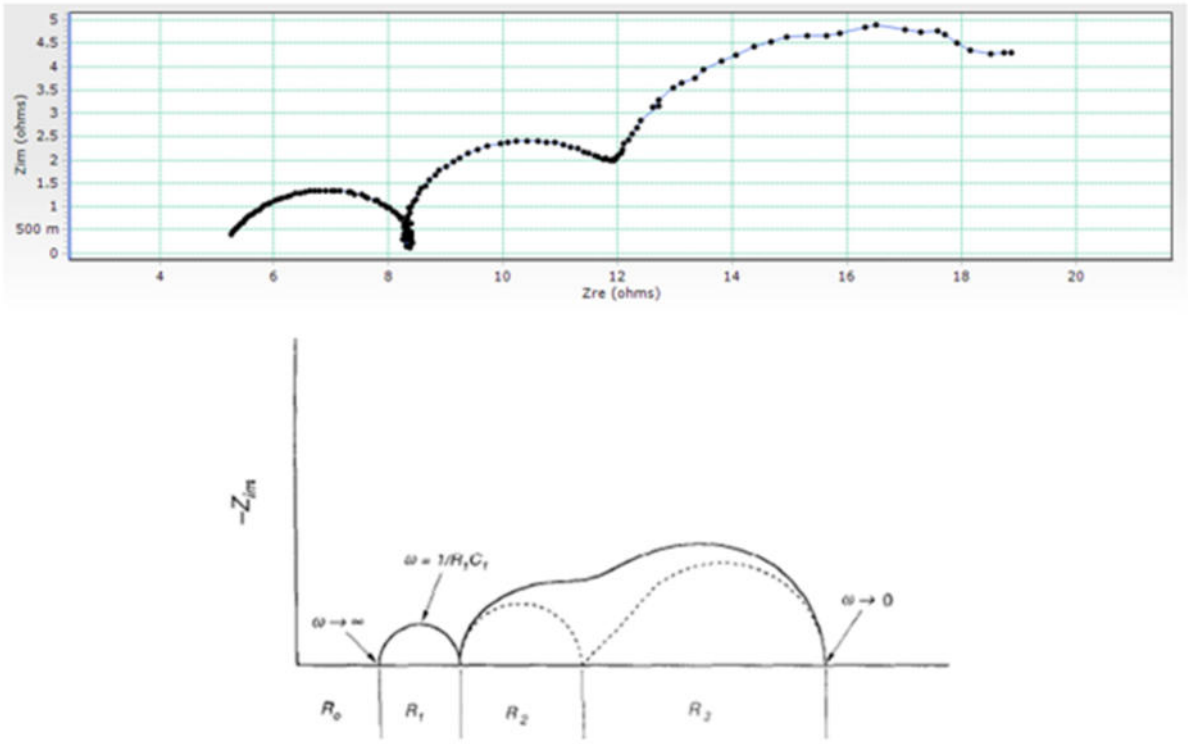

Figure 41: Typical impedance signal obtained for 316 steel in sulfuric acid/phosphoric acid bath (top) and the theoretical signal corresponding to an adsorbate acceptor model (low)

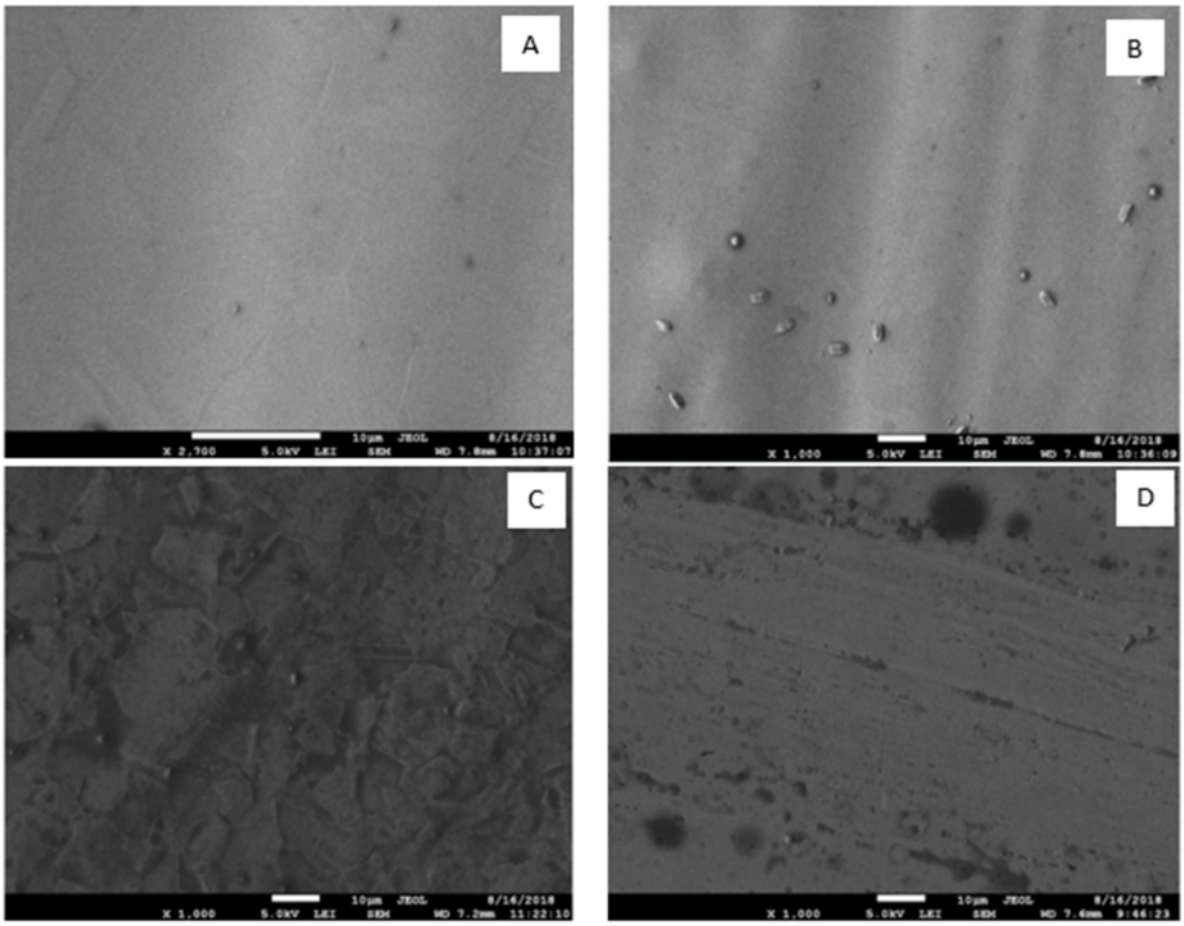

Figure 42: Scanning electron microscopy images (A, B) characteristics of an electropolished a surface in conditions where the impedance signal shown in the previous figure is observed. C and D illustrate the surface state when the impedance signal differs from the previous figure

A systematic screening of various additives and bath compositions are still to be realized. This screening will focus on the impedance signal and on the surface state obtained.

The description of the electrochemical impedance spectroscopy (EIS) has been realized in the previous annual report.

During this second year, a systematic study of the EIS response of stainless steels on phosphoric/sulphuric acid electrolyte has been performed.

The standard manipulation consists in a polarization of a sample in the chosen electrolyte. After 20 minutes of stabilization, an EIS spectrum is recorded. The sample is then polarized at a slightly higher potential (by steps of 50 mV or 25 mV) and the manipulation is realized again. This kind of measurement is realized between the OCP (typically around 0.200 V *vs.* SCE) up to an applied potential of 3.00 V *vs.* SCE.

Figure 43 shows the evolution of the recorded current density as a function of the applied potential for a sample of AISI 430 stainless steel in a phosphoric/sulphuric acid electrolyte. The standard electrolyte for most of the experiment is made of 71 wt. % H_3PO_4/16 wt. % H_2SO_4 and 13 wt. % H_2O. Figure 43 also illustrates the three typical impedance spectra observed on AIS 430. They can be described as:

In zone I: a high frequency capacitive loop followed by a low frequency inductive loop

In zone II: three capacitive loops

In zone III: two capacitive loops

The parameters of those loops (diameter, top frequency) vary as a function of applied potential and this variation has been used to formulate hypothesis about the mechanism.

It is worth noting that the three different impedance spectra are known in the literature[1–4]. The strong link between the observed impedance spectra and the surface resulting from an electropolishing in the same conditions is reported in the literature as well. Figure 43 illustrates the fact that the best electropolishing results are obtained at applied potentials corresponding to the electropolishing plateau and to the three capacitive loops spectrum. As a consequence, this three capacitive loops structure has been the focus of the mechanistic study. The mechanistic study is detailed in annex 2.2-1 in the form of an article to be submitted in “journal of the electrochemical society”.

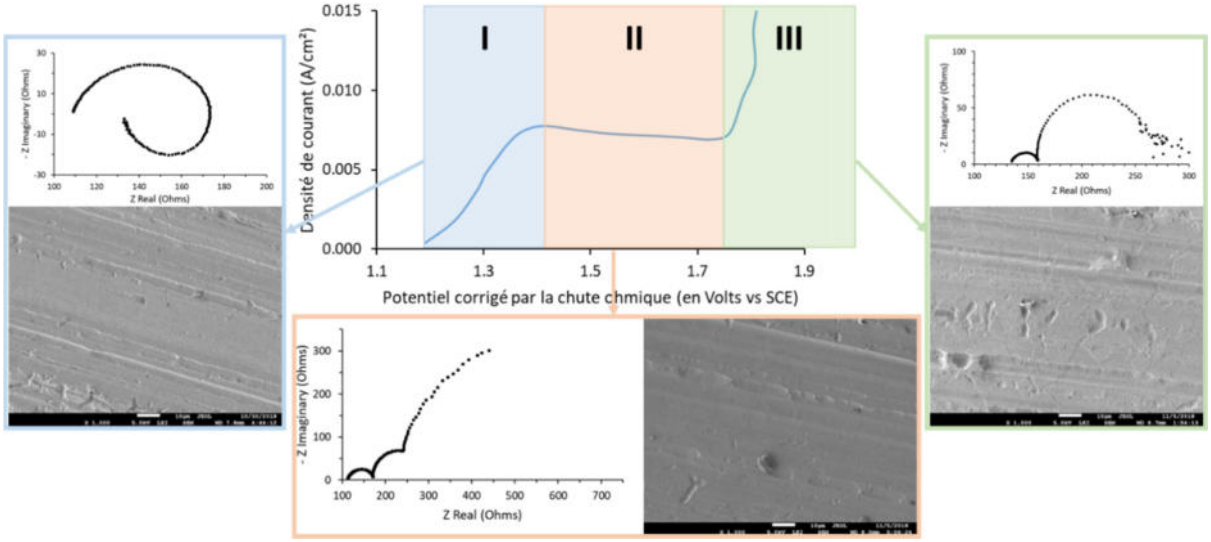

Figure 43: Intensity-potential curve for AISI 430 in acid electrolyte. The various typical impedance spectra and the surface state corresponding to electropolishing at the corresponding potentials are also disclosed

Briefly, the mechanistic study demonstrates that:

- The mechanism is characterized by a step of diffusion through a thin layer;
- At potentials corresponding to the electropolishing plateau, the limiting step is not the charge transfer but the diffusion of a chemical species through the thin layer. This corresponds to the principle of electropolishing where the reaction is not limited by charge transfer but rather by matter transfer;
- The thin layer consists of a porous salt film made of oxidation products;
- The thickness of the thin layer is a function of the applied potential but also of the water and ions content in the electrolyte. **Therefore, the electropolishing bath evolve during electropolishing but this evolution can be monitored**;
- The nature of the diffusing species may be dichromate formed at the electrode and diffusing towards the solution or the water needed for the chromium reaction (Eq. 1) and diffusing from the electrolyte towards the surface;
- The mechanistic study cannot clear cut between the two possible diffusing species. However, the water diffusion may explain more easily some experimental details.

$$[1] \quad 2\,Cr + 7\,H_2O \rightarrow Cr_2O_7^{2-} + 14\,H^+ + 12\,e^-$$

Briefly, we proved that for AISI 430 in acid electrolyte, the impedance spectroscopy is a powerful *in situ* investigation technique. EIS allows determining *in-situ* if the applied conditions will produce a good electropolishing. Moreover, EIS allows the monitoring of the bath aging. We also demonstrate that by the control of the amount of water it is possible, to some extent, to regenerate a used polishing bath.

EIS has also been applied to the case of AISI 304 and 316 in the same acid electrolyte. All the observations made for AISI 430 are applicable for both AISI 304 and 316. Still, there is an important difference. Figure 44 illustrates the intensity/potential curve for AISI 304 and the zones corresponding to the various kinds of impedance spectra. **AISI 304 and 316 are characterized by the presence of an EIS signal that is not observed for AISI 430**. This signal can be described as two capacitive loops, the low frequency one being related to a negative resistance.

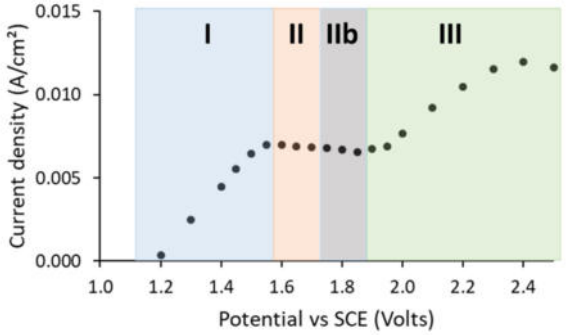

Figure 44: Intensity/potential curve for AISI 304 in acid electrolyte and the potential range where the various type of impedance spectra are encountered

We hypothesize that this ne signal is related to the presence of high amount of nickel in those alloys. This point is supported by the fact that pure nickel shows the same impedance signal for the same applied potentials. It is worth noting that in the potential range where signal IIb is observed, the surface state obtained after electropolishing is extremely bad. The impedance behavior of AISI 304 and AISI 316 stainless steels in acid electrolytes are not reported in the literature. The results obtained in this project have been published (**Annex 2.2-2**).

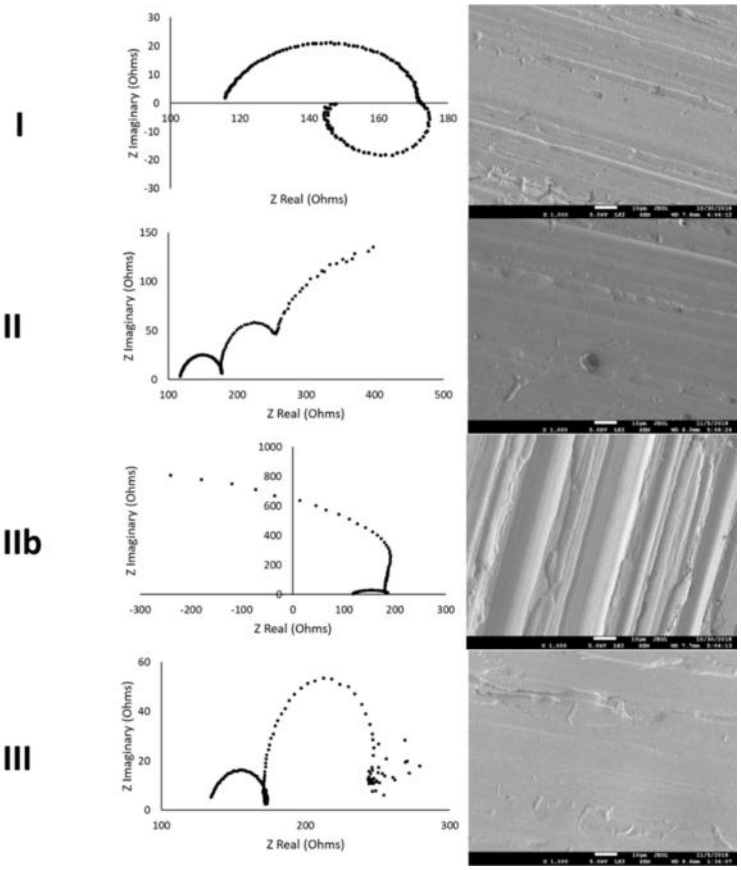

Figure 45: The different kind of impednce spectra corresponding to the potentials range defined in figure 2 and the surface state obtained by electropolishing at those potentials

1. C. Rotty, *PhD thesis*, 1–271 (2018).

2. M. Matlosz, S. Magaino, and D. Landolt, *J. Electrochem. Soc.*, **141**, 410–418 (1994).

3. S. Magaino, M. Matlosz, and D. Landolt, *J. Electrochem. Soc.*, **140**, 1365–1373 (1993).

4. M. Matlosz, *Electrochim. Acta*, **40**, 393–401 (1995).

Task 2.3: Investigation of electropolishing mechanisms in IL-based baths

This work has been carried out the basis of the multi-technique approach described in task 1.5.

In the frame of AdEPT project, the electropolishing in DES media has been studied. This approach is the subject of a master thesis at UNamur.

DESs are solvents formed by the mixture of two (or more) compounds in proportions characterized by a strong eutectic. This eutectic has for consequence a strong diminution of the fusion temperature. By using this technic, it is possible to obtain a liquid from the mixture of two solid compounds. DESs being made by at least one ionic compound (usually a metal chloride or choline chloride) have physico-chemical properties close to the ones of ionic liquids. The major advantages of DES are their low cast and, for many of them, their eco-friendly aspect.

The choline chloride/urea DES presents an impedance signal characteristic of a compact salt film mechanism. According to this mechanism the electropolishing occurs when the limiting step in the reaction is the solubilization of the metallic cations produced by the oxidation of the surface. The consequence of this limitation step is an accumulation of a cations film at the surface. Anions, coming from the solution, ensure the electroneutrality and produce a salt film at the metal surface.

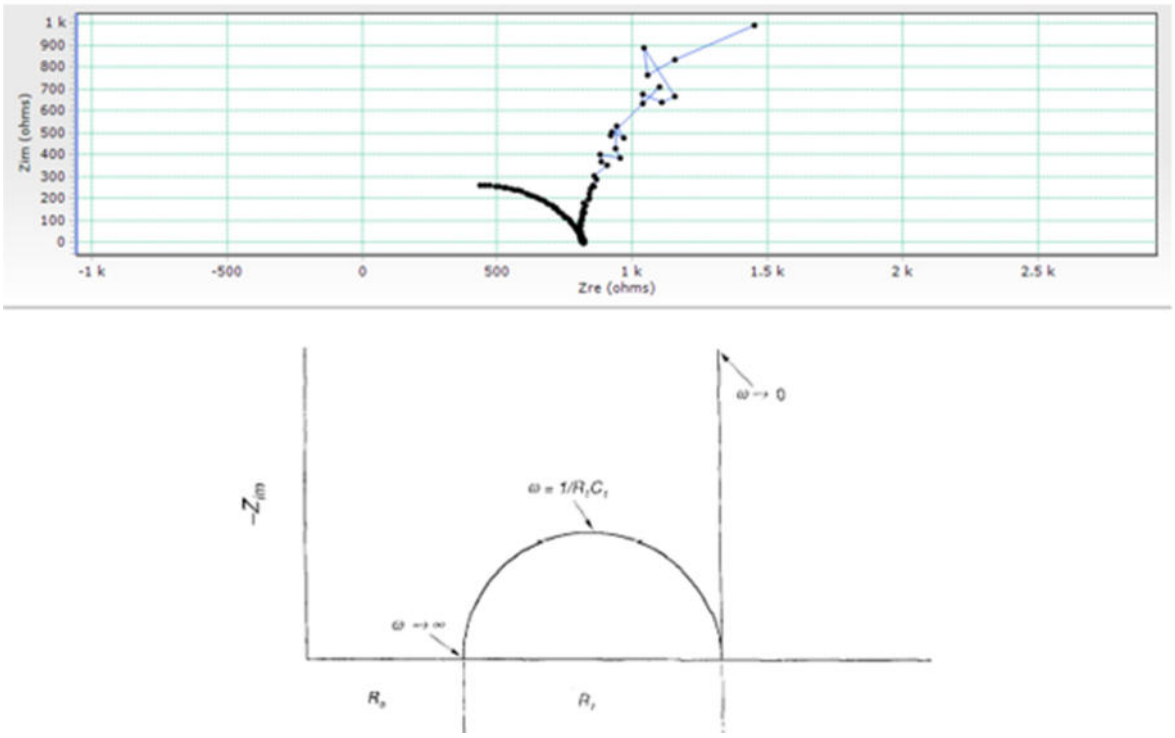

Figure 46: Impedance signal obtained for 316 stainless steel in the choline chloride/urea bath (top) and the theoretical impedance signal for a salt film mechanism (bottom)

In this DES, some tests have been done with the addition of sulfuric acid. This additive leads to changes in the impedance signal (A new polishing plateau and a change in the salt film conductivity and/or thickness).

The same procedure has been used for the choline chloride/ethylene glycol DES. The impedance signals point to a more complicated mechanism, probably of the salt film type, but with an additional step which could be a chemical reaction prior to the dissolution. More investigations are needed in order to understand the mechanism for this DES.

Some studies have already been published about the electropolishing of steels in DES electrolyte. A few by Abbott et al.[1–3], the pioneering research group for DES, then by other researcher such as Rotty[4,5], Dsouza[6], Alrbaey[7] and Loftis[8].[1] This is a very recent research

[1] 1. A. P. Abbott, G. Capper, K. J. McKenzie, A. Glidle, and K. S. Ryder, *Phys. Chem. Chem. Phys.*, **8**, 4214 (2006).
2. A. P. Abbott, G. Capper, D. L. Davies, K. J. McKenzie, and S. U. Obi, *J. Chem. Eng. Data*, **51**, 1280–1282 (2006).
3. A. P. Abbott, G. Frisch, J. Hartley, W. O. Karim, and K. S. Ryder, *Prog. Nat. Sci. Mater. Int.*, **25**, 595–602 (2015) http://dx.doi.org/10.1016/j.pnsc.2015.11.005.
4. C. Rotty et al., *Surfaces and Interfaces*, **6**, 170–176 (2017).
5. C. Rotty, *PhD thesis*, 1–271 (2018).
6. N. Dsouza et al., *MATEC Web Conf.*, **14**, 13007 (2014) http://www.matec-conferences.org/10.1051/matecconf/20141413007.
7. K. Alrbaey, D. I. Wimpenny, A. A. Al-Barzinjy, and A. Moroz, *J. Mater. Eng. Perform.*, **25**, 2836–2846 (2016).
8. J. D. Loftis and T. M. Abdel-Fattah, *Colloids Surfaces A Physicochem. Eng. Asp.*, **511**, 113–119 (2016) http://dx.doi.org/10.1016/j.colsurfa.2016.09.013.

subject. The DES used in these studies are made of choline chloride, in combination with urea or ethylene glycol.

In the frame of a master thesis, the electropolishing of two steels (AISI 316 stainless steel and 1.2343 tool steel) has been studied in two different DES. The electropolishing of tool steel in DES electrolyte has never been disclosed in the literature. The first studied DES is the mixture of choline chloride and urea. It has been used in the literature for the electropolishing of AISI 316 stainless steel. This is not the case of the second studied DES, zinc chloride/ethylene glycol.

Some preliminary tests have been realized on the two steels. We can observe that:

- Some combinations DES/Steel/Temperature/Applied potential allow to obtain a strong decrease of roughness;
- However, the shiny surface characteristic of stainless steel electropolishing in acid mixture cannot be reproduced in DES electrolyte;
- The two investigated DES produce interesting results. The best results are obtained with choline chloride/urea for AISI 316 and with zinc chloride/ethylene glycol for tool steel;
- Depending on the applied potential and temperature, the oxide layer structure is highly variable on AISI 316. Some conditions produces a nickel oxide or a molybdenum oxide rich surface;
- For all the samples, two to three morphologically different zones have been observed after the electropolishing (Figure 47). Those morphological differences are a consequence of a flow effect. The flow is known in the literature to be able to deform the viscous layer[9] and this viscous layer is a key player in the electropolishing process[10–12].[2] Because of this observation, it has been decided to use an experimental setup allowing the control of the flow.

Figure 47: AISI 316 sample electropolished in DES and showing two different zone due to flow effect

The structure of the cell allowing a control of the flow is represented in Figure 48. This cell certifies a constant 10 mm distance between the sample and the counter-electrode. The use of a peristaltic pump allows a flow rate control. The cell geometry has been chosen to correspond to the one used in the publication of Lee and al.[9]

[2] 9. S.-J. Lee, J.-J. Lai, and Y.-T. Lin, *WIT Trans. Eng. Sci.*, **48**, 203–213 (2005) https://www.witpress.com/elibrary/wit-transactions-on-engineering-sciences/48/14762.
10. R. Kirchheim, *J. Electrochem. Soc.*, **128**, 1027 (2006).
11. K. TAJIMA et al., *Dent. Mater. J.*, **27**, 258–265 (2008).
12. J. B. Mathieu, *J. Electrochem. Soc.*, **125**, 1044 (2006).

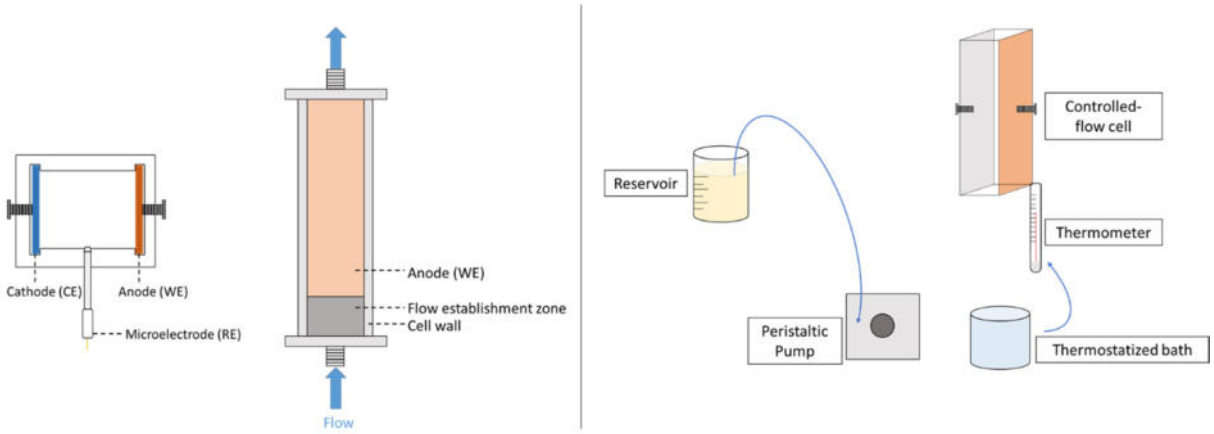

Figure 48: the controlled-flow cell and the complete system allowing the flow and temperature control

During the first tests on the flow-controlled cell with AISI 316 stainless steel and a choline chloride/urea electrolyte, it appears that the amount of water in the electrolyte drastically affects the electropolishing plateau current (Figure 49). It is worth noting that the link between the amount of water and the electropolishing plateau current is coherent with the hypothesis about the role of water described in task 2.2. The electropolishing mechanism of stainless steel in DES need the presence of water and is probably similar to the mechanism taking place in acid electrolytes. Moreover, the amount of water needed to obtain a high electropolishing plateau current is close to the amount of water in the acid electrolyte described in task 2.2.

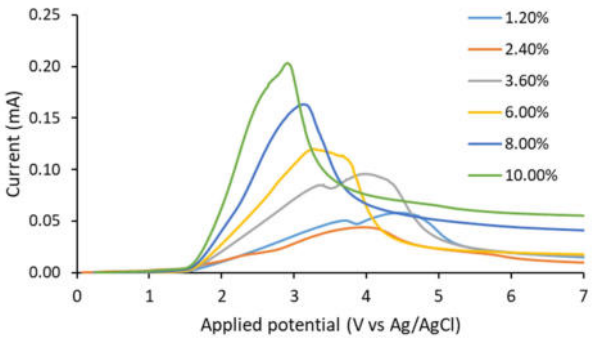

Figure 49: Evolution of the I/V curve as a function of the amount of water added in the DES

The effect of flow rate has been studied with a controlled amount of water. It appears that a too high flow rate cause the deformation of the viscous layer bringing the formation of two morphologically different zone on the electrode. The “flame” of the low part zone (which is a consequence of the flow) increases in size when the flow increases (Figure 50). Tests realized using various flow-rates confirms that a low but non-null flow rate is needed to obtain the lowest Ra and the more homogenous samples (Figure 51).

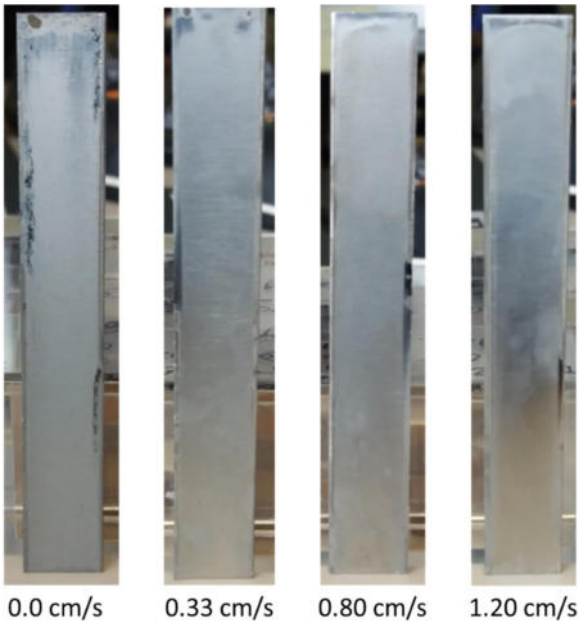

Figure 50: Evolution of the sample morphology for different flow rate, 25 °C, Charge = 200 C, 5 V

With a constant flow and a constant amount of water, various electropolishing tests of AISI 316 in the DES choline chloride/urea have been realized. The evolution of roughness as a function of the applied potential and temperature is summarized in Figure 51. Those results demonstrate that it is possible to strongly reduce the roughness on AISI 316 in this DES provided that the good parameters are chosen.

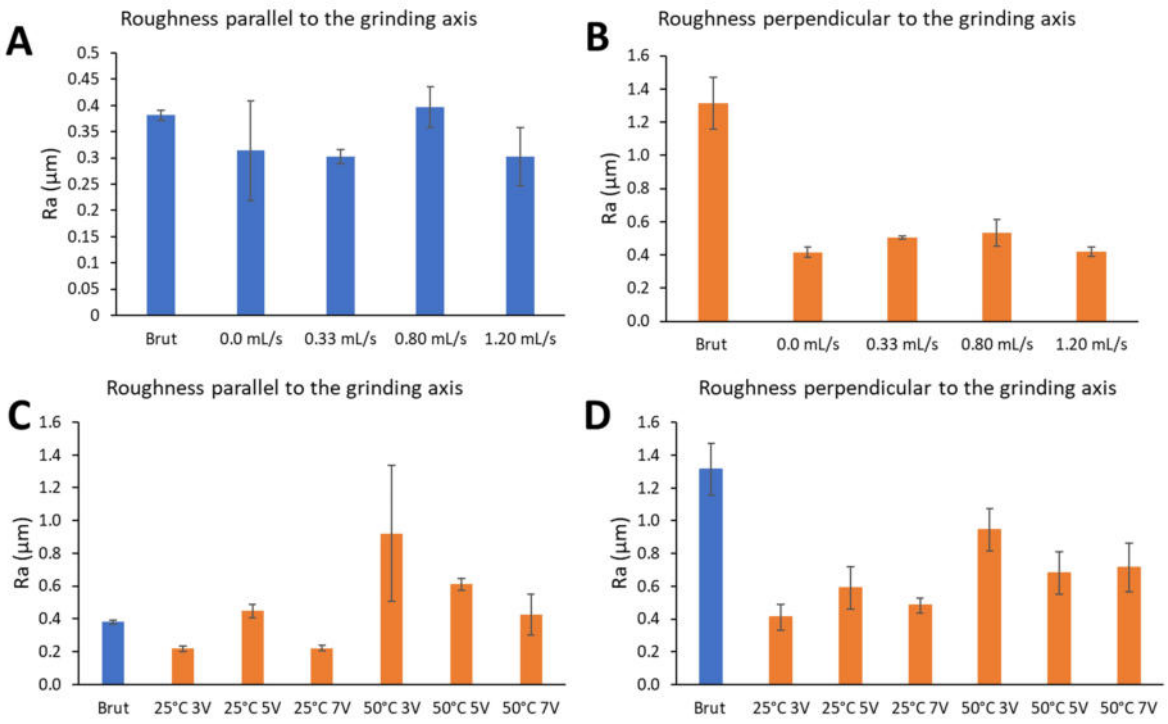

Figure 51: Evolution of the roughness measured parallel and perpendicular to the grinding axis for (A and B) various flow rate (same conditions than figure 4) and (C and D) for various applied potential and temperature (Q = 200 Coulombs)

Task 2.4: Implementation of advanced electropolishing baths: impact on process parameters and electropolishing performances

Electrochemical impedance spectroscopy has been used as investigating tool to characterize the effects of additives in acid electrolytes.

In the following chapter, we will focus on the effects of additives on R1. This parameter corresponds to the diameter of the high frequency capacitive loop in the EIS spectra. R1 is related to the charge transfer resistance (the easiness with which the oxidation reaction will happen) and to the blocking level of the electrode by an adsorbate species. R1 is directly related to the current density at steady state. For a given applied potential, the higher is R1, the lower is the current density and the rate of the oxidation reaction (thus the electropolishing speed).

a) Effect of the addition of an ions mixture

The graph in Figure 52 shows the evolution of R1 as a function of the amount of ions in the electrolyte. To load the electrolyte with ions, a sample of AISI 316 stainless steel has been polarized inside. This polarization allows the solubilization of solution in the form of Fe (III), Cr (VI), Ni (II) and probably Mo (VI). Because of the used experimental setup, the addition of ions goes hand with hand with the removal of water. Therefore, in Figure 52, the higher is the ions concentration; the lower is the water concentration in the electrolyte.

The addition of ions and the loss of water correspond to the situation encountered in the case of an industrial electropolishing of a big amount of steels samples in the same electrolyte.

We can see that the higher the ions concentration is (and the lower the water concentration is), the higher R1 is. **The electropolishing became increasingly difficult when the electropolishing bath aged.**

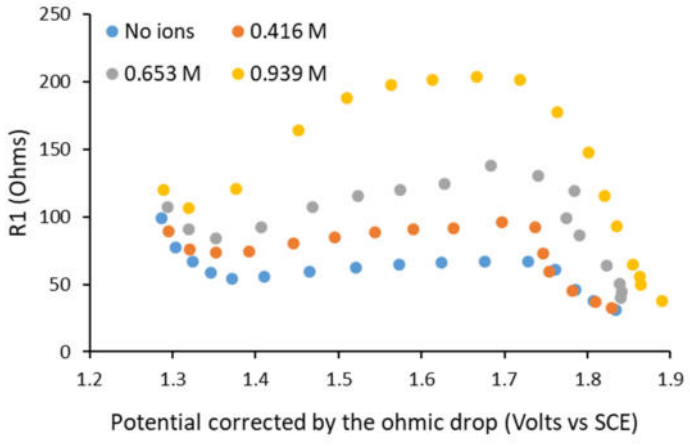

Figure 52: Evolution of R1 as a function of the applied potential and of the ions concentration in the electropolishing bath

b) Effect of the addition of Fe^{3+} ions

The addition of Fe^{3+} ions in the bath has been realized by polarizing a pure Fe surface in the electrolyte. The polarization has the side effect to remove water from the electrolyte. Figure 53 shows the evolution of R1 as a function of the applied potential and of the amount of Fe^{3+}

ions in the electrolyte. We can draw the same conclusion than for Figure 52; the aging of the bath by the addition of Fe^{3+} ions (and the removal of water) make the electropolishing increasingly difficult.

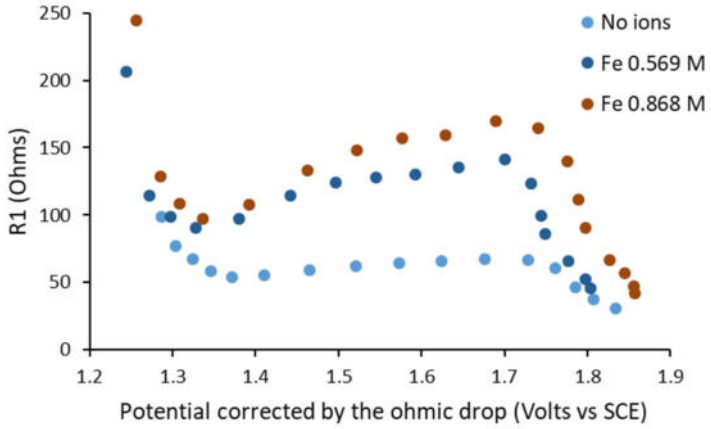

Figure 53: Evolution of R1 as a function of the applied potential and of the amount of Fe3+ ions in the electropolishing bath

c) Effect of the addition of water

The loading of the electrolyte with ions by polarization of a stainless steel or iron surface has also for consequence its depletion in water. This effect is similar to the aging of industrial electrolyte during intensive use.

Figure 54 shows the evolution of R1 as a function of the applied potential and the amount of ions and water. After loading of the electropolishing bath with ions (and depletion in water, orange dots), an addition of water has been realized in order to compensate the previous loss (grey dots).

We can observe that the control of the amount of water allows to, at least partially, regenerate the bath efficiency.

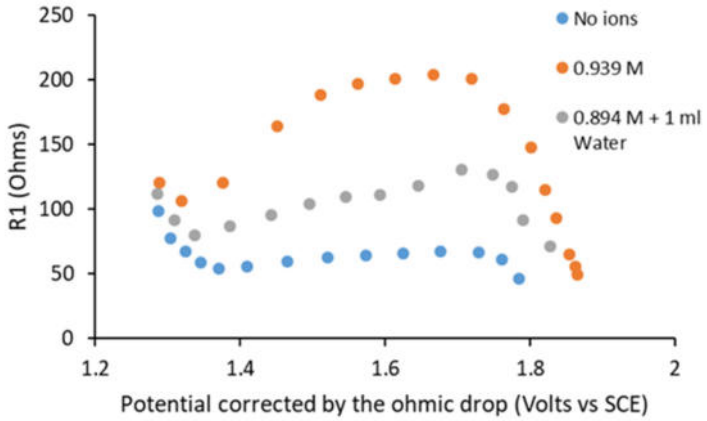

Figure 54: Evolution of R1 as a function of the applied potential, the amount of ions and amount of water

d) Effect of chromium addition

In the frame of the study of the additives, an addition of chromium ions has been realized. The electrolyte has been loaded with ions by polarization of a pure chromium surface. In the applied conditions, the metallic chromium probably oxidized on the form of a mixture of Cr(III) and Cr(VI). Moreover, based on the mass loss of the chromium sample and the amount of electric charge exchanged, it appears that almost no solvent has been oxidized during the polarization. As a consequence, the solution is loaded with Cr(III) and Cr(VI) ions without change in the water content.

In Figure 55, we observe a decrease of R1 after the loading of the electrolyte with chromium ions. Therefore, the electropolishing reaction is easier after the loading of the electrolyte. **Chromium ions seems to act as a catalyst in the reaction.** The addition of water still decrease R1, as previously observed in Figure 54.

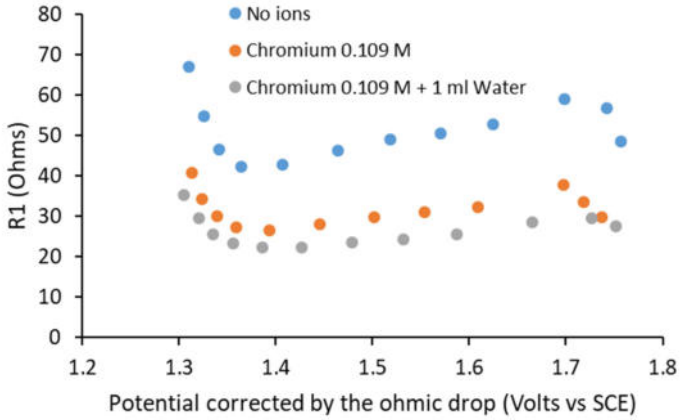

Figure 55: Evolution of R1 as a function of the applied potential and of the amount of chromium ions before and after the addition of water

e) Case of a commercial electrolyte

A commercial acid electrolyte, provided by « Chimiderouil » has been investigated. During the polarization of a sample of AISI 430 stainless steel in this electrolyte, a strong increase of the value of R1 is observed. This is correlated to a strong decrease of the current density. This behavior quickly disappears after aging of the electropolishing bath (Figure 56). As soon as a small amount of ions has been dissolved (amount corresponding to the electropolishing of one to one or two samples), R1 decrease to values similar to those observed in the phosphoric/sulphuric acid electrolyte (71 wt. % H_3PO_4/16 wt. % H_2SO_4 and 13 wt. % H_2O).

It seems that the new « Chimiderouil » electrolyte contains some additives and that this additive hinders the reaction. Moreover, this additive seems to disappear quickly during the aging of the bath. This disappearance may be explained by the complexation of ions by the additives or by its oxidation at the electrode.

Figure 57 shows that this behavior is also observed during the electropolishing of AISI 304 stainless steel in the same electrolyte.

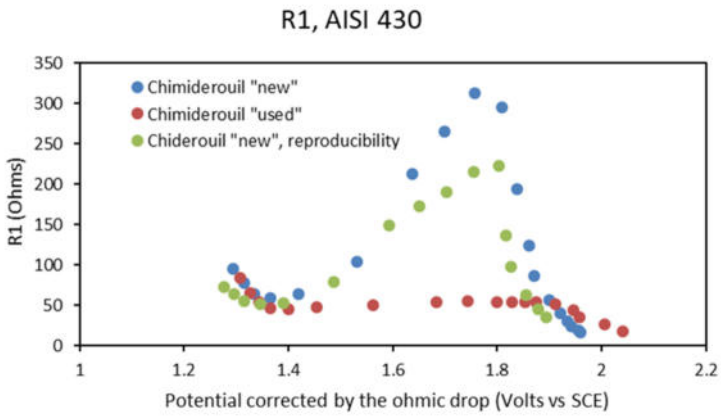

Figure 56: Evolution of R1 in the « Chimiderouil » electrolyte as a function of the applied potential. Case of the electropolishing of AISI 430

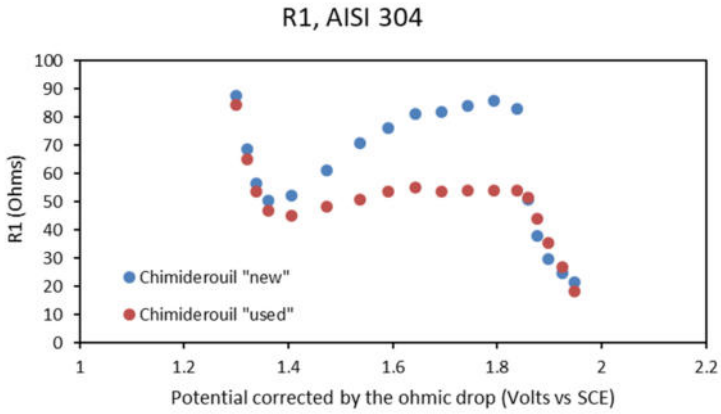

Figure 57: Evolution of R1 in the « Chimiderouil » electrolyte as a function of the applied potential. Case of the electropolishing of AISI 304

ENAS:

As advanced electropolishing bath a deep eutectic solvent (DES: urea-choline chloride) and the ionic liquid, which was also used for the Al depositions, were characterized. Unfortunately, the linear scan voltammetry showed no typical EP behavior for both liquids. In the DES the Al was dissolved and the liquid became milky, when applying the potential. The ionic liquid showed only the straight slope while increasing the potential during the LSV. Hence, the focus for the Al-EP process was set to the optimization of the EP parameters with the solution from Electronic Thingks. This was working for Al and is quite cheap.

CRM:

ECM - type baths

ECM-type baths have been investigated. Electrochemical machining (ECM) is based on the removal of metallic matter by an electrochemical process. ECM is normally used to give the desired geometry to a metallic piece, generally extremely hard or difficult to machine conventionally. The cathode shaped like the contour of the workpiece is advanced to the latter separated by a small gap (100 - 1000 µm) to give the desired shape of the workpiece by its dissolution.

In order for the current to flow between the electrodes, the bath must be highly conductive; this is why concentrated aqueous salts are generally used. Two kinds of electrolytes are to be differentiated: the passivating electrolytes such as $NaNO_3$ and the non-passivating electrolytes such as NaCl (corrosive effect of Cl^- ions).

The electropolishing of 1.2343 tool steel in NaCl is a quick process to decrease the roughness by a factor of 2 in very short times (1 - 2 min), giving the sample a homogeneous dull aspect. Neither the surface condition nor the roughness seems to be much influenced by the average current density or the process time longer than 2 min.

Since electropolishing in ECM-type electrolyte led to good results in terms of roughness diminution but to a poor surface finish, a second step following the EP in NaCl was considered. The test consisted of a first electropolishing step in NaCl during 2 min to rapidly decrease the average roughness; followed by a longer EP in Poligrat E520 (5 - 10 min) to further reduce the roughness and give better surface conditions (Figure 58).

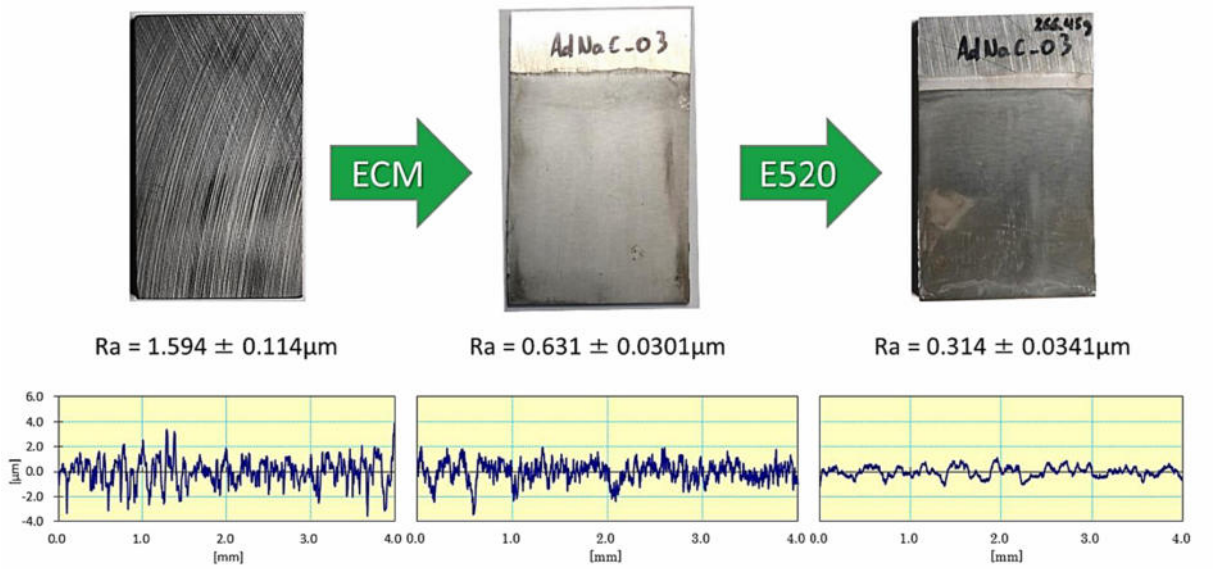

Figure 58: Illustration of the electropolishing process in two steps by using first NaCl followed by a conventional step using Poligrat E520

By this process, it is possible to decrease the sample's roughness by a factor of 3. Further studies will be performed in larger electrolyte volumes in the future in order to use higher current densities and minimize the heating of the bath.

Acid bath + additives

Based on various sources in the electropolishing field, the electropolishing of tool steels in acid-based bath containing additives was considered. Seven baths have been compared, including the commercial Poligrat bath (methane sulfonic acid-based) and the acid-based bath (H_3PO_4 - H_2SO_4 - H_2O). The latter served as the basis for the preparation of additives-containing baths:

- Citric acid 30 g/L;
- Ascorbic acid 30 g/L;

- Dextrose 58 g/L;
- Glycerol 7 vol. %;
- Lactic acid (aq.) 46.5 vol. %.

Tests were performed with the Hull cell configuration (Figure 59 and Figure 60) on three tool steel grades (1.2343, 1.2311 and 1.2379) for each bath.

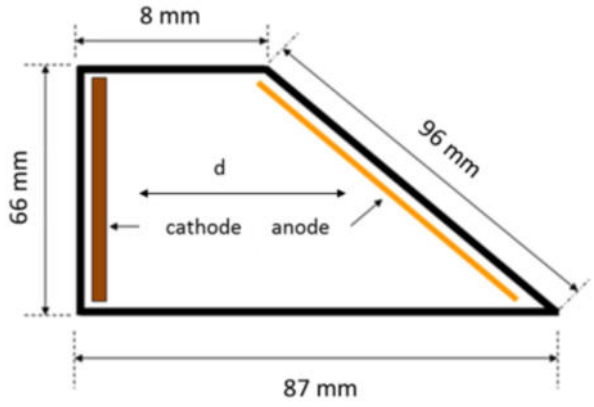

Figure 59: Top view of a schematic representation of a Hull cell configuration

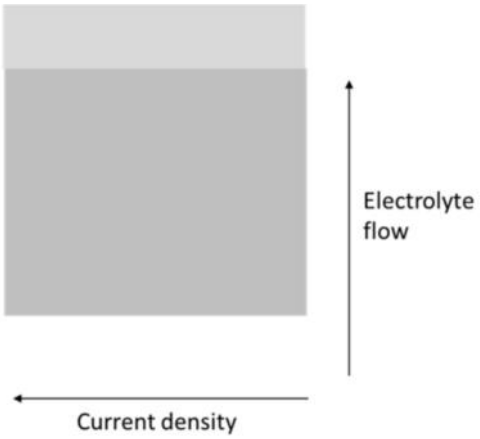

Figure 60: Front view of a schematic representation of a sample in the Hull cell configuration

Owing to the similar conductivity and temperature working range, the Hull tests were carried out with the same control parameters for most of the baths, the initial applied current density, temperature and time of treatment had to be tuned for the lactic acid-containing bath and Poligrat for the results to be comparable with each other.

The resulting samples presented a well-polished zone in the high current densities region (left) of variable widths depending on the bath. The highest and lowest current density of the polished region (calculated from the distances on the anode) were plotted into a graph as displayed in Figure 61 for each bath and each tool grade.

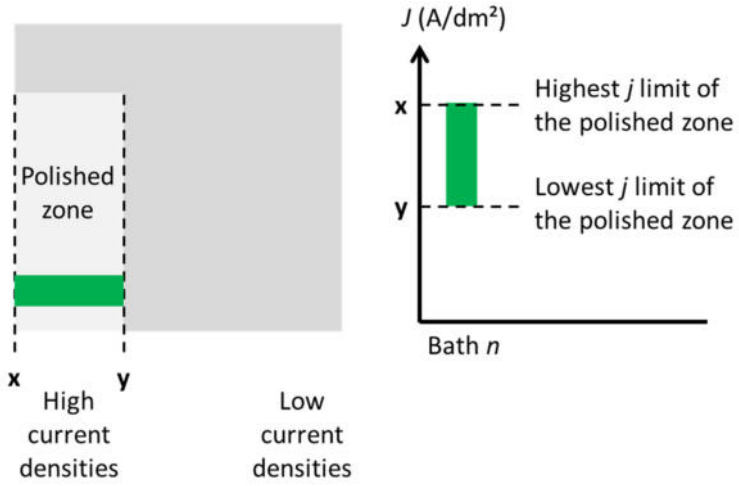

Figure 61: Methodology adopted to compare the different baths based on the polished region

Figure 62 displays the methodology applied to 1.2343 tool steel. Based on the roughness measurements performed on the polished zones and the visual look of the sample after the tests for each grade and each bath, the most promising bath which could compete with Poligrat for the three grades was the acid-based with citric acid as an additive. Therefore, this electrolyte had been chosen for further investigations.

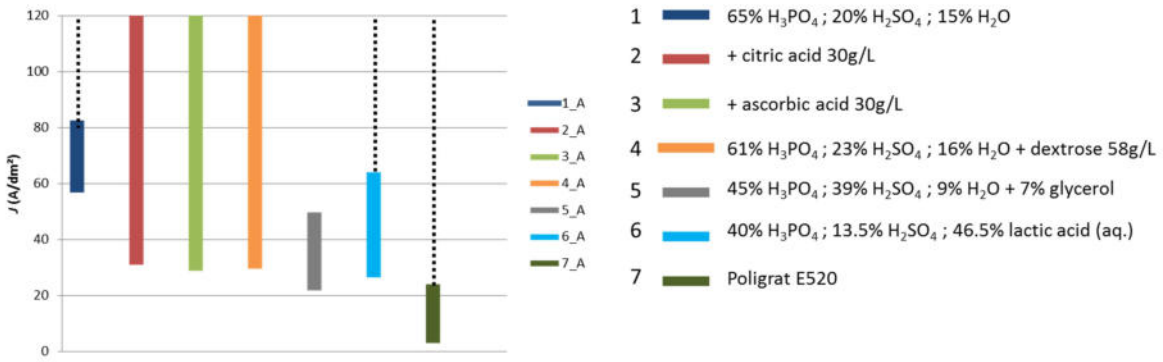

Figure 62: Highest and lowest current densities of the polished zone of 1.2343 tool steel in the different baths and the corresponding color legend

A new series of tests were performed on 1.2343 steel with an initial Ra of about 0.45 µm. In order to compare the performances of the two electrolytes, similar electropolishing trials were made. Due to a limited number of available samples, the only changing parameters were the current density and the type of electric current (direct, pulsed or reverse pulsed). Figure 63 displays the average roughness of the best conditions tested during these trials.

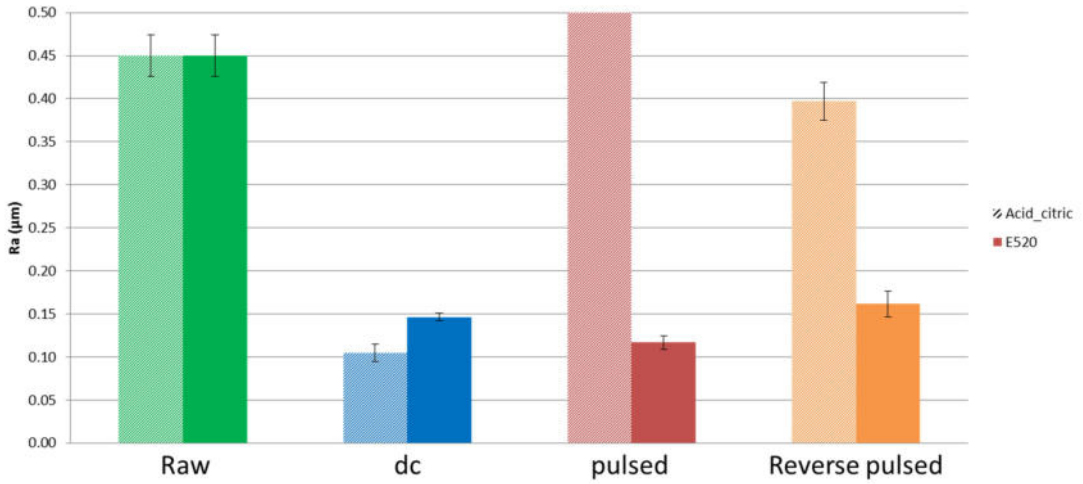

Figure 63: Average roughness of 1.2343 tool steel in acid-based bath (striped) and Poligrat E520 (plain) before (green) and after electropolishing using direct (blue), pulsed (red) and reverse pulsed (orange) currents

While the Poligrat allowed the decrease of Ra by one third of the initial one in the three electric configurations, it is clear that the tested pulsed and reverse pulsed parameters in the acid-based bath barely improved or in some cases even worsened the surface condition after electropolishing. To this day, the reason behind such different behaviors is still not understood and to our knowledge, is not reported in the literature for the electropolishing of this tool grade in this bath. One possible explanation could lie in a difference in mechanisms. Indeed, one electrolyte is composed of mineral aqueous acids while the other is composed of organic acids free of water, a limiting step could be negatively affected by the pulsed currents, which would lead to a poor electropolishing. Nonetheless, it should be noted that the reverse pulsed currents tested do not lead to better surface condition than pulsed or DC currents as it was previously observed when the initial Ra was higher.

The evolution of the average roughness with the charge transported during the electropolishing (directly related to the time of electropolishing) of 1.2343 steel in acid + citric and Poligrat bath is represented in Figure 64. By comparing these two graphs, it can be observed that the decrease of Ra is similar in both baths when DC is used, that is to say a significant decrease during the first half of the electropolishing followed by a slower yet continuous decrease in the last part. The reason why the charge/dm^2 is lower in the case of Poligrat is because this electrolyte is much more resistive (less conductive) than the other one, which means that the flow of current in the cell is much lower in Poligrat than in acid-based for the same voltage. In fact, comparing the two electrolytes in terms of Ra loss *vs.* energy (i × V), the two baths behave also similarly (Figure 65).

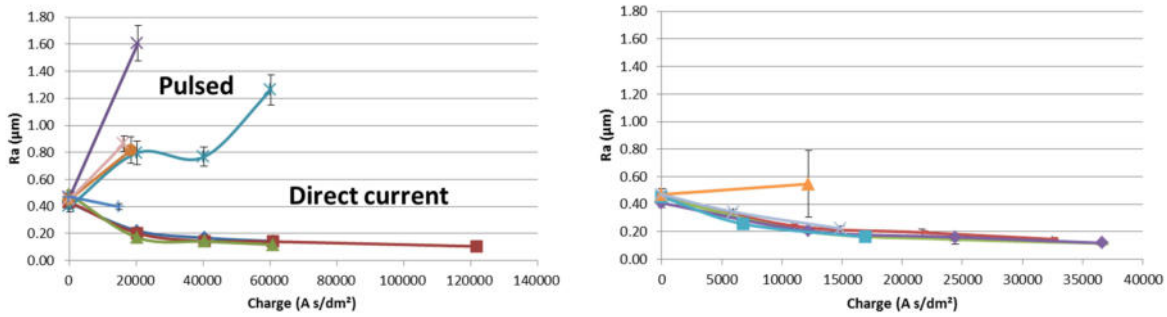

Figure 64: Evolution of Ra with the charge/dm^2 of 1.2343 steel in acid + citric (left) and Poligrat (right) for different applied current densities

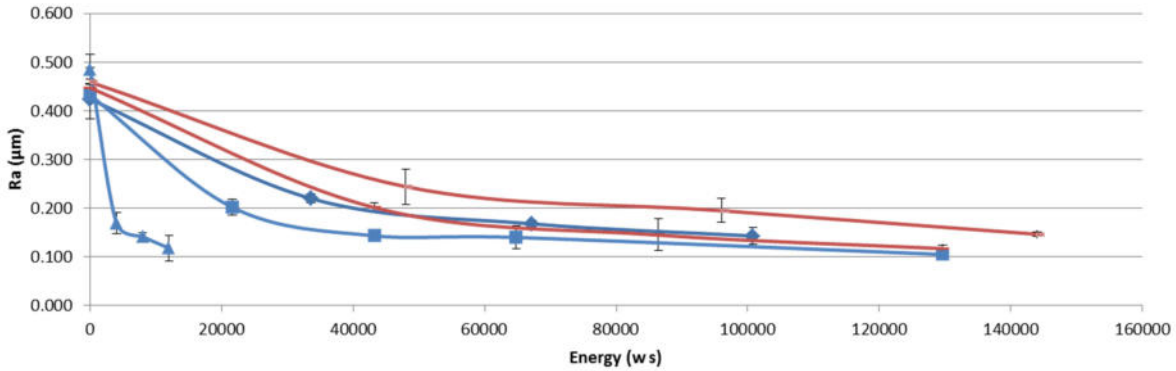

Figure 65: Evolution of Ra with the energy required for the electropolishing of 1.2343 in acid + citric (blue) and Poligrat (red) for different applied current densities

The last criterion used to differentiate the performances of the two electrolytes was the surface aspect. In the case of the acid bath, the surface after electropolishing was matte/dull with a milky appearance while in the case of Poligrat, the sample came out bright and shiny. Gloss[3] measurements were performed after the treatment, the graph is shown in Figure 66. It can be seen that for all the samples, the gloss increased when electropolishing with Poligrat while it decreased with the other bath, thus giving the dull appearance. In order to understand the difference at the macroscopic level (as seen with the naked eye), observations at the microscopic level (by secondary electron microscopy - SEM) were performed (Figure 67). The two samples had almost identical Ras (0.143 ± 0.018 and 0.146 ± 0.004 µm) and only differed from the aspects and gloss values. By looking at the microscopic pictures, one can see the striking difference that is the pitting of the sample is

[3] indicates how well a surface reflects the incident light in a specular (mirror-like) direction, the higher the gloss, the higher the perceived brightness and brilliance.

much more significant in Figure 67a than Figure 67b. This causes the light to be more diffused rather than reflected thus decreasing the gloss value.

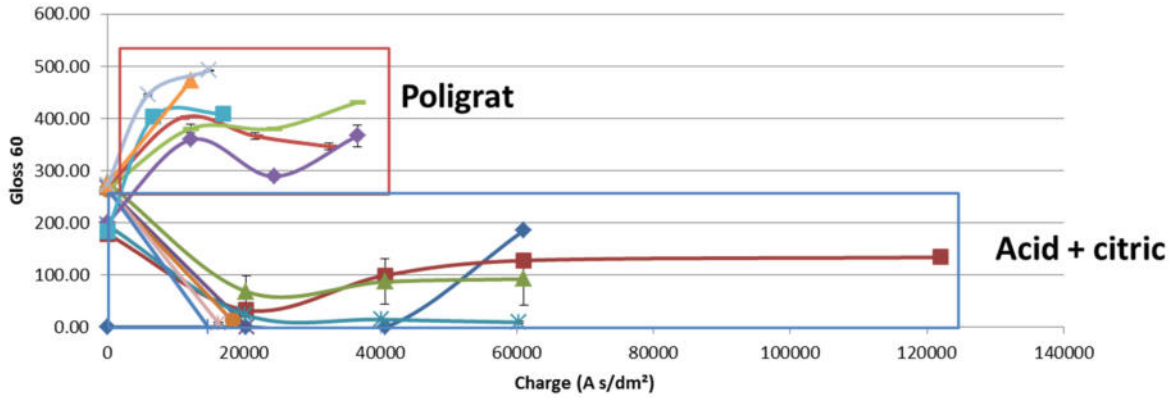

Figure 66: Gloss evolution with the charge of 1.2343 steel in acid + citric (blue) and Poligrat (red) for different applied current densities

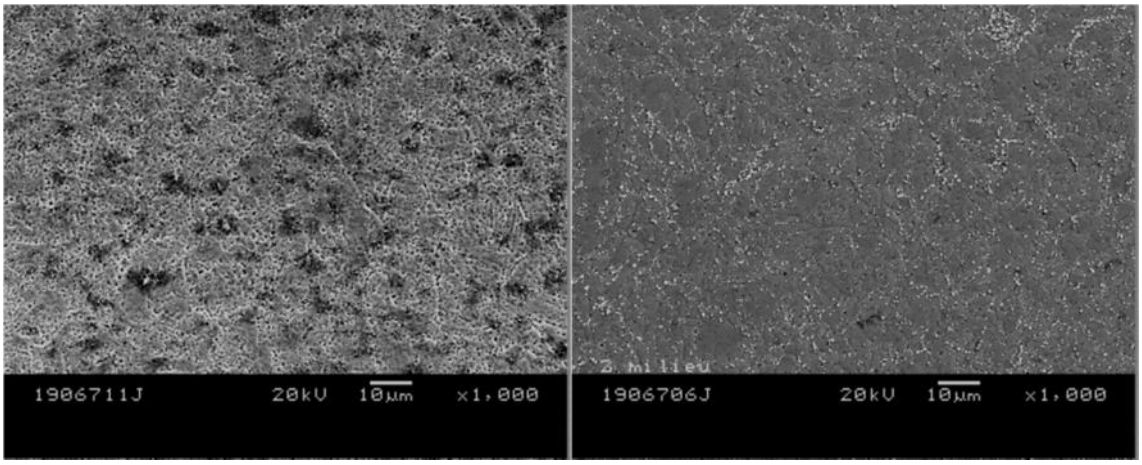

Figure 67: SEM pictures of 1.2343 tool steel electropolished in acid-citric (a) and Poligrat (b). The two samples have identical Ras

On the basis of these observations, the commercial Poligrat bath had been chosen for the treatment of the 3D demonstrator parts, because although the easier-to-operate acid-based bath can give identical Ra loss to those obtained with Poligrat, the surface condition after the treatment is critical for the intended use.

3. Work package 3: Investigation of advanced electrical parameters

Task 3.1: Update of the literature review on advanced electrical parameters

ZFM:

The international literature in the topic of pulse or pulse reverse electro polishing is limited. A review on guiding principles for pulse/pulse reverse EP is given Taylor et al. [1]. The authors describe how the pulses work and which effect the pulse parameters have on different microstructures. A summary of the work is given in a separate document to the partners.

Makarov et al. has written a report about the use of pulse mode for electro polishing of stainless steel AISI-304L in non-chromium electrolytes. The authors used an electrolyte containing sulfuric and phosphoric acid as base. They added three different additives named tartaric acid, urotropine and lactic acid. The temperature was set to 50 to 55 °C. The anode and cathode are from the same stainless steel material. To observe how the pulse mode influences the EP process, the authors used the three electrolyte mixtures and direct current (DC) as well as pulse current (PC) for EP trials. The roughness values over polishing time are recorded with the result that the DC-EP with tartaric acid shows the greatest smoothing effect. However, in corrosion tests the PC-EP samples of all electrolyte mixtures show 2-3 times less pits than DC-EP. As a conclusion, the PC-EP can improve the corrosion resistance of the used stainless steel. Furthermore, the removal rate with PC-EP is 1.5-2 times less than DC-EP [2].

Task 3.2: Electro polishing trials under pulsed currents and voltages + Task 3.3: Characterizations

ZFM:

The ZFM did not perform experiments with pulsed currents and voltages during the EP because the parameter variance would be more challenging than the constant potential approach. The setting up for a basic EP process with the electroplated Al and the comparable thin layers took a long time to achieve sufficient results. Therefore, the parameter scan with pulsed currents could not be managed during the project duration.

CRM:

Two types of advanced current parameters had been studied: simple pulsed currents by applying anodic pulses and reverse pulsed currents by alternating between anodic and cathodic current pulses (Figure 68).

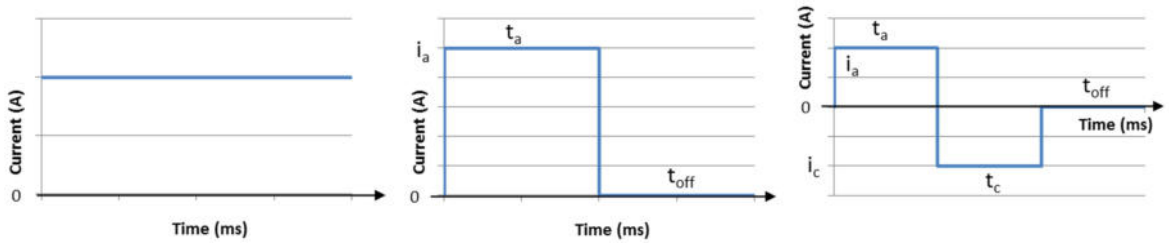

Figure 68: Schematic representations of different electrical parameters: direct (a), pulsed (b) and reverse pulsed (c) current. a = anodic, c = cathodic and toff = resting time (no current)

In addition to the applied current density during the process, the use of pulsed and reverse pulsed currents introduce other parameters to consider for the optimization of the conditions: the intensity of the pulses (ia and ic), the duration of these pulses (ta and tc), as well as the resting time (toff).

Electropolishing of AISI 316 in acidic bath

While electropolishing using direct (DC) current or voltage has been well referenced for many years and used at the industrial scale, few reports talk about EP using pulsed/reverse pulsed

currents. Preliminary trials of EP using pulsed currents were carried out on 316 stainless steel before applying it to tool steels.

Pulsed currents First, simple anodic pulses were investigated. The insertion of off times (toff) between the pulses make it possible to apply pulses of high intensity, while maintaining the average current density relatively low and thus avoid an overheating of the bath.

After a optimizing the different parameters, the most conclusive ones had been selected to study the evolution of the average roughness as a function of the time of EP, the plot of these values is presented in Figure 69. In addition, plots of Ra vs. charge using DC (13 and 22 A/dm²) are also represented for comparisons.

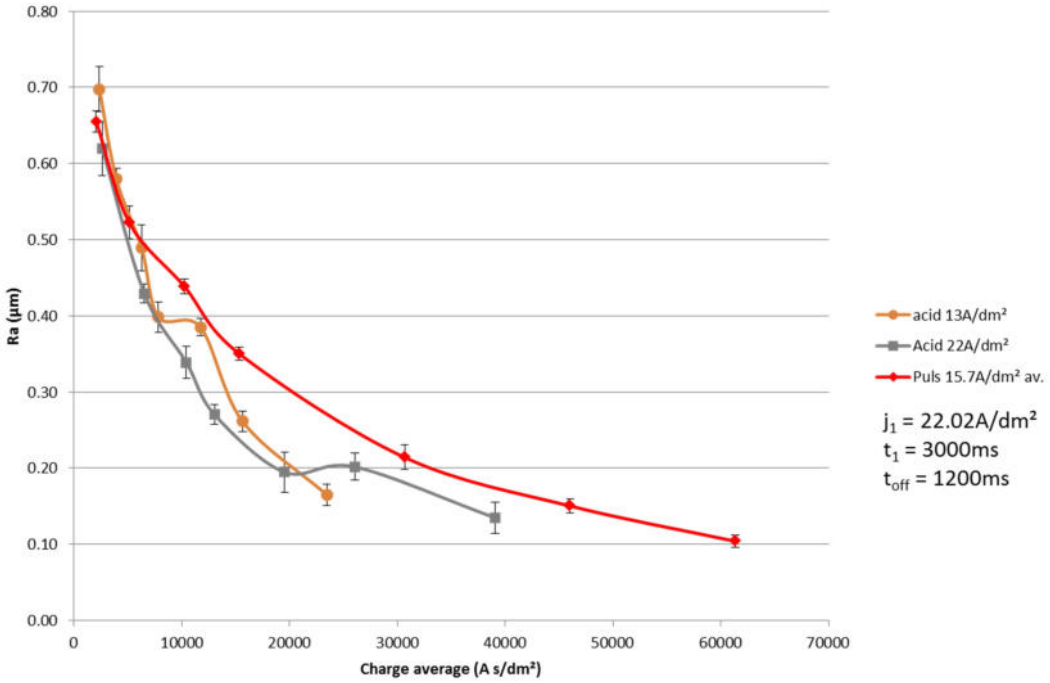

Figure 69: Average roughness vs. time of electropolishing (represented by the total charge) of AISI 316 in acidic bath using pulsed currents

Reverse pulsed currents To complete the advanced electrical parameters study on AISI 316, electropolishing tests were carried out using reverse pulsed currents. The introduction of cathodic pulses between anodic ones would serve to depassivate the sample's surface to remove the surface oxide that forms on passivating samples.

Parameters of reverse pulsed currents were chosen to yield current densities similar to those of pulsed currents and the electropolishings were carried out during 15 minutes. Average roughness values for the best conditions in pulsed currents and for the firsts trials with reverse pulsed currents are presented in Figure 70. According to these first results on AISI 316, it appears that although simple anodic pulses doesn't upgrade the performances of EP, the introduction of cathodic pulses somehow help for the electropolishing of this substrate.

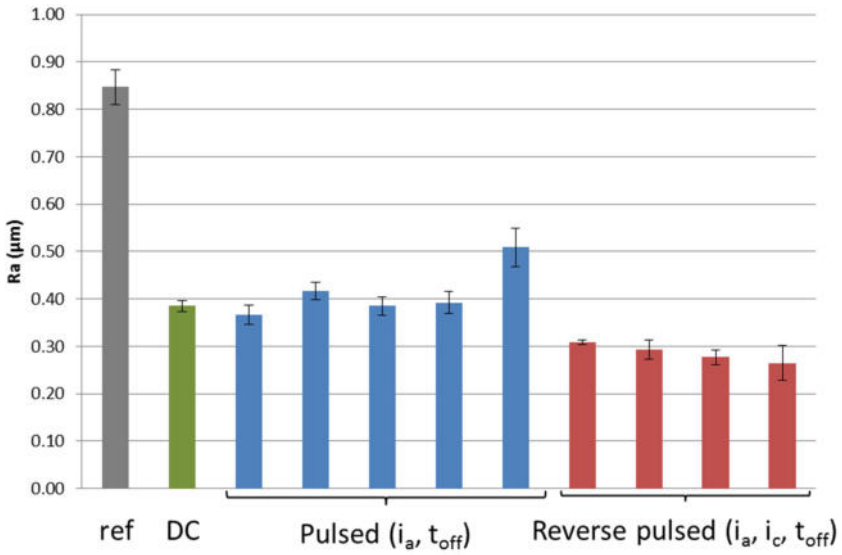

Figure 70: Average roughness of AISI 316 samples electropolished in the acidic bath using either pulsed (blue) or reverse pulsed (red) currents. Tests were performed during 15min, using similar average current densities

Electropolishing of tool steel using pulsed currents

Based on the results above, reverse pulsed currents were chosen for the study of EP of tool steels with advanced electrical parameters. From the preliminary trials, promising results were obtained on both of the tool steel studied, with in the best conditions, a decrease of the roughness by a factor of nearly three.

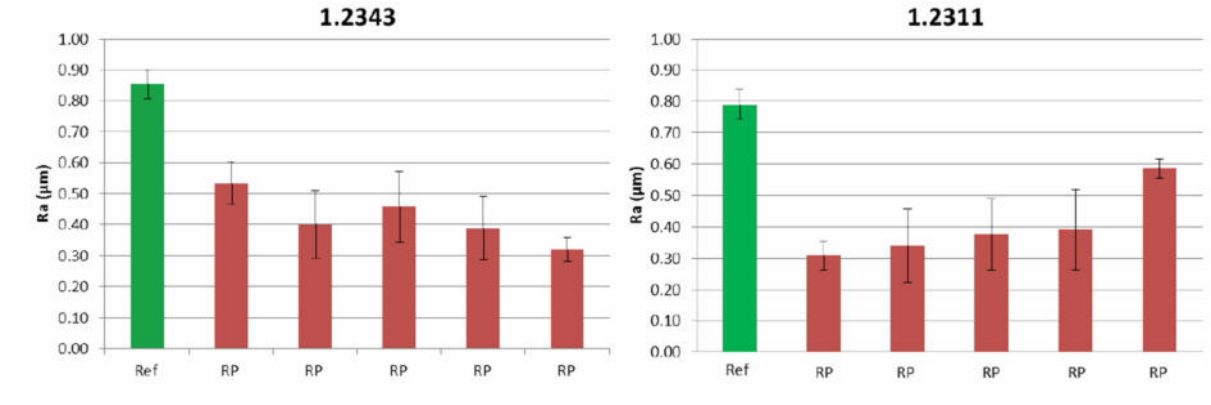

Figure 71: Average roughness of 1.2343 and 1.2311 tool steel electropolished in Poligtat E520 bath using reverse pulsed currents (red) compared to reference samples (green) for the preliminary trials

The surface profiles of the best electropolishing results on 1.2343 and 1.2311 are presented on Figure 72. Both surface profiles are alike and display a decrease of the surface defects, with similar roughness parameters (Ra, Rz, Rt).

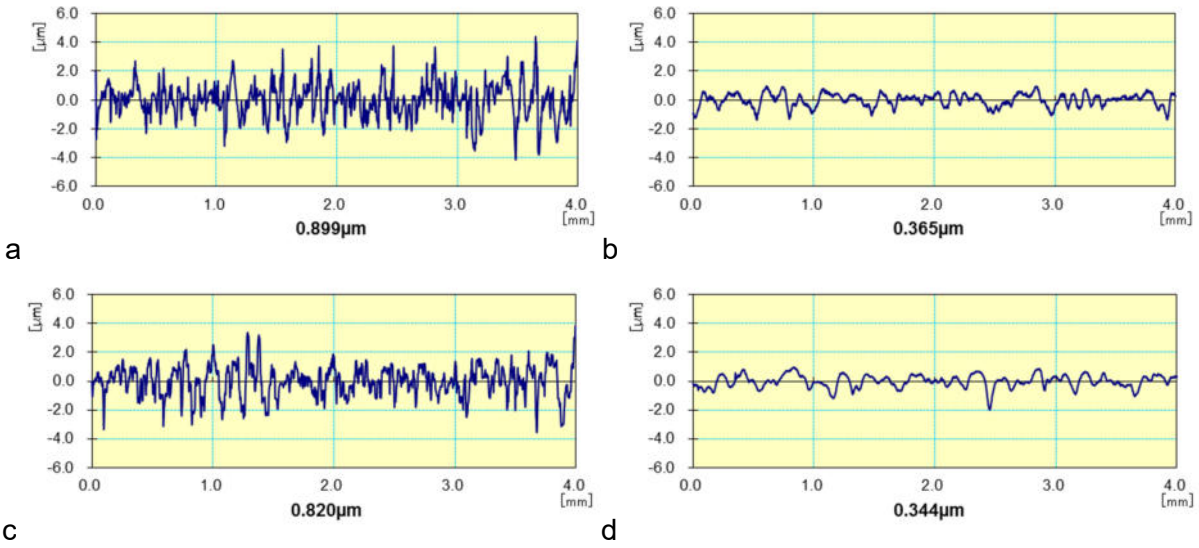

Figure 72: Surface profiles of 1.2343 tool steel before (a) and after (b) EP and 1.2311 tool steel before (c) and after (d) EP

As already stated above, pulsed/reverse pulsed currents process optimization imply many degrees of freedom that are not necessarily connected to each other (e.g. if good results can be achieved with low anodic peaks without cathodic peaks, when these are inserted in between it may be necessary to use higher anodic peaks). That is why establishment of methodologies using pulse/reverse pulsed currents is more tricky than DC.

Based on these preliminary results, two further trials were performed on 1.2343 and 1.2379 tool steels (Figure 73Figure 74). For the EP of 1.2343 steel, two series of pulsed current were tested by changing the anodic pulse and keeping the frequency (time of pulse and time off). Concerning the bipolar pulses, the influence of the ratio between the anodic and cathodic pulses was tested in order to keep the same average anodic current density.

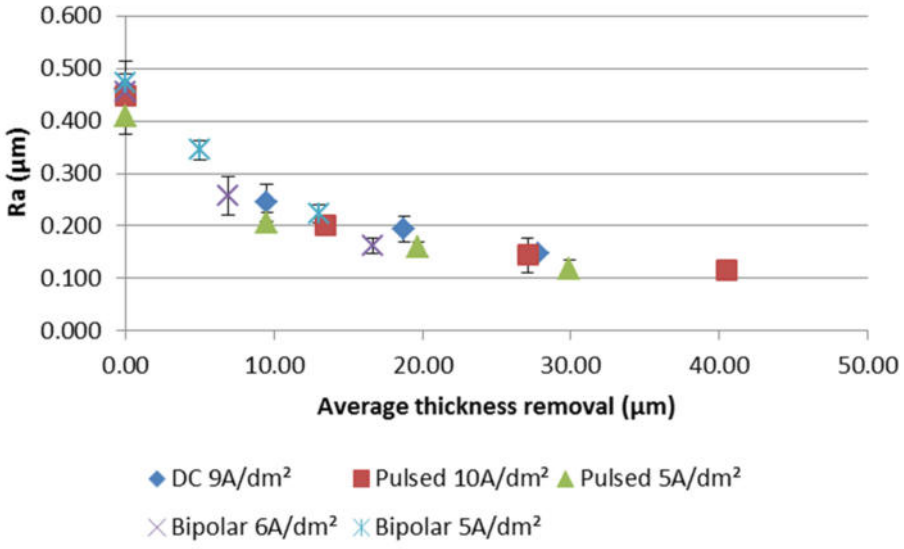

Figure 73: Ra *vs.* average thickness removal for the electropolishing of 1.2343 tool steel using direct, pulsed and reverse pulsed currents in Poligrat E520

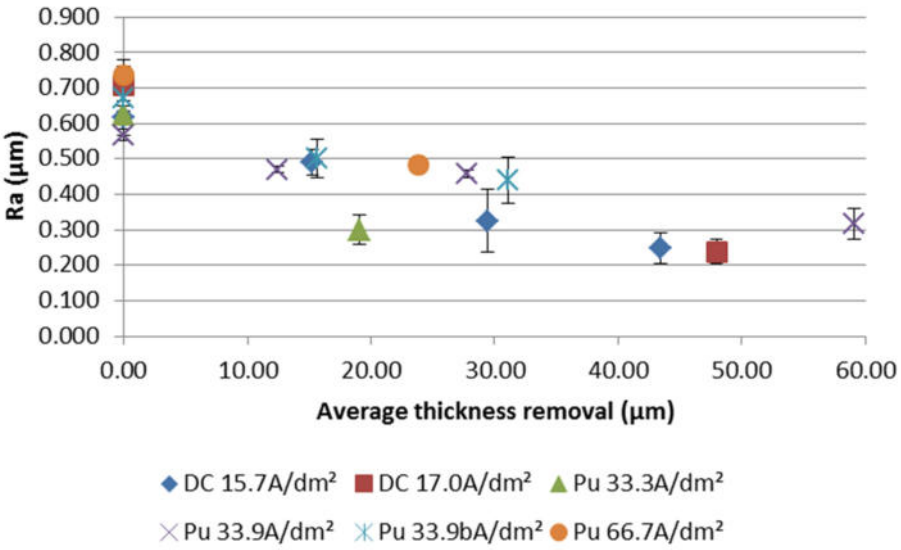

Figure 74: Ra *vs.* average thickness removal for the electropolishing of 1.2379 tool steel using direct and pulsed currents in Poligrat E520

Based on these trials, the tested conditions of pulsed and bipolar pulsed currents did not allow a significative improvement over the direct current trials. However, it can be observed in both graphs that the same final Ra can be achieved with a smaller thickness removal by using pulsed and bipolar pulsed currents with respects to direct current (up to 10 - 15 µm less, and possibly even less by fine selection of the process parameters) which is a huge advantage for micrometric parts.

4. Work package 4: Investigations of advanced configurations and tooling

Task 4.1: Update of the literature review on advanced configuration and tooling

Task 4.2: Modeling

In the framework of the AdEPT project, CRM performed the modeling of the electropolishing process using the Comsol electrodeposition module. A flow channel whose geometry corresponds to that of the electropolishing cell used in this project in its parallel electrodes configuration was modeled as a first step (Figure 75a).

The following step was to retrieve the physico-chemical and electrochemical proper ties of the sample and the electrolyte, for this mean, the bath had been characterized (conductivity, viscosity…) and a polarization curve was made on the sample to extract the Tafel coefficients and the exchange current density to insert in the model.

In order to be able to see the the material removal (at the µm-scale) due to the electropolishing and the rounding up of the edges, a very fine meshing had to be done around the edges (Figure 75b).

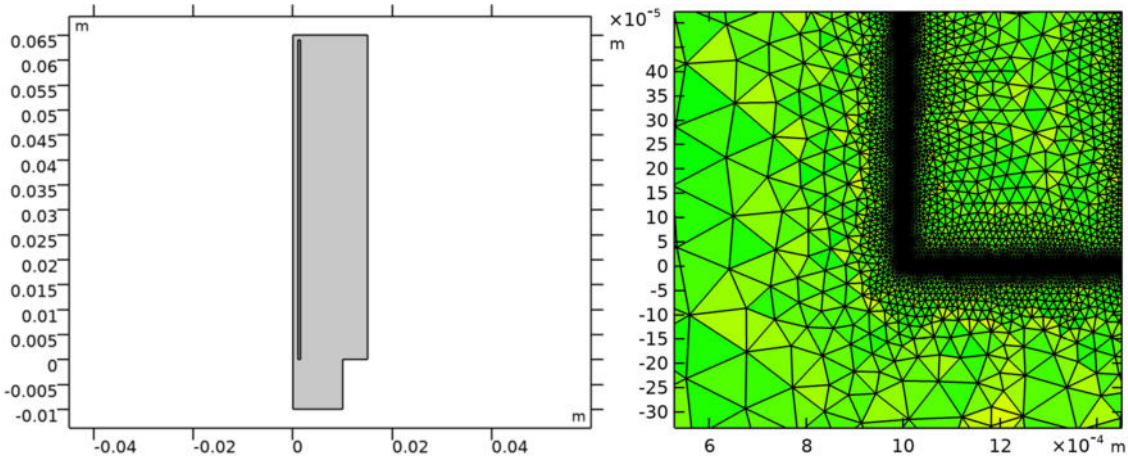

Figure 75: Modeling of the electropolishing cell's geometry (a) and the fine meshing around the edges (b)

With these included in the model, it was possible to simulate the electropolishing of the substrate and follow the change of shape as the process time increases (Figure 76). Some refinement of the model still has to be done to match better the reality. The thickness loss of a trial with defined parameters will be measured in order to compare to and affine the simulation, then the geometry will be upgraded in 3D and in the following, the geometry will be modified by adding microscopic details to simulate the micromachined cavities, or by modifying the anode conductivity to approach the difficulties related to the electropolishing of thin films.

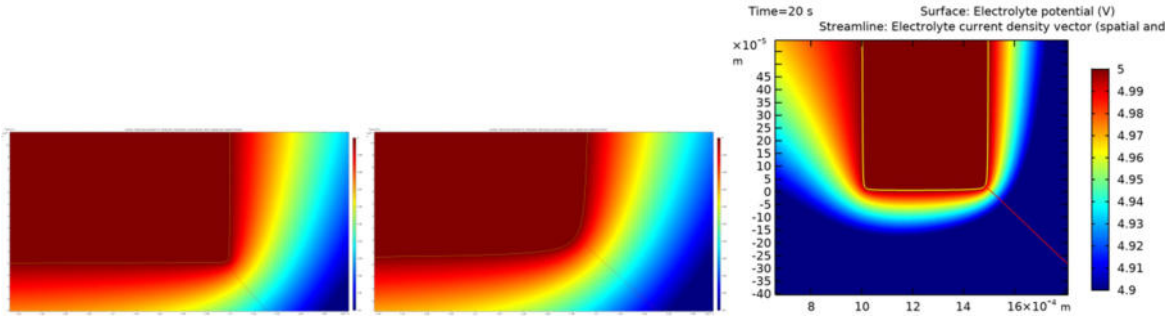

Figure 76: Evolution of the substrate deformation and surface electrolyte potential of the electropolishing cell modeled using Comsol electrodeposition module after electropolishing times of 1s (a) and 20s (b and c)

Task 4.3: Design and construction of tools and cells for the electropolishing of thin films

After appropriate considerations, it has been decided that the electropolishing of 2D thin films didn't need specific cells modifications, as good results could be obtained with the simple configurations.

Task 4.4: Design and construction of cells for the electropolishing of micro-features + 4.5: Testing of the cells and characterization of processed surfaces

In order to be able to electropolish micro-features, several possibilities were considered.

The first approach was to do the electropolishing treatment with the conventional method (batch electropolishing) by placing the part in front of a counter-electrode in the electrolyte. This method, although easy to implement and execute has several limitations. The batch electropolishing with parallel electrodes can only be used for planar parts and cause an uneven current distribution on the surface containing micro-features. This can be partly solved by adapting the counter-electrode to the part to be treated. For example, cylindrical parts that have to be electropolished in the inside were treated with a cylinder/rod as cathode.

Electropolishing of parts supplied by the user committee

In addition to the 3D demonstrator, the user committee provided CRM with parts to be electropolished. This was an opportunity to design and test specific cells for the electropolishing of microfeatures.

Three parts were supplied by the user committee. The first one was a small cylinder with a central thread to be polished made of 1.2083 steel, the second one was a gear of 1.2379 steel with the inside teeth to be polished and the last one consisted of a complex part of 1.2379 steel with an internal thread (which makes up 1/3 of the part) to be polished. Each sample required a special apparatus for the electropolishing the specific area to be treated (Figure 77).

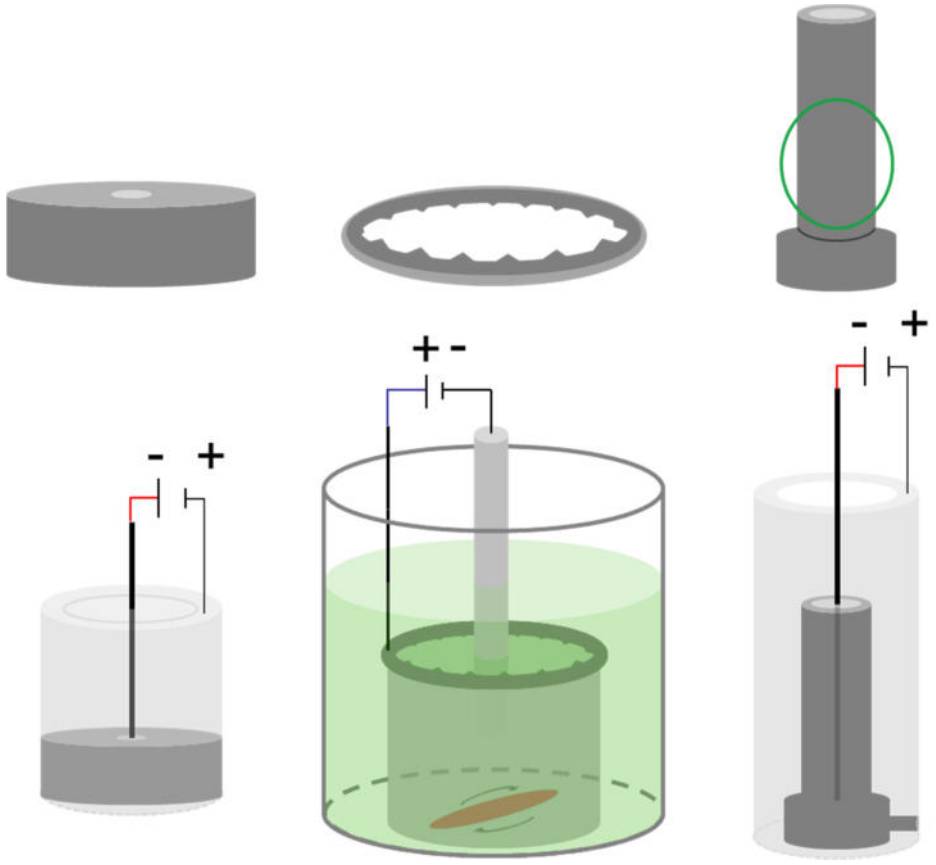

Figure 77: Parts supplied by the user committee and specific cells designed for their electropolishing

For the small cylinder, two polishing strategies were investigated: batch electropolishing where the sample was maintained horizontally from the counter-electrode, this lead to the polishing of the front part facing the cathode with a risk of inhomogeneous polishing of the thread. The other strategy was to place the part in a holder in such way that the counter-

electrode stands in the middle of the hole and to immerse the whole apparatus in the electrolyte.

The same principle was adapted for the third parts, the only difference being the presence of holes in the bottom of the holder to allow its positioning so that only the threaded part was immersed and electropolished. Since two identical parts were available, tests using direct current and pulsed currents were carried out as a mean of comparison. The gear part was electropolished on a hollow holder that allowed the agitation of the bath and the positioning of a central cathode. The rotation of the magnetic agitator was such that the electrolyte flux came in contact with the inside of the teeth.

Electropolishing of parts from task 1.2

The batch electropolishing was tested for the treatment of the sample containing micro-features presented in task 1.2. A large number of tests have been carried out by CRM on the samples supplied, in direct current, unipolar and bipolar pulsed, in the electrolyte E520 already presented. Figure 78 illustrates the pulse parameters of the different frequencies used in this study. The treated samples were then subjected to metrological examination at Hahn-Schickard. Figure 79 shows the evolution of the roughness of the parts, in the raw and machined areas, as a function of the load used for polishing. The corresponding polishing times are between 3 and 10 min. It is observed that these polishing conditions make it possible to reduce the roughness of the different zones by a factor of 3, which is appreciable. In parallel, Figure 80 shows the evolution of the radius of curvature measured at a step. It can be seen that this increases as the polishing time increases (and therefore that the roughness decreases). This has encountered in evidence a critical aspect relating to the polishing of this type of structure: there will always be a compromise to be found between improving the surface quality and preserving the geometry. On the basis of these tests, operating windows could be defined for the processing of the demonstrator parts.

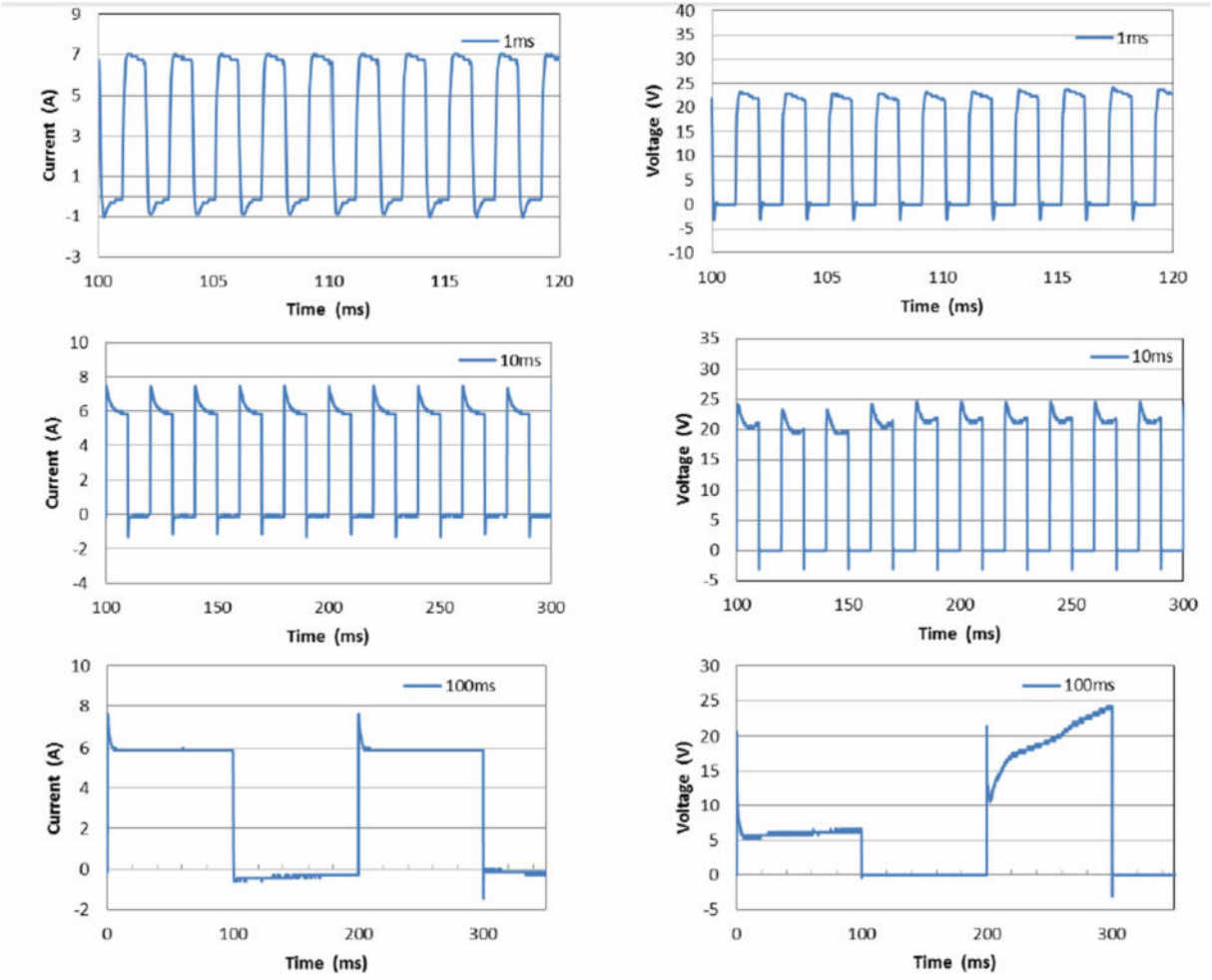

Figure 78: Current sequences and voltages applied during pulsed current electropolishing tests on 1.2343 steel. Four different pulse durations were tested, between 1 and 1000 ms (only the first 3 are shown above)

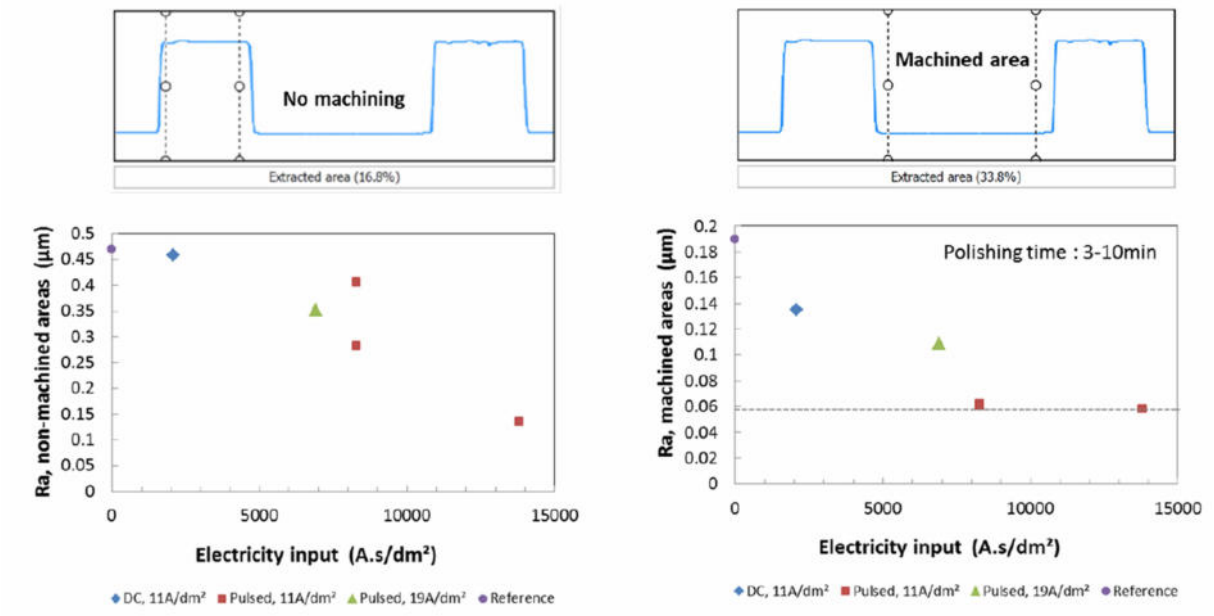

Figure 79: Results of pulsed current electropolishing tests on micro-machined parts: Evolution of the roughness of unmachined (left) and machined (right) areas depending on the load consumed

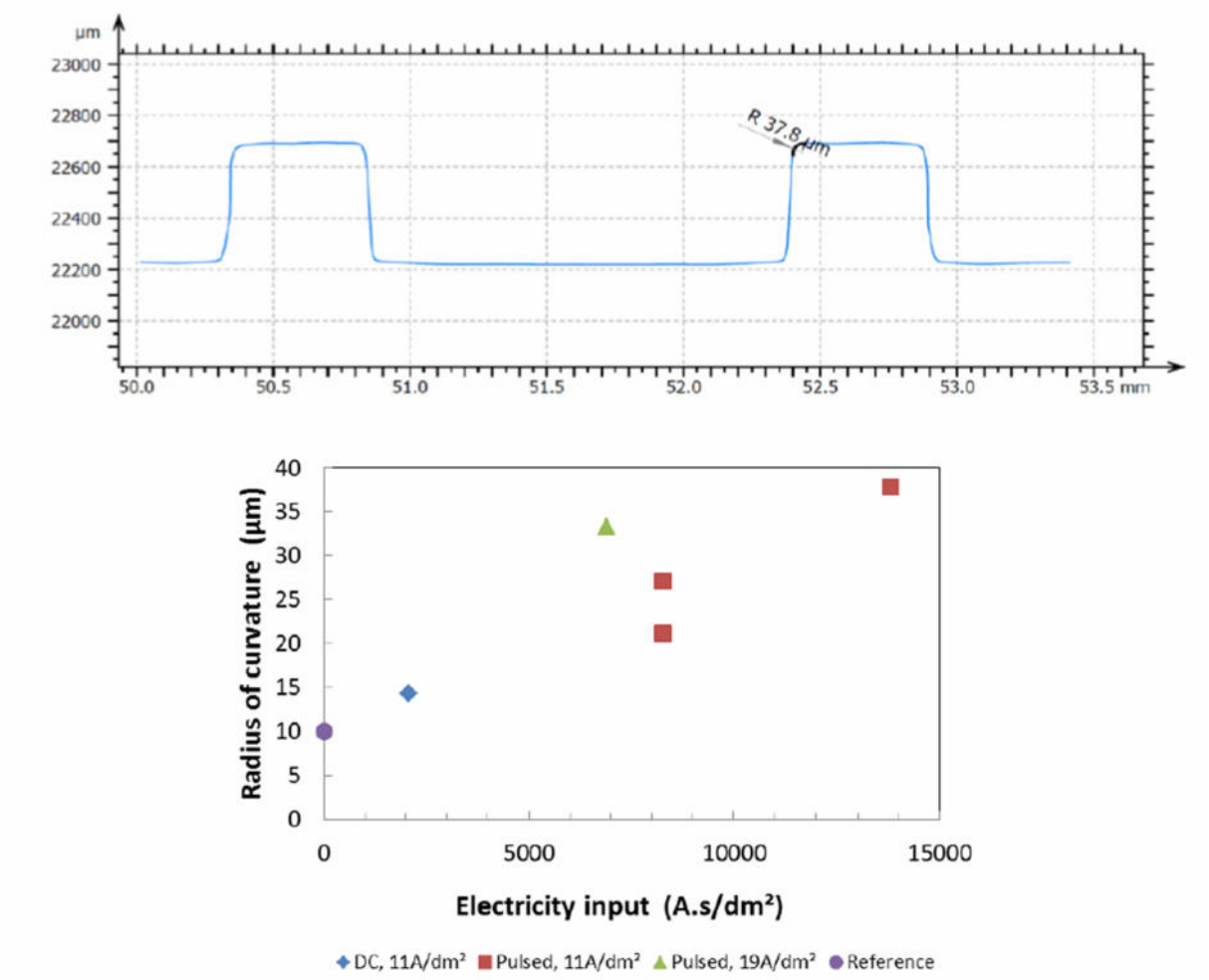

Figure 80: Results of pulsed current electropolishing tests on micro-machined parts: Evolution of the radius of curvature of the edges of the trenches according to the load consumed

A second approach was the local electropolishing of the parts by using an electropolishing pen. A first electropolishing pen prototype was designed and constructed in CRM. This pen was similar to a felt marker equipped with an electrolyte reservoir and a felt tip of 3 mm in diameter. To use this pen, one must simply fill it with electrolyte and connect it to an external power supply. The small diameter of the tip allows the local EP of parts difficult to access (*e.g.* shaped surfaces) to a mm-scale.

Preliminary results showed that the process efficiently cleans the surface and remove asperities. However, the blocking point for progressing in the tests was the robustness of the felt tip to the acid. Recently, the felt tip was replaced with a brush made out of carbon fiber (Figure 81). This allowed the electropolishing pen to be used for trials on parts with millimetric details without any damage to the tip.

Figure 81: Electropolishing pen prototype (left) and the newly replaced carbon fiber tip

In order to establish its efficiency, a series of different AISI 316 stainless steel metrics (from 3 to 8) screws were electropolished by two methods: batch electropolishing and electropolishing pen, both methods were carried out at room temperature using the standard H_3PO_4 - H_2SO_4 - H_2O electrolyte.

Figure 82 displays the two extreme metrics tested (M3 and M8) screws before and after electropolishing. With the electropolishing pen, it is possible to treat cavities and areas that are difficultly accessible by other means. This allows for example the polishing of the area between the screw thread without affecting the size of the latter, making it a highly advantageous tool for the treatment of microdetails. On the other hand, if the part to be electropolished is too large, the treatment becomes more time-consuming and gives equal results to those obtained by batch electropolishing.

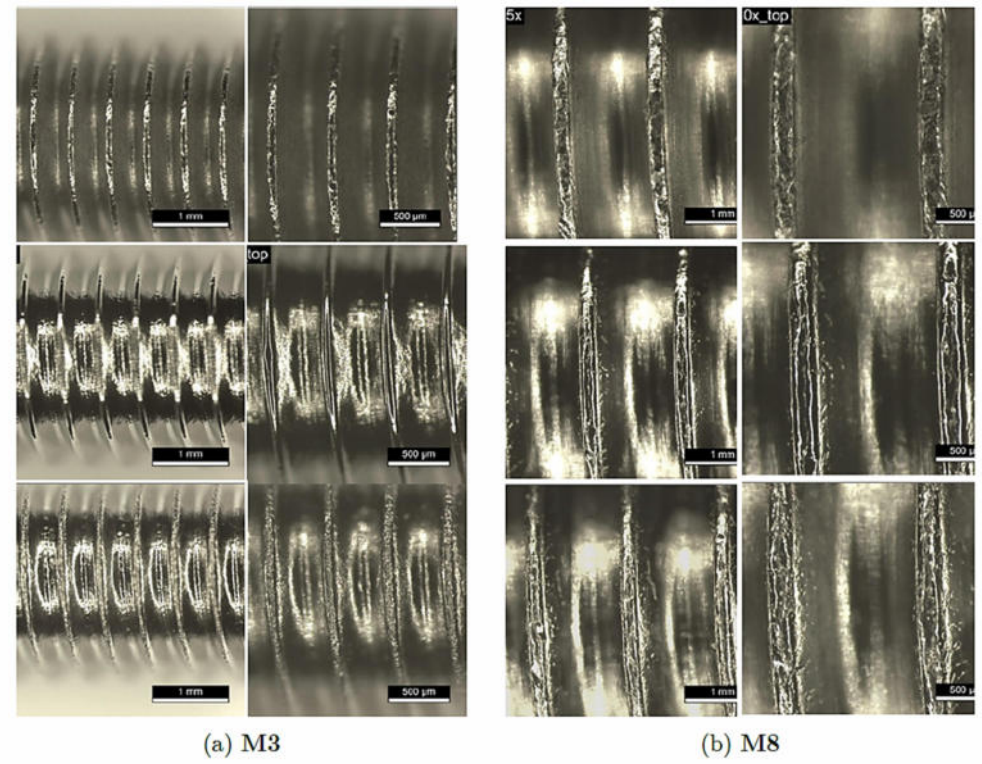

Figure 82: M3 (a) and M8 (b) screws before (top) and after electropolishing with the pen (middle) and in batch (bottom)

Based on these tests and observations, several conclusions can be drawn:

Batch electropolishing	Electropolishing pen
× Requires a special device (cylindrical counter-electrode);	✓ Very easy to handle;
× condition of the parts uncontrollable during treatment;	✓ control of the parts condition *in-situ*;
× higher current density on edges and peaks;	✓ access to cavities with the brush (reduced leveling effect);
✓ temperature control;	✓ identical current density regardless of the sample size (always the same contact area);
✓ treatment of larger parts.	× low electrolyte volume in the tank;
	× heating of electrolyte at the tip of the pen.

The last approach considered was using a scanning electrochemical microscope. Scanning electrochemical microscopy (SECM) is a technique generally intended to measure (mapping) the local electrochemical behavior of surfaces by measuring the diffusion-limited current response at the micro-electrode after applying a potential through it in a redox-containing electrolyte.

In this approach, the electrolyte is replaced by the electropolishing bath and the micro-electrode serves as the counter electrode (cathode - Figure 83).

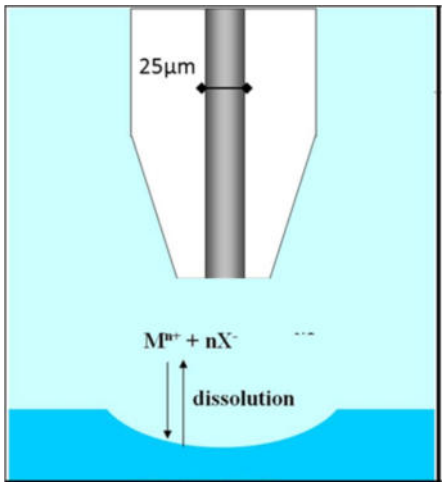

Figure 83: Schematic representation of the use of the SECM micro-electrode for localized electropolishing at the µm scale

A first series of tests was carried out by increasing the voltage between the electrodes (micro-electrode and sample). The sample's dimensions allowed to test 8 conditions on one sample, but only the 3 last ones (highest voltages) resulted in significant results (Figure 84).

The area modified in the harshest conditions shows two different morphologies, which are caused by a difference in distances between the two electrodes, and thus differences in potentials and current densities. The center seems to have been eroded while the outer side seems to have been modified but not significantly eroded (Figure 84b).

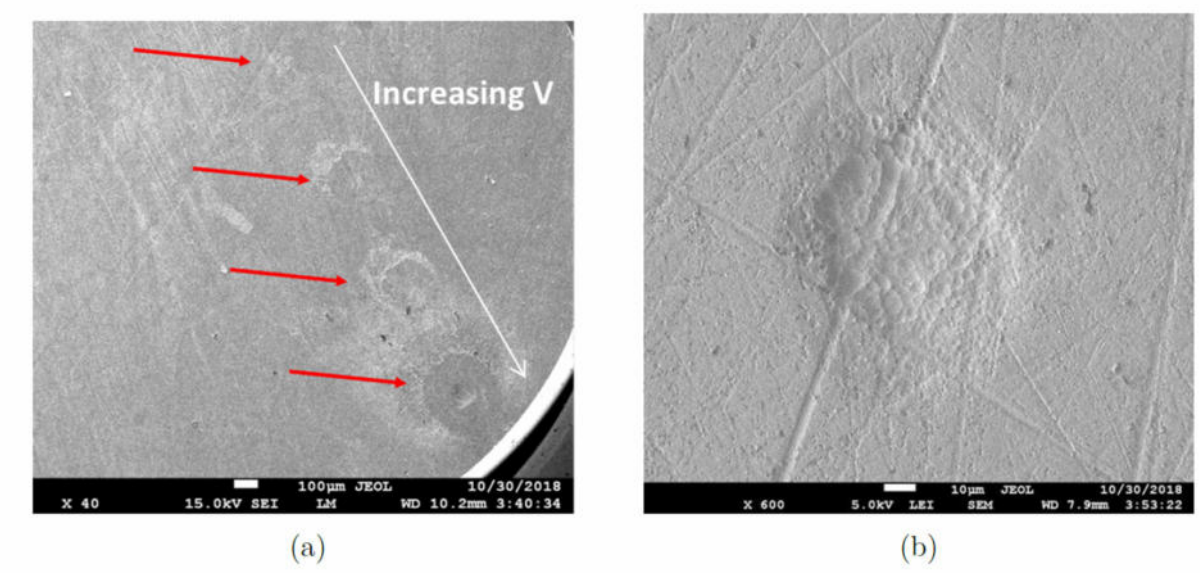

Figure 84: SEM image of 304 SS locally electropolished using a micro-electrode with increasing voltage (a) and surface electropolished with the highest voltage (b)

The outer side presents a highly pitted area (Figure 85a) at higher magnification. The structure of the central area looks like whole grains from the steel were dissolved. The surface has different morphologies depending on the position in the pit: either smooth, scaled of pitted (Figure 85b and c).

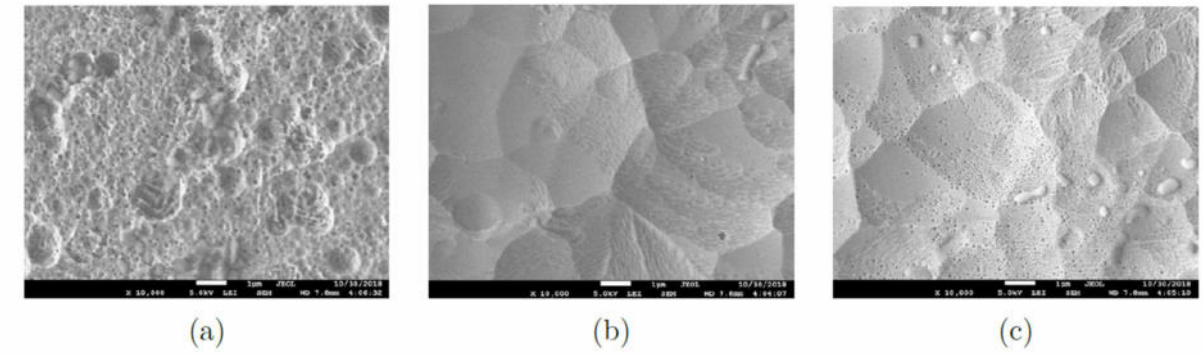

Figure 85: Outer area (a) and center (b and c) area of the surface modified in the harshest conditions

This approach could have led to more advanced electropolishing technologies, but due to the encountered difficulties of probing reference samples even though there were planar (*i.e.* the easiest shape to probe), this solution was abandoned for the treatment of parts containing irregularities and details such as micro-features.

5. Work package 5: Construction and Validation of demonstrators for 2D applications

Task 5.1: Selection of 2D case studies

ZFM:

The 2D case studies were electroplated Al wafer with bonding frames. The goal was to reduce the roughness of the deposited Al in order to achieve bondable surfaces. The preparation and a figure is already given in Task 1.2. In Figure 86 a photograph of a prepared wafer is shown. Those wafers were diced in smaller pieces to fit in the current beaker set up. A goal was to try also the EP on wafer level. However, the project progress was too slow to set up a bigger cell in a plating equipment.

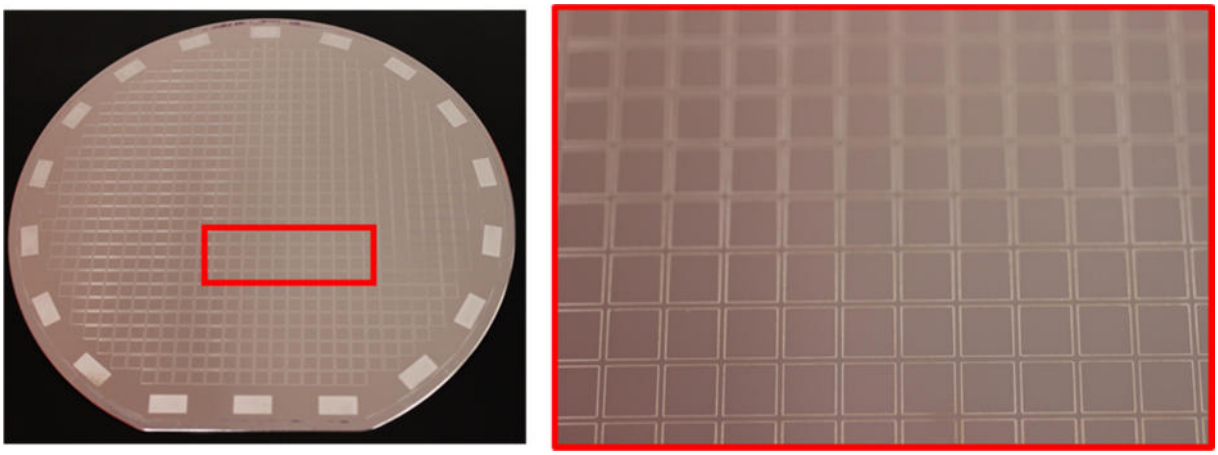

Figure 86: photograph of an electroplated Al on Al seed layer on 150 mm wafer

Task 5.2 Adaption of EP cell and preparation of parts to be treated

Regarding the time consuming set up of the EP process, the cell was not adapted for the micro feature polishing. The prepared wafer were diced in 2.8 x 4 cm² to use the same set up than before for the full-surface polishing experiments.

For the EP of the bonding frames, the defined parameters of 75 °C electrolyte temperature and a potential of 22.5 V were applied. The polishing time was varied (300 s, 600 s, 900 s) to investigate the influence of the time. Before EP of the 2D features, a test run of reference samples was performed to find the right position for the porous stone. The EP in bonding frames with a width of 60 µm was promising. The results for the different EP durations are shown in Figure 87 The main problem during the polishing is the strong attack of the seed layer for durations longer than 300 s even though it was protected with the resist. The measurement of layer thickness and roughness was challenging due to a missing reference surface. Thus, the evaluation of the polishing result is more qualitative than quantitative regarding the roughness. From the 3D images of the confocal microscopy in Figure 87, it can be concluded that 300 s improve the layer quality sufficiently. The higher EP durations resulted in a U-shaped frame profile. That is not intended to achieve. The SEM pictures show a slight rough surface, which looks porous in higher magnifications. This was detected for all EP durations and could be related to an oxidizing of the Al. However, this was not analyzed.

Summarizing, the EP can be used for the polishing of ECD-Al microstructures but the process has to be optimized in terms of cell construction, N_2-bubbling and process integration into microsystem fabrication.

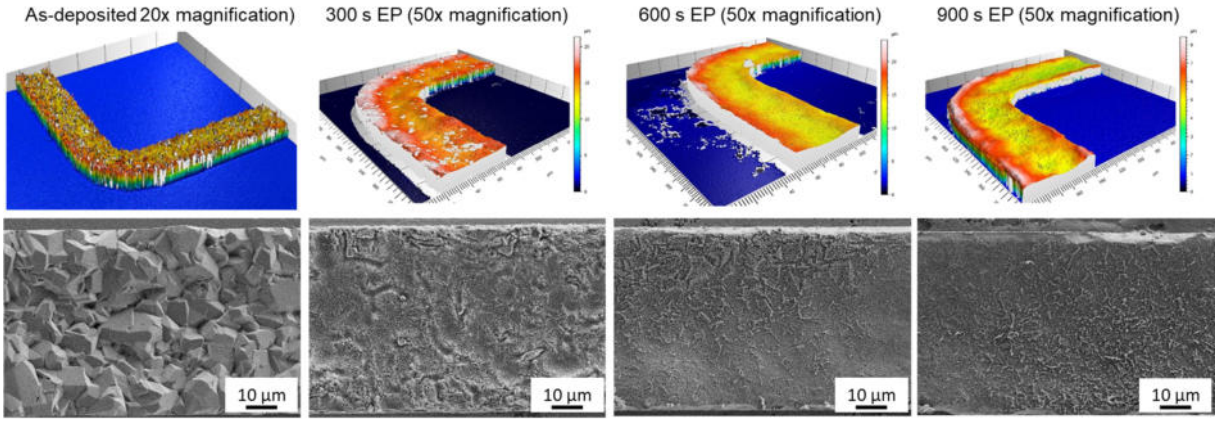

Figure 87: Analyzation of the EP results in bondings frames; top: 3D images from confocal microscopy; bottom: SEM pictures of polished 2D features

Task 5.3. Electropolishing optimization

The optimization process was mainly done on the full-surface Al layers. The main results and development steps are shown in Task 1.4.

Task 5.4 Testing of EP parts under real conditions

The polished bonding frames could not be tested in a followed bonding step regarding the small sample size. A useful comparison of wafer bonding with Al layers needs at least a complete wafer level processing step.

Task 5.5 performance analysis

A comparison of the performance of a non 100 % optimized EP process with an industrial standard process for layer smoothening, like chemical mechanical polishing (CMP), seems unfair. Nevertheless, the Figure 88 shows three 3D images of a confocal microscope of electroplated Al. The as-deposited Al is very rough at the surface. After a CMP process of 2 min with very low pressure, the layer was flattened nicely. The EP process was also able to flatten the Al even if the procedure was not that homogeneous than the CMP. However, during the CMP some of the large crystals were peeled off, which results in scratches over the whole surface of the Al. Additionally, the buffing sheet had to be changed for following wafer preparations. This is the benefit of the EP process: the removal is not through a mechanical attack but through electrochemical dissolution. At any point, the electrolyte needs to be changed. But the used one is very inexpensive compared to the CMP slurry and buffing sheet. Overall, the EP should be considered as a preparation for a fine polishing using CMP.

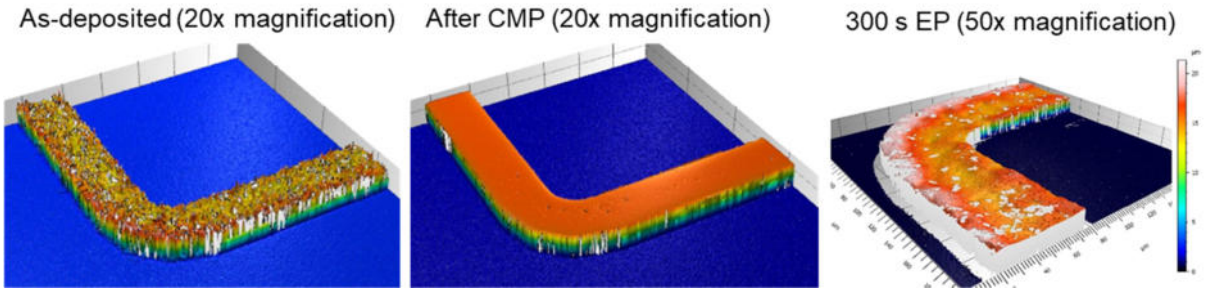

Figure 88: Comparison of CMP and EP process with an as-deposited Al layer

Furthermore, the process should also be considered as an additional step before CMP for other materials, like Cu. Cu is a common material in microelectronics. A usual process is the damascene process where vertical interconnects (vias) are filled with Cu. The Cu is also deposited on the surface of the wafer. The planarization of the Cu to the vias is challenging because of dishing and erosion processes. A pre-EP process could remove the Cu easily and prepare the wafer for CMP. The CMP process itself will take shorter time. Thus, dishing and erosion will have less time to occur and the overall polishing will show a better result.

As a summary, the EP process is a powerful process, which should be used more in microsystem technology. Unfortunately, the setup of the reference conditions in this project and the analyzation took too long time. Hence, a complete integration in a process example was not possible. The outcome of the project should be followed and brought into wafer level applications.

6. Work package 6: Construction and Validation of demonstrators for 3D applications

Task 6.1: Selection of 3D case studies

For the 3D demonstrators, mold inserts are fabricated and treated by EP. To evaluate the influences on the molding process, the mold insert are integrated into an injection molding tool before and after the EP process. Thereby differences in the molding process and part quality will be compared. For the molding trials, an injection molding tool is required. The design of the molding tool is shown in Figure 89. The molding tool has dimensions of 196x196 mm² with a 100x130 mm² mold insert. The mold inserts will be structured using milling and electric discharge machining. With every mold insert, molding trials will be performed before and after the EP process and the molding results will be compared. Using electric discharge machining as a fabrication method was explicitly recommended by the user committee, since mold inserts used for industrial applications are often fabricated by this technology.

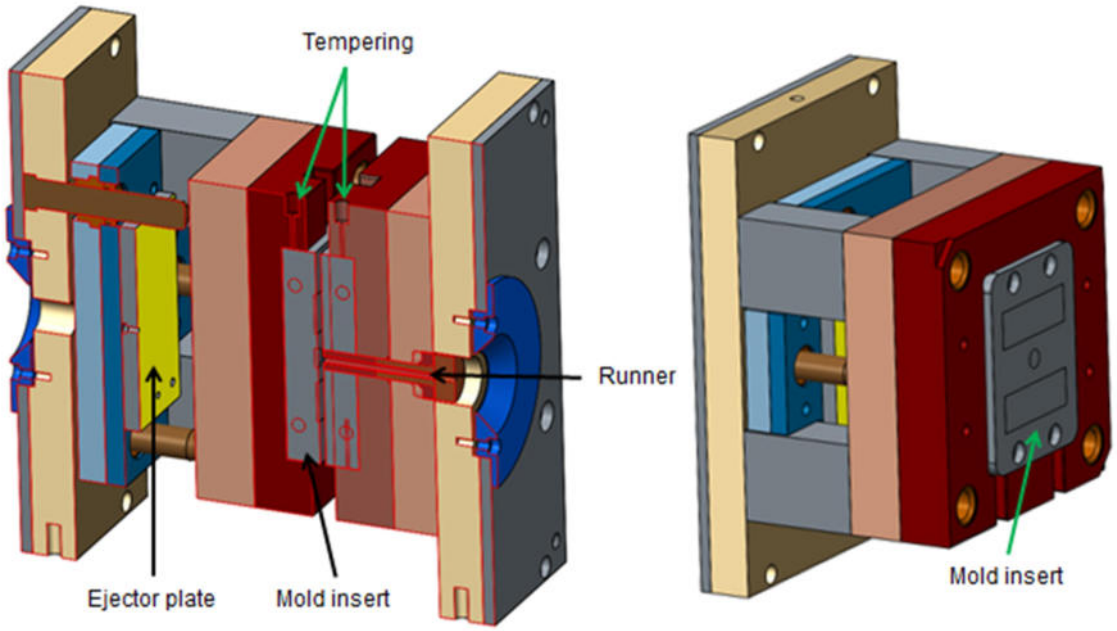

Figure 89: Design of the molding tool (left) with a detailed view of the moveable side (right)

A detailed view of the structured mold inserts are shown in Figure 90. Two microfluidic designs were chosen, whereby Design 2 was provided by Stratec as part of the user committee. Both designs include two similar cavities with microfluidic designs consisting of small chambers, microstructures and channels. The designs were chosen, since microfluidic structures are very often small and difficult or impossible to polish with traditional methods. Therefore, EP would be a significant improvement for the resulting surface quality in the mold inserts as well as the molded parts. Furthermore, decasting during the molding process could be improved. Every cavity is equipped with a single gate. To remove the parts from the mold inserts, every cavity is equipped with ejector pins which can be seen as holes in the designs. Furthermore, 3 ejector pins are placed at the runner system.

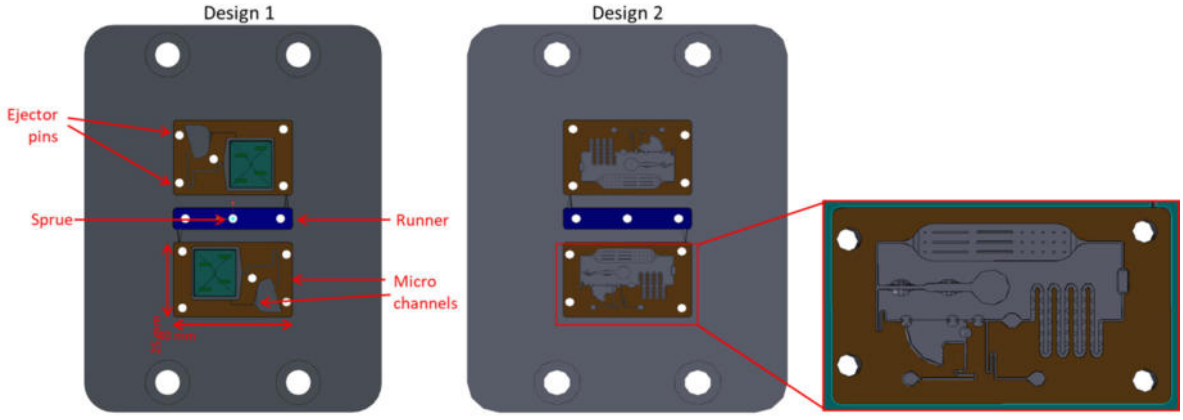

Figure 90: 3D demonstrator mold inserts with microfluidic structures

Mold inserts were fabricated using 1.2343 ESU and M333 steel grade.

Task 6.2: Adaptation of electropolishing cell and preparation of parts to be treated + 6.3: Electropolishing study

The device was set up in order to treat the 3D demonstrator. In order to optimize the conditions of electropolishing for the demonstrator in the new set-up, preliminary tests were started on flat samples of the same size that the demonstrator, several challenges arose when doing so. Because of the different of electrodes size, electrolyte volume and mean of agitation, the optimized conditions identified on small samples didn't transpose on the new equipment and new optimizations had to be done for the treatment of these parts.

The problem of an inhomogeneous surface finish after treatment was resolved by replacing the large cathode by a smaller one of the size of the sample. Because of the time needed to adjust the parameters, an aging of the bath was observed. Indeed, the Poligrat bath is highly hygroscopic and tends to deteriorate over time, it is thus needed to replace it. Because of a shortage of one constituent of the bath (Poligrat E520 KB which constitutes 70 vol. %), the bath could not be replaced. However, since E520 KB is mainly composed of ethylene glycol (EG), it was decided to substitute KB by EG. To ensure that the new bath would behave in the same manner, current-potential plots were recorded (Figure 91). The same trend in the response is recorded, showing a well distinct electropolishing plateau.

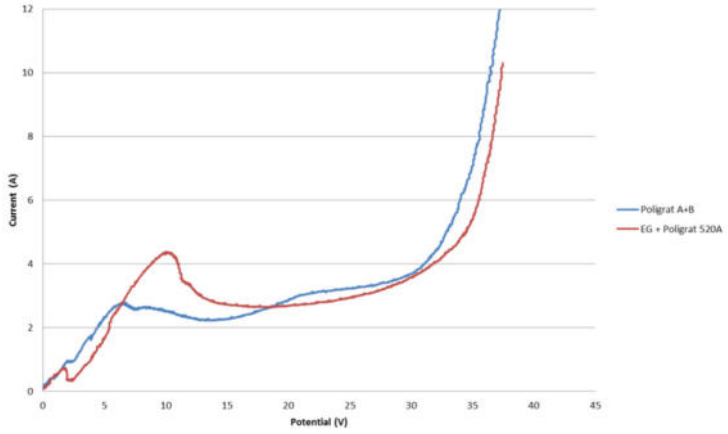

Figure 91: Current-potential curves of 1.2343 tool steel in Poligrat (A + B) and Poligrat A + ethylene glycol

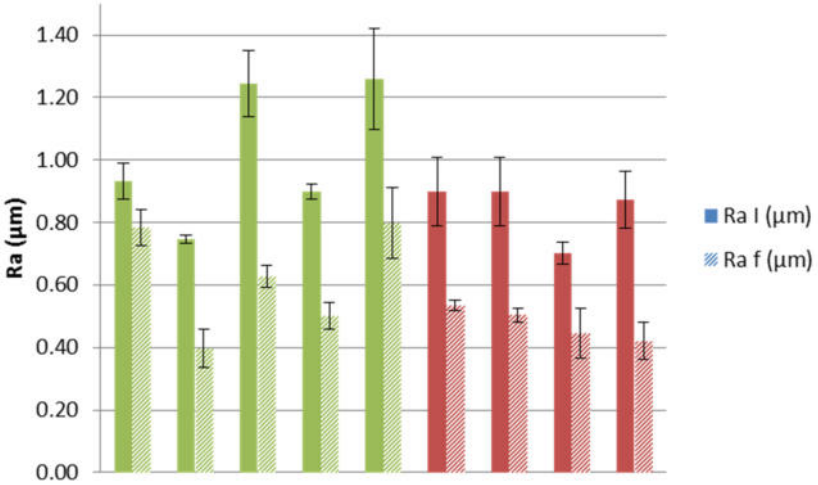

Figure 92: Initial (plain) and final (dashed) Ras for galvanostatic (green) and potentiostatic (red) electropolishing tests

Different parameters were investigated, the galvanostatic (current-controlled) electropolishing required an initial voltage ramp during a short time in order to in the electropolishing region (plateau), while potentiostatic (voltage-controlled) electropolishing didn't require such ramp. Figure 92 displays the decrease of Ra for both type of polishing. The potentiostatic electropolishing gave the best results in terms of Ra loss and surface finish after treatment.

Once the appropriate optimizations had been realized, the demonstrators were electropolished in the 50 liters tank containing the Poligrat electrolyte with the best conditions (Figure 93).

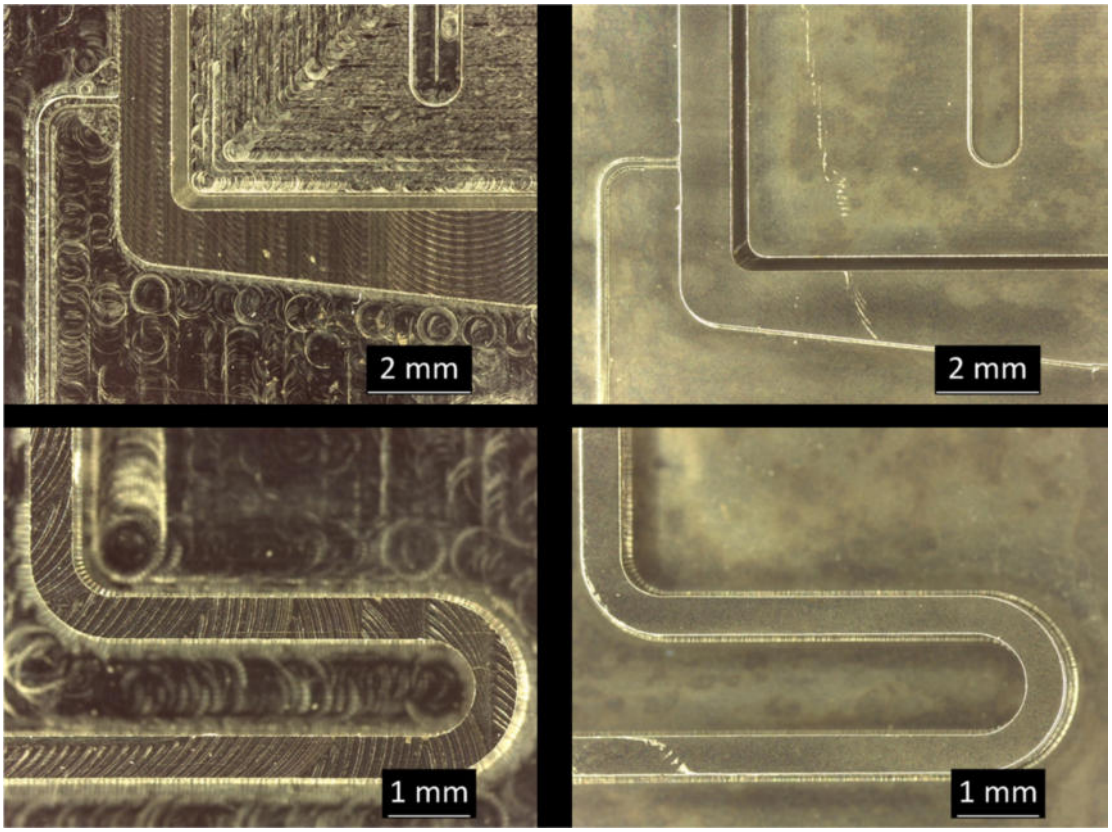

Figure 93: Micromachined details of one demonstrator before (left) and after (right) electropolishing

Task 6.4: Testing of electropolished parts under real conditions

The electropolishing of the mold inserts was performed by CRM group due to the existing size limitations in the electropolishing cell at Hahn-Schickard. Mold inserts after the electropolishing process are shown in Figure 94.

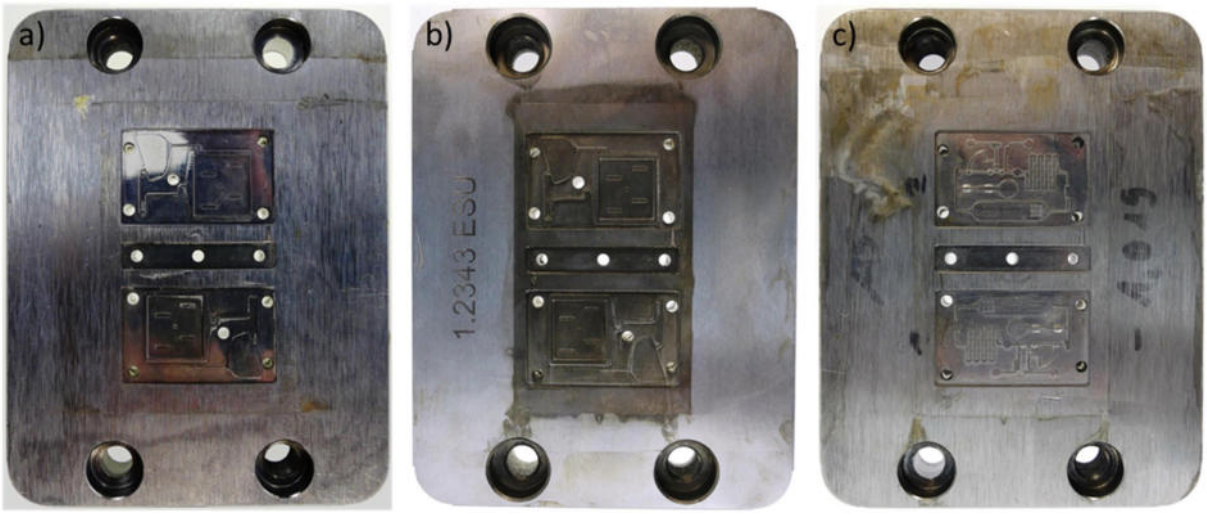

Figure 94: a) Milled mold insert after electropolishing, b) mold insert fabricated by means of discharge machining after electropolishing and c) milled mold insert with the design by Stratec after electropolishing

To evaluate the mold inserts under real conditions, injection molding trials were performed using an Arburg 375 Allrounder molding machine. As the molding material, COP (cycloolefin-copolymer) was used, which is a frequently used material for microfluidic chips. The molding parameters are shown in Table 7: Injection molding parameters. No differences in the molding behavior between the untreated and treated mold inserts could be identified. However, surface quality was visibly better with the samples of the treated mold inserts. The decasting of the molded parts was good with the untreated and treated mold inserts. However, for components which are hard to eject due to their geometry, electropolishing might have a significant benefit due to the possibility of improving the surface quality and thereby reducing the attachment of the part to the mold insert.

Table 7: Injection molding parameters

Material	COP
Melt temperature	295 °C
Mold temperature	90 °C
Injection pressure	1700 bar
Holding pressure	900 bar
Cycle time	33 s

Comparing the molded parts before and after electropolishing, a significant difference is visible, especially when the mold insert was fabricated by means of discharge machining. Due to the significant improvement of the surface quality by the electropolishing process, the molded parts become more transparent, as shown in Figure 95.

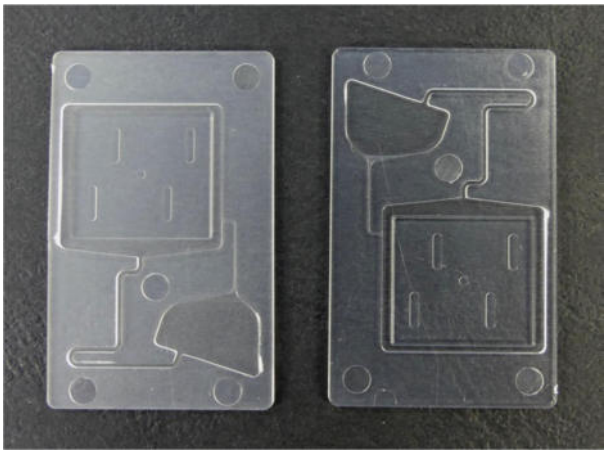

Figure 95: Comparison of a molded part before (left) and after (right) electropolishing

Task 6.5: Analysis of the performances

To analyse the performance of the electropolishing process, different features of the mold inserts were measured before and after the polishing process as well as the molded component fabricated with the polished mold insert. The mold inserts and molded parts were analyzed using a laser autofocus system (Mitaka MLP-3). Figure 96 show the measurement results of a milled 1.2343 ESU steel mold. The surface roughness was measured on the top surface (on the bottom surface respectively for the molded part). Using the electropolishing process, the surface roughness could be reduced from Ra = 0.2 µm (Rz = 1.3 µm) to Ra = 0.05 µm (Rz = 0.4 µm) which is a significant improvement. The measurement of the molded part is more difficult, since the component is transparent. Using the same measurement system (Mitaka MLP-3), a surface roughness of Ra = 0.03 µm (Rz = 0.3 µm) was measured. Due to the transparent properties of the part, the steep was cannot be measured correctly, which can be seen in Figure 96 as an additional step, which does not exist in the part. Looking at the edges, only small rounding effects can be seen. Other areas of the mold insert showed similar results. Therefore, it can be concluded that the electropolishing process is suitable to improve the quality of a mold insert made of 1.2343 ESU steel.

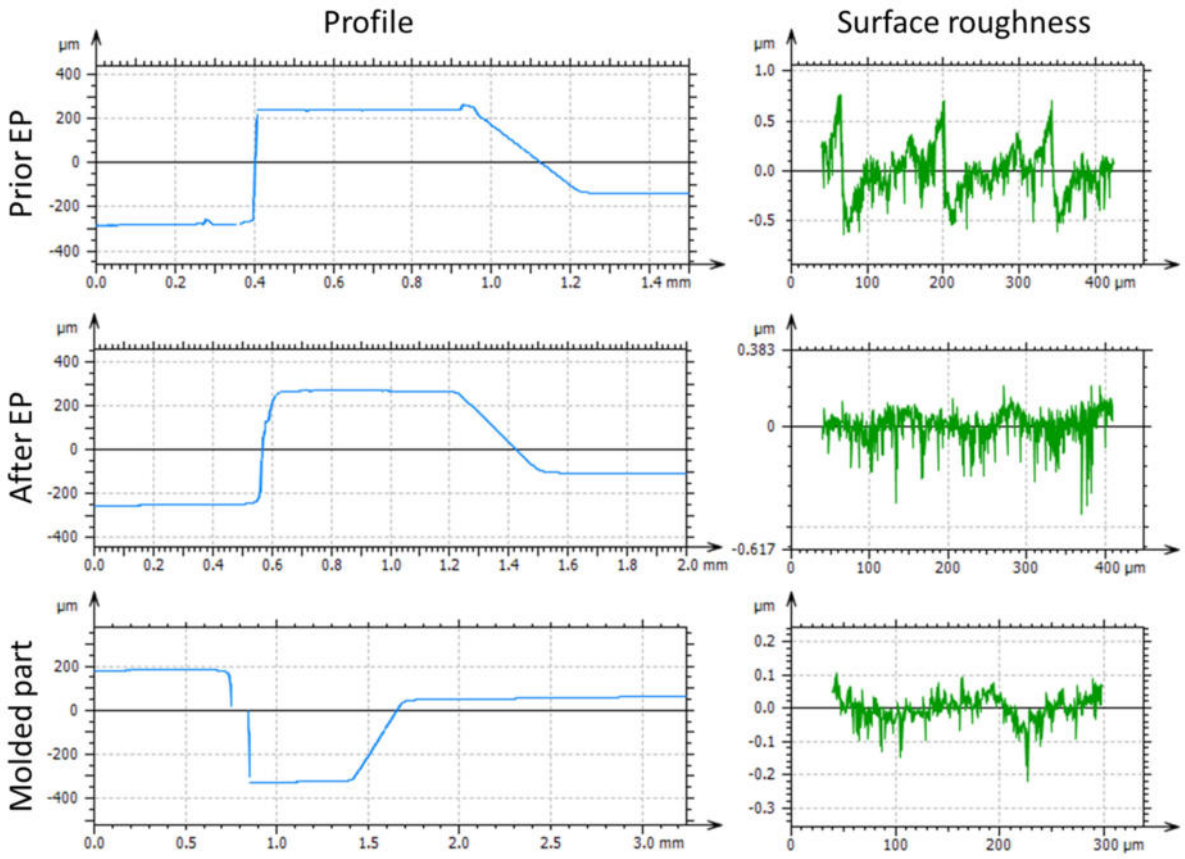

Figure 96: Exemplary comparison of a micro feature in the mold insert prior and after polishing as well as in the molded part. The mold insert was milled in 1.2343 ESU steel

In addition to a milled mold insert, a mold insert fabricated by electrical discharge machining (by Hack as part of the user committee) was investigated. For the mold insert hardened 1.2343 ESU steel was used. Compared to the milled mold insert it can be seen in Figure 97, that the initial surface roughness is significantly higher (Ra = 1.1 µm, Rz = 6.6 µm) due to the machining principal. However, using the electropolishing process, a significant improvement of the surface quality can be achieved, reducing the roughness to Ra = 0.4 µm (Rz = 1.8 µm). Especially the reduction in the Rz value is high, since surface peaks are reduced significantly. Looking at the edges of the microstructures, no significant changes are visible. Comparing the profile and roughness of the mold insert with the molded part, a very good accordance can be seen, which is expected. As already shown in Figure 95, the improvement of the molded part is very obvious, since the part is significantly more transparent.

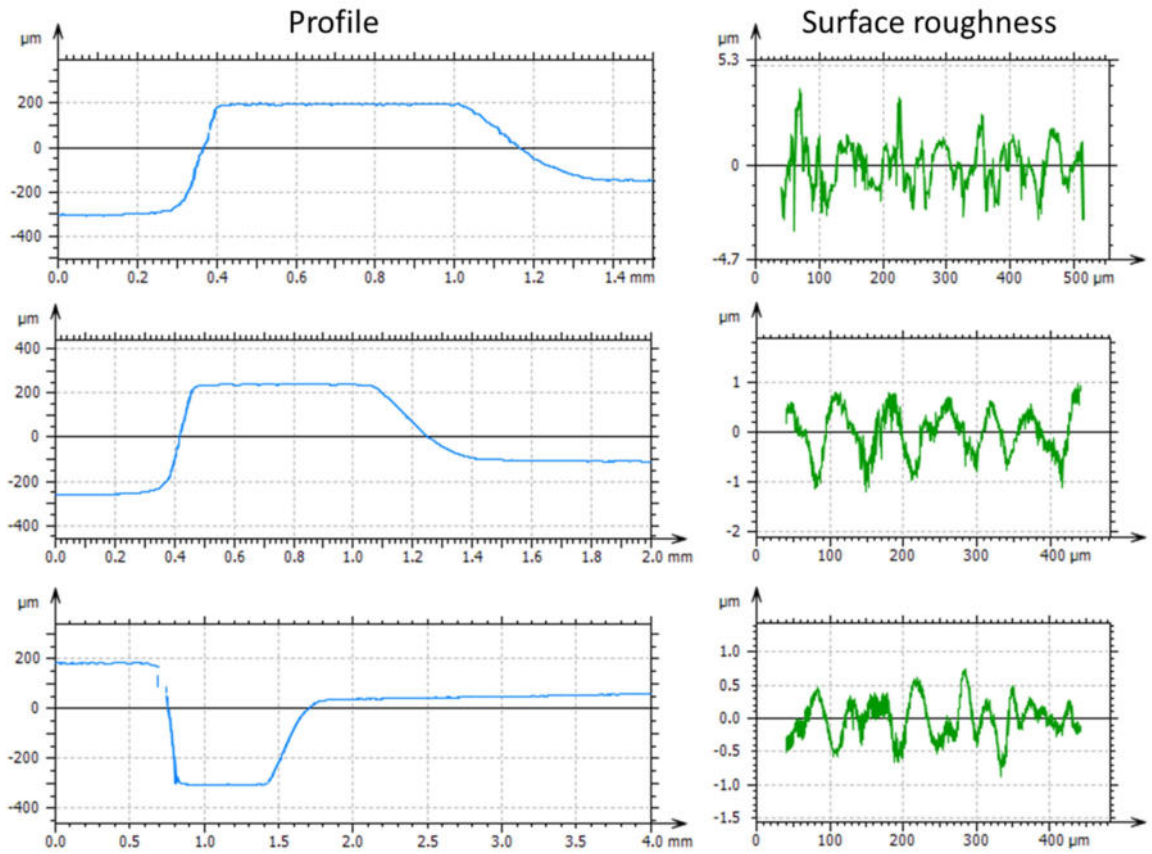

Figure 97: Exemplary comparison of a micro feature in the mold insert prior and after polishing as well as in the molded part. The mold insert was fabricated in 1.2343 ESU steel using electrical discharge machining

Furthermore, the second mold insert design was investigated. Figure 98 shows exemplary the measurement results at one feature prior and after the electropolishing process. It can be seen, that the edges are significantly rounded. Therefore, for this structure the polishing time should be reduced. The surface roughness was reduced from Ra = 0.2 µm (Rz = 0.9 µm) to Ra = 0.06 µm (Rz = 0.3 µm) which equals a reduction of more than 60 %. Due to the transparency of the molded part, no conclusive measurement of the micro feature could be acquired.

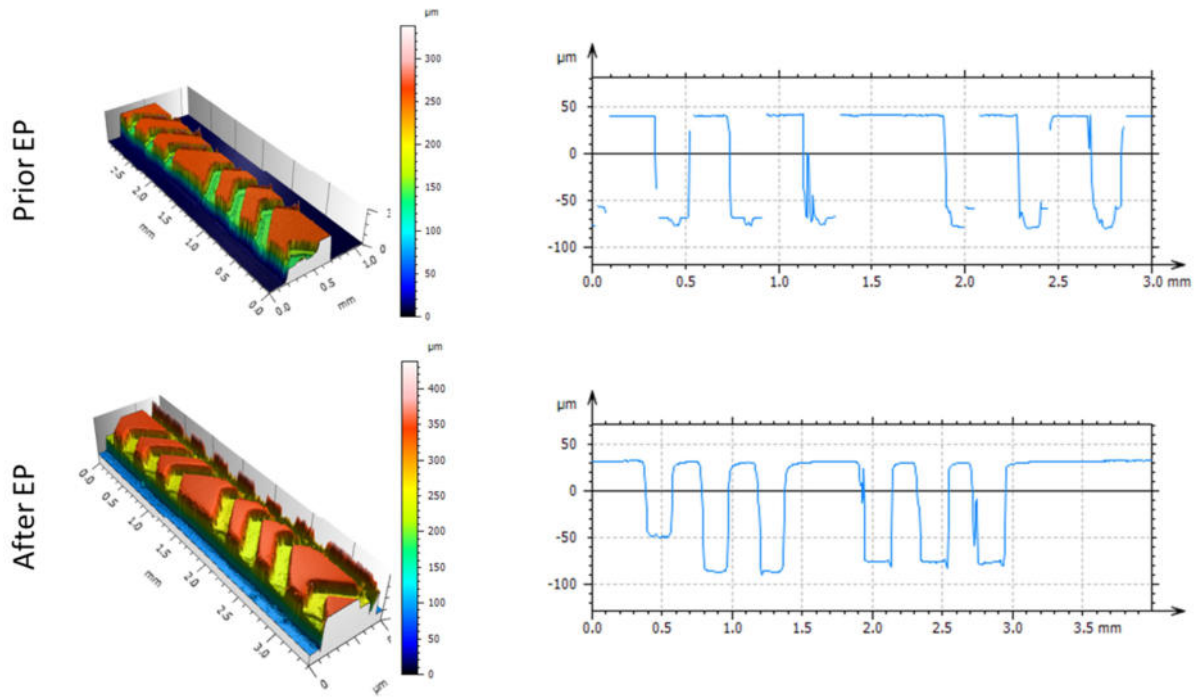

Figure 98: Measurement of the mold insert with the second design prior and after electropolishing

Conclusions:

The following conclusions can be made from the results of the polishing and replication trials:

- Electropolishing is a suitable method to improve surface quality of different steel grades;
- The method is a promising method to improve the quality of mold inserts fabricated by milling or discharge machining;
- The process can be used for hardened steel, which allows a finishing process at the end of the fabrication process;
- The electropolishing process can also be used in micro features like channels and holes, even when the structures are very small (300 µm and smaller);
- The duration of the polishing process is the most critical parameter to consider, since the edges of the structures get rounded, if the polishing time is too long;
- The quality of the initial surface is critical to achieve good results with the electropolishing process. Therefore, it is mandatory to have already good surface quality with the initial machining process like milling or discharge machining.;
- Surface quality Ra can be reduced about 50-75 % using electropolishing with steel substrates;
- Especially surface peaks can be removed very good using electropolishing and therefore reducing the Rz value significantly.

Conclusions and perspectives

The AdEPT project's stated objective was to "push the boundaries" of the electropolishing technology. This ambitious objective was achieved by improving the understanding of the process, by evaluating the various improvements described in the literature and by studying its applicability in various fields where it is not currently used. At the end of the project, we can take stock of these different objectives.

Significant progress has been made in the understanding of the mechanisms of electropolishing, at the molecular level, using the tools and methodologies developed by the University of Namur. These tools are based on electrochemical impedance spectroscopy, in correlation with chemical surface analyzes by XPS. These results have been the subject of two scientific publications (1 in preparation).

Several improvements to the electropolishing processes have been evaluated at the laboratory scale, particularly with regard to improved bath chemistry or electrical parameters.

One of the major results of the project is the demonstration of the potential of electropolishing in two new technological fields. The first area is that of finishing the steels used to manufacture injection molds for plastic parts. The technique is an interesting alternative to the conventional mechanical polishing for parts with a geometry that makes manual polishing difficult. However, electropolishing is of even of greater interest in the case of surface finishing of molds for parts with micro-machined details (eg microfluidic applications). For this type of parts, mechanical polishing is not possible and electropolishing therefore makes it possible to solve a real need for improving the surface quality of these parts. The performance of electropolishing for this application could be demonstrated by real injection tests, which gives hope that the technology will arouse the interest of mold makers, well represented in the Walloon and German user committees. These developments have been achieved thanks to an effective partnership between CRM and Hahn-Schickard.

The second, very broad field of application is that of microelectronic manufacturing processes. The potential of electropolishing technology has been demonstrated here for the specific case of electrodeposited aluminum deposits used for wafer bonding. The results obtained at the laboratory scale are very conclusive. It is regrettable here that the demonstration trials could not be carried out up to the full wafer scale, making it possible to assess the effect on the wafer bonding application. Upscaling to this level is however expected in the coming months. These results were obtained at the Zentrum fur Mikroteknologien in Chemnitz.

In addition to the results mentioned above, the AdEPT project has enabled the development of know-how and expertise in the study of electropolishing processes at the level of the various partners involved, particularly in terms of available equipment and characterization procedures (morphology surface, optical characterization).

References

[1] I. V Antsikhovich and A. A. Chernik, “Using pulse modes in non-chromium electrolytes for electropolishing antsikhovich i.v., chernik a.a.,” no. Vi, pp. 74–80.

[2] E. M. Beamud, P. J. Núñez, E. García-Plaza, D. Rodríguez, A. González, and J. García, “Impact of electrolyte concentration on surface gloss in electropolished stainless steel,” *Procedia Manuf.*, vol. 13, pp. 663–670, 2017.

[3] M. Datta and D. Vercruysse, “Transpassive dissolution of 420 stainless steel in concentrated acids under electropolishing conditions,” *J. Electrochem. Soc.*, vol. 137, no. 10, pp. 3016–3023, 1990.

[4] D. R. Gabe, “Electropolishing of mild steel in phosphoric and perchloric acid containing electrolytes,” *Corros. Sci.*, vol. 13, no. 3, pp. 175–185, 1973.

[5] G. Jeyashree, A. Subramanian, T. Vasudevan, S. Mohan, and R. Venkatachalan, “Electropolishing of Stainless Steel,” *Bull. Electrochem.*, vol. 16, no. 9, pp. 388–391, 2000.

[6] P. S. Kao and H. Hocheng, “Optimization of electrochemical polishing of stainless steel by grey relational analysis,” *J. Mater. Process. Technol.*, vol. 140, no. 1–3 SPEC., pp. 255–259, 2003.

[7] E. S. Lee, “Machining characteristics of the electropolishing of stainless steel (STS316L),” *Int. J. Adv. Manuf. Technol.*, vol. 16, no. 8, pp. 591–599, 2000.

[8] C. C. Lin and C. C. Hu, “Electropolishing of 304 stainless steel: Surface roughness control using experimental design strategies and a summarized electropolishing model,” *Electrochim. Acta*, vol. 53, no. 8, pp. 3356–3363, 2008.

[9] C. C. Lin, C. C. Hu, and T. C. Lee, “Electropolishing of 304 stainless steel: Interactive effects of glycerol content, bath temperature, and current density on surface roughness and morphology,” *Surf. Coatings Technol.*, vol. 204, no. 4, pp. 448–454, 2009.

[10] S. Magaino, M. Matlosz, and D. Landolt, “An Impedance Study of Stainless-Steel Electropolishing,” *J. Electrochem. Soc.*, vol. 140, no. 5, pp. 1365–1373, 1993.

[11] M. Matlosz, S. Magaino, and D. Landolt, “Impedance Analysis of a Model Mechanism for Acceptor-Limited Electropolishing,” vol. 141, no. 2, pp. 410–418, 1994.

[12] P. J. Núñez, E. García-Plaza, M. Hernando, and R. Trujillo, “Characterization of surface finish of electropolished stainless steel AISI 316L with varying electrolyte concentrations,” *Procedia Eng.*, vol. 63, pp. 771–778, 2013.

[13] L. Ponto, M. Datta, and D. Landolt, “Electropolishing of iron-chromium alloys in phosphoric acid-sulphuric acid electrolytes,” *Surf. Coatings Technol.*, vol. 30, no. 3, pp. 265–276, 1987.

[14] Z. ur Rahman, K. M. Deen, L. Cano, and W. Haider, “The effects of parametric changes in electropolishing process on surface properties of 316L stainless steel,” *Appl. Surf. Sci.*, vol. 410, pp. 432–444, 2017.

[15] S. J. Lee and J. J. Lai, “The effects of electropolishing (EP) process parameters on corrosion resistance of 316L stainless steel,” *J. Mater. Process. Technol.*, vol. 140, no. 1–3 SPEC., pp. 206–210, 2003.

[16] P. Sojitra, C. Engineer, D. Kothwala, A. Raval, H. Kotadia, and G. Mehta, “Electropolishing of

316LVM stainless steel cardiovascular stents: An investigation of material removal, surface roughness and corrosion behaviour," *Trends Biomater. Artif. Organs*, vol. 23, no. 3, pp. 115–121, 2010.

[17] M. Matlosz and D. Landolt, "Shape Changes in Electrochemical Polishing" The Effect of Temperature on the Anodic Leveling of Fe-24Cr," *J. Electrochem. Soc. Corros. J. Boden, ibid. J. B. Cott. I. R. Sch. Br. Corros. J. J. Electron Spectrosc. Relat. Phenom. G. Lewis, Corros. Corros. Sci*, vol. 136, no. 4, pp. 40–1246, 1989.

[18] S. Habibzadeh, L. Li, D. Shum-Tim, E. C. Davis, and S. Omanovic, "Electrochemical polishing as a 316L stainless steel surface treatment method: Towards the improvement of biocompatibility," *Corros. Sci.*, vol. 87, pp. 89–100, 2014.

[19] A. M. Awad, E. A. Ghazy, S. A. Abo El-Enin, and M. G. Mahmoud, "Electropolishing of AISI-304 stainless steel for protection against SRB biofilm," *Surf. Coatings Technol.*, vol. 206, no. 14, pp. 3165–3172, 2012.

[20] C. Rotty, A. Mandroyan, M. L. Doche, and J. Y. Hihn, "Electropolishing of CuZn brasses and 316L stainless steels: Influence of alloy composition or preparation process (ALM vs. standard method)," *Surf. Coatings Technol.*, vol. 307, pp. 125–135, 2016.

[21] M. Hernando, P. J. Núñez, E. García-Plaza, and R. Trujillo, "Effect of Electrolyte on the Surface Smoothness Obtained by Electropolishing of Stainless Steel," *Mater. Sci. Forum*, vol. 713, pp. 55–60, 2012.

[22] A. Latifi, M. Imani, M. T. Khorasani, and M. D. Joupari, "Electrochemical and chemical methods for improving surface characteristics of 316L stainless steel for biomedical applications," *Surf. Coatings Technol.*, vol. 221, pp. 1–12, 2013.

[23] P. J. Nunez *et al.*, "Metrology of surfaces applied to the electrochemical polishing process," *Mater. Sci. Forum*, vol. 853, pp. 52–57, 2016.

[24] R. Rokicki and T. Hryniewicz, "Enhanced oxidation–dissolution theory of electropolishing," *Trans. IMF*, vol. 90, no. 4, pp. 188–196, 2012.

[25] K. Rokosz and T. Hryniewicz, "XPS study of AISI 316L SS surfaces after mechanical and electrochemical polishing and chelating/electro-chelating treatments," *Adv. Mater. Sci.*, vol. 14, no. 1, pp. 31–41, 2014.

[26] K. Rokosz, J. Lahtinen, T. Hryniewicz, and S. Rzadkiewicz, "XPS depth profiling analysis of passive surface layers formed on austenitic AISI 304L and AISI 316L SS after high-current-density electropolishing," *Surf. Coatings Technol.*, vol. 276, pp. 516–520, 2015.

[27] K. Rokosz, T. Hryniewicz, F. Simon, and S. Rzadkiewicz, "Comparative XPS analyses of passive layers composition formed on Duplex 2205 SS after standard and high-current-density electropolishing," *Teh. Vjesn. - Tech. Gaz.*, vol. 23, no. 3, pp. 731–735, 2016.

[28] C. Rotty, M. L. Doche, A. Mandroyan, J. Y. Hihn, G. Montavon, and V. Moutarlier, "Comparison of electropolishing behaviours of TSC, ALM and cast 316L stainless steel in H3PO4/H2SO4," *Surfaces and Interfaces*, vol. 6, pp. 170–176, 2017.

[29] F. Nazneen, P. Galvin, D. W. M. Arrigan, and M. Thompson, "Electropolishing of medical - grade stainless steel in preparation for surface nano - texturing," pp. 1–25.

[30] H. Zhao, J. Van Humbeeck, J. Sohier, and I. De Scheerder, "Electrochemical polishing of 316L stainless steel slotted tube coronary stents," *J. Mater. Sci. Mater. Med.*, vol. 13, no. 10, pp. 911–916, 2002.

[31] C. An Huang, “AC Impedance Responses of the Inconel 718 Alloy During Electropolishing in Perchloric-Acetic Mixed Acids,” *Int. J. Electrochem. Sci.*, vol. 12, pp. 3503–3515, 2017.

[32] Y. Han, J. Mei, Q. Peng, E. H. Han, and W. Ke, “Effect of electropolishing on corrosion of nuclear grade 316L stainless steel in deaerated high temperature water,” *Corros. Sci.*, vol. 112, pp. 625–634, 2016.

[33] G. Han, Z. Lu, X. Ru, J. Chen, Q. Xiao, and Y. Tian, “Improving the oxidation resistance of 316L stainless steel in simulated pressurized water reactor primary water by electropolishing treatment,” *J. Nucl. Mater.*, vol. 467, pp. 194–204, 2015.

[34] H. Tsuchiya, T. Suzumura, Y. Terada, and S. Fujimoto, “Formation of self-organized pores on type 316 stainless steel in organic solvents,” *Electrochim. Acta*, vol. 82, pp. 333–338, 2012.

[35] C. Ma, E. H. Han, Q. Peng, and W. Ke, “Effect of polishing process on corrosion behavior of 308L stainless steel in high temperature water,” *Appl. Surf. Sci.*, vol. 442, pp. 423–436, 2018.

[36] T. S. Hahn and A. R. Marder, “Effect of electropolishing variables on the current density-voltage relationship,” *Metallography*, vol. 21, no. 4, pp. 365–375, 1988.

[37] V. Vignal, J. C. Roux, S. Flandrois, and A. Fevrier, “Nanoscopic studies of stainless steel electropolishing,” *Corros. Sci.*, vol. 42, no. 6, pp. 1041–1053, 2000.

[38] A. Bhuyan, B. Gregory, H. Lei, S. Y. Yee, and Y. B. Gianchandani, “PULSE AND DC ELECTROPOLISHING OF STAINLESS STEEL FOR STENTS AND OTHER DEVICES,” *Sensors IEEE*, no. 1, pp. 314–317, 2005.

[39] D. Nakar, D. Harel, and B. Hirsch, “Electropolishing effect on roughness metrics of ground stainless steel: A length scale study,” *Surf. Topogr. Metrol. Prop.*, vol. 6, no. 1, pp. 1–18, 2018.

[40] S. E. Ziemniak, M. Hanson, and P. C. Sander, “Electropolishing effects on corrosion behavior of 304 stainless steel in high temperature, hydrogenated water,” *Corros. Sci.*, vol. 50, no. 9, pp. 2465–2477, 2008.

[41] A. P. Abbott, G. Capper, K. J. McKenzie, A. Glidle, and K. S. Ryder, “Electropolishing of stainless steels in a choline chloride based ionic liquid: an electrochemical study with surface characterisation using SEM and atomic force microscopy,” *Phys. Chem. Chem. Phys.*, vol. 8, no. 36, p. 4214, 2006.

[42] A. P. Abbott, G. Capper, K. J. McKenzie, and K. S. Ryder, “Voltammetric and impedance studies of the electropolishing of type 316 stainless steel in a choline chloride based ionic liquid,” *Electrochim. Acta*, vol. 51, no. 21, pp. 4420–4425, 2006.

[43] K. Alrbaey, D. I. Wimpenny, A. A. Al-Barzinjy, and A. Moroz, “Electropolishing of Re-melted SLM Stainless Steel 316L Parts Using Deep Eutectic Solvents: 3 × 3 Full Factorial Design,” *J. Mater. Eng. Perform.*, vol. 25, no. 7, pp. 2836–2846, 2016.

[44] C. Rotty, M.-L. Doche, A. Mandroyan, and J.-Y. Hihn, “Electropolishing behavior of additive layer manufacturing 316l stainless steel in deep eutectic solvents,” *ECS Trans.*, vol. 77, no. 11, pp. 1199–1207, 2017.

[45] K. Rokosz, F. Simon, T. Hryniewicz, and S. Rzadkiewicz, “Comparative XPS analysis of passive layers composition formed on AISI 304 L SS after standard and high-current density electropolishing,” *Surf. Interface Anal.*, vol. 47, no. 1, pp. 87–92, 2015.

[46] L. S. Andrade, S. C. Xavier, R. C. Rocha-Filho, N. Bocchi, and S. R. Biaggio, “Electropolishing of AISI-304 stainless steel using an oxidizing solution originally used for electrochemical coloration,” *Electrochim. Acta*, vol. 50, no. 13, pp. 2623–2627, 2005.

[47] M. Datta, “Surface Finishing of High Speed Print Bands,” *J. Electrochem. Soc.*, vol. 145, no. 9, p. 3047, 1998.

[48] T. Hryniewicz, “On discrepancies between theory and practice of electropolishing,” *Mater. Chem. Phys.*, vol. 15, no. 2, pp. 139–154, 1986.

[49] T. Hryniewicz, “Concept of microsmoothing in the electropolishing process,” *Surf. Coatings Technol.*, vol. 64, no. 2, pp. 75–80, 1994.

[50] O. Piotrowski, C. Madore, and D. Landolt, “Electropolishing of tantalum in sulfuric acid-methanol electrolytes,” *Electrochim. Acta*, vol. 44, no. 19, pp. 3389–3399, 1999.

[51] R. Vidal and a C. West, “Copper Electropolishing in Concentrated Phosphoric-Acid .1. Experimental Findings,” *J. Electrochem. Soc.*, vol. 142, no. 8, pp. 2682–2689, 1995.

[52] A. Chandra, M. Sumption, and G. S. Frankel, “On the Mechanism of Niobium Electropolishing,” *J. Electrochem. Soc.*, vol. 159, no. 11, pp. C485–C491, 2012.

[53] K. Kojima and C. W. Tobias, “Interpretation of the Impedance Properties of the Anode-Surface Film in the Electropolishing of Copper in Phosphoric Acid,” *J. Electrochem. Soc.*, vol. 120, no. 9, p. 1202, 1973.

[54] R. D. Grimm, A. C. West, and D. Landolt, “An a.c. impedance study of anodically formed salt film on iron in chloride solution,” *J. Electrochem. Soc.*, vol. 139, no. 6, pp. 1622–1629, 1992.

[55] C. Clerc, M. Datta, and D. Landolt, “On the theory of anodic levelling: model experiments with triangular nickel profiles in chloride solution,” *Electrochim. Acta*, vol. 29, no. 10, pp. 1477–1486, 1984.

[56] C. Clerc and D. Landolt, *On the theory of anodic levelling: behaviour of macroprofiles*, no. c. 1987.

[57] M. Datta and D. Landolt, “Surface Brightening during High Rate Nickel Dissolution in Nitrate Electrolytes,” *J. Electrochem. Soc.*, vol. 122, no. 11, pp. 1466–1472, 1975.

[58] M. Datta and D. Landolt, “On the Role of Mass Transport in High Rate Dissolution of Iron and Nickel in ECM electrolytes—I. Chloride Solutions,” *Electrochim. Acta*, vol. 25, no. 10, pp. 1255–1262, 1980.

[59] C. L. Faust, “Technical Notes and Reviews Surface Preparation by Electropolishing,” vol. 62, no. 2, pp. 62–72.

[60] J. M. Fitz-gerald and J. A. Mcgeough, “Mathematical theory of electrochemical machining 1. Anodic smoothing,” *IMA J. Appl. Math. (Institute Math. Its Appl.*, vol. 5, no. 4, pp. 387–408, 1969.

[61] P. A. Jacquet, “Electrolytic and Chemical Polishing,” *Metall. Rev.*, vol. 1, no. 1, pp. 157–238, 1956.

[62] D. Landolt, “Fundamental aspects of electropolishing,” *Electrochim. Acta*, vol. 32, no. 1, pp. 1–11, 1987.

[63] M. Matlosz, “Modeling of impedance mechanisms in electropolishing,” *Electrochim. Acta*, vol. 40, no. 4, pp. 393–401, 1995.

[64] R. Sautebin, H. Froidevaux, and D. Landolt, “Theoretical and Experimental Modeling of Surface Leveling in ECM under Primary Current Distribution Conditions,” *J. Electrochem. Soc.*, vol. 127, no. 5, pp. 1096–1100, 1980.

[65] R. Sautebin, “Anodic Leveling under Secondary and Tertiary Current Distribution Conditions,”

J. Electrochem. Soc., vol. 129, no. 5, p. 946, 1982.

[66] C. Wagner, “Contribution to the Theory of Electropolishing,” pp. 225–228, 1954.

[67] T. P. Hoar, “Mechanism of electropolishing,” *Nature*, vol. 165, no. 4185, pp. 64–65, 1950.

[68] A. P. Abbott, K. S. Ryder, and U. König, “Electrofinishing of metals using eutectic based ionic liquids,” *Trans. IMF*, vol. 86, no. 4, pp. 196–204, 2008.

[69] S. Mohan, D. Kanagaraj, R. Sindhuja, S. Vijayalakshmi, and N. G. Renganathan, “Electropolishing of stainless steel - A review,” *Trans. Inst. Met. Finish.*, vol. 79, no. 4, pp. 140–142, 2001.

[70] A. Bekmurzayeva, W. J. Duncanson, H. S. Azevedo, and D. Kanayeva, “Surface modification of stainless steel for biomedical applications: Revisiting a century-old material,” *Mater. Sci. Eng. C*, p. #pagerange#, 2018.

[71] E. J. Taylor, H. McCrabb, H. Garich, T. Hall, and M. Inman, “A pulse/pulse reverse electrolytic approach to electropolishing ans through mask electroetching,” 2011.

[72] I. Makarova and A. A. Chernik, “USING OF PULSE MODES IN NON-CHROMIUM ELECTROLYTES FOR,” 2017.

Anlage 1: Gegenüberstellung der geplanten Arbeiten und erzielten Projektergebnisse

Tabelle 1: Zusammenfassung der geplanten Arbeiten und erzielten Projektergebnisse in den Arbeitspaketen

AP	Arbeitspaket	Geplante Arbeiten	Erzielte Ergebnisse
1	Definition von Vergleichsproben	• Auswahl geeigneter Vergleichsproben mit einfacher Geometrie und vergleichbaren Oberflächen • Präparation von Proben mit speziellen Mikrostrukturen • Implementierung von Elektropolierzellen- und Verfahren • Elektropolierversuche an den Vergleichsproben • Charakterisierung der Proben	ZFM: • Prozessetablierung für 6“ Waferlevel Abscheidung von Al für die Probenherstellung zum Elektropolieren (vollflächig und strukturiert) • Aufbau zweier EP-Zellen und Einsatz verschiedener Parametersätze für die Vergleichsproben • Umfangreiche Charakterisierung der Proben vor und nach dem EP Hahn-Schickard: • Als geeignete Werkzeugstähle wurden 1.2343, 1.2379 und M333 ausgewählt • 3D Strukturen wie Mikrokanäle und Mikrobohrungen wurden hergestellt • Elektropolierzelle wurde aufgebaut und eingesetzt • Proben wurden bei verschiedenen EP-Parametern behandelt und die Oberflächenrauheit charakterisiert
2	Untersuchung von neuartigen Badzusammensetzungen	• Implementierung von neuartigen Badzusammensetzungen	ZFM: • die getesteten Flüssigkeiten (DES und IL) sind nicht für das EP von Al geeignet Hahn-Schickard: • Für das EP-Bad wurde E520 (Poligrat) eingesetzt

3	Untersuchung von erweiterten elektrischen Parametern	• Literaturrecherche zum Puls-Elektropolieren • Elektropoliertests mit gepulsten Strömen und Potentialen • Charakterisierung der Proben	ZFM: • Literaturrecherche zum Puls-EP zeigt Grundlagen der Parametervariationen auf • Keine Ansätze für Puls-EP von dünnen Schichten oder Al • Keine direkte Anwendung im Projektverlauf für Al-Schichten
4	Untersuchung von neuartigen Anlagenkonfigurationen	• Design und Konstruktion einer EP-Zelle für dünne Schichten • Untersuchung des Einflusses des Zellaufbaus auf das Polierergebnis	• Modifizierung des Laboraufbaus durch unterschiedliche Umwälzarten • Beste Polierergebnisse mit feinperligen Stickstoffbläschen durch einen porösen Luftstein
5	Herstellung und Validierung von Demonstratoren für 2D-Anwendungen (ZFM)	• Auswahl 2D-Anwendungsfälle • Anpassung der EP-Zelle • Herstellung der zu bearbeitenden Proben • Optimierung des EP-Prozesses • Einsatz und Vergleich der polierten Proben im Vergleich zu unpolierten Proben	ZFM: • Anwendung: Al-Thermokompressionsbonden für das System Packaging • Probenherstellung durch Pattern Plating • EP der Proben mit und ohne Resist • Gute Polierergebnisse bereits ab 300s Prozessdauer • Ableitung einer verbesserten Prozesskette für den EP-Prozess • Darstellung der Einsatzfähigkeit, aber kein Performancevergleich möglich
6	Herstellung und Validierung von Demonstratoren für 3D-Anwendungen (HS)	• Auswahl 3D-Anwendungsfälle • Anpassung der EP-Zelle • Herstellung der zu bearbeitenden Proben • Optimierung des EP-Prozesses • Einsatz und Vergleich der polierten Proben im Vergleich zu unpolierten Proben	Hahn-Schickard • Zwei verschiedene Mikrofluidik Strukturen wurden ausgewählt. Eines der Designs wurde vom PBA Mitglied geliefert • Die EP Zelle wurde in Kooperation mit CRM Group angepasst und durchgeführt • Die Einsätze wurden aus den Werkzeugstählen 1.2343 ESU und M333 mittels Fräßen und Erodieren hergestellt. • Mit den Einsätzen wurden Bauteile mit COP Material

	spritzgegossen und eine Verbesserung der Oberflächenrauheit und der optischen Güte festgestellt

Anlage 2:

1. Darstellung des wissenschaftlich-technischen und wirtschaftlichen Nutzens für KMU

Innerhalb des Projektes „AdEPT“ sind verschiedene Stähle und verhältnismäßig dünne Aluminiumschichten auf ihre Elektropoliercharakteristik untersucht worden. Daher können unterschiedliche Branchen von den Ergebnissen profitieren.

Zu den Ergebnisse des ZFM zählt vor allem die Etablierung der galvanischen Abscheidung von Al auf 6“ Wafer, sowohl vollflächig als auch strukturiert. Das Einsatzgebiet liegt bisher in die Leiterplatten- und Elektroindustrie sowie der Mikrosystemtechnik. Das Elektropolieren der Schichten zeigt das Potential, das aufwendige CMP-Prozesse (Chemisch-Mechanisches Polieren) ersetzt werden können. Gerade für KMU und deren Prozessintegration ist das ein treibender Faktor. Das wirtschaftliche Potential für KMU ist somit gegeben. Die Ergebnisse des Projektes „AdEPT“ können aber nicht direkt transferiert werden, da die Technologie noch einige Optimierungsarbeiten erfahren muss.

Im Bereich der Werkzeugstähle konnte gezeigt werden, dass diese nach der Herstellung elektropoliert werden können. Dadurch konnte die Oberflächenrauheit signifikant gesenkt werden. Stand der Technik ist, dass Werkzeughersteller entweder Fachkräfte einsetzen, die die Einsätze manuell nachbearbeiten oder steigen bei der Herstellung auf die kostenintensive Variante der Diamantbearbeitung um, um die Oberflächengüte an die Anforderungen anzupassen. **Die KMU können die im Projekt AdEPT entwickelten Methoden für die Verbesserung der Oberflächenqualität ihrer Werkzeuge, kostengünstiger als alternative Methoden, einsetzen**. Dabei müssen sie nur in gewissen Maßen sich Grundwissen im Bereich der Galvanik aneignen und die notwendigen Bäder beschaffen**. Durch die verbesserte Oberflächenqualität können die KMU auch neuere Anwendungsfelder wie Mikrooptik und Mikrofluidik bedienen.**

2. Notwendigkeit und Angemessenheit der geleisteten Arbeit

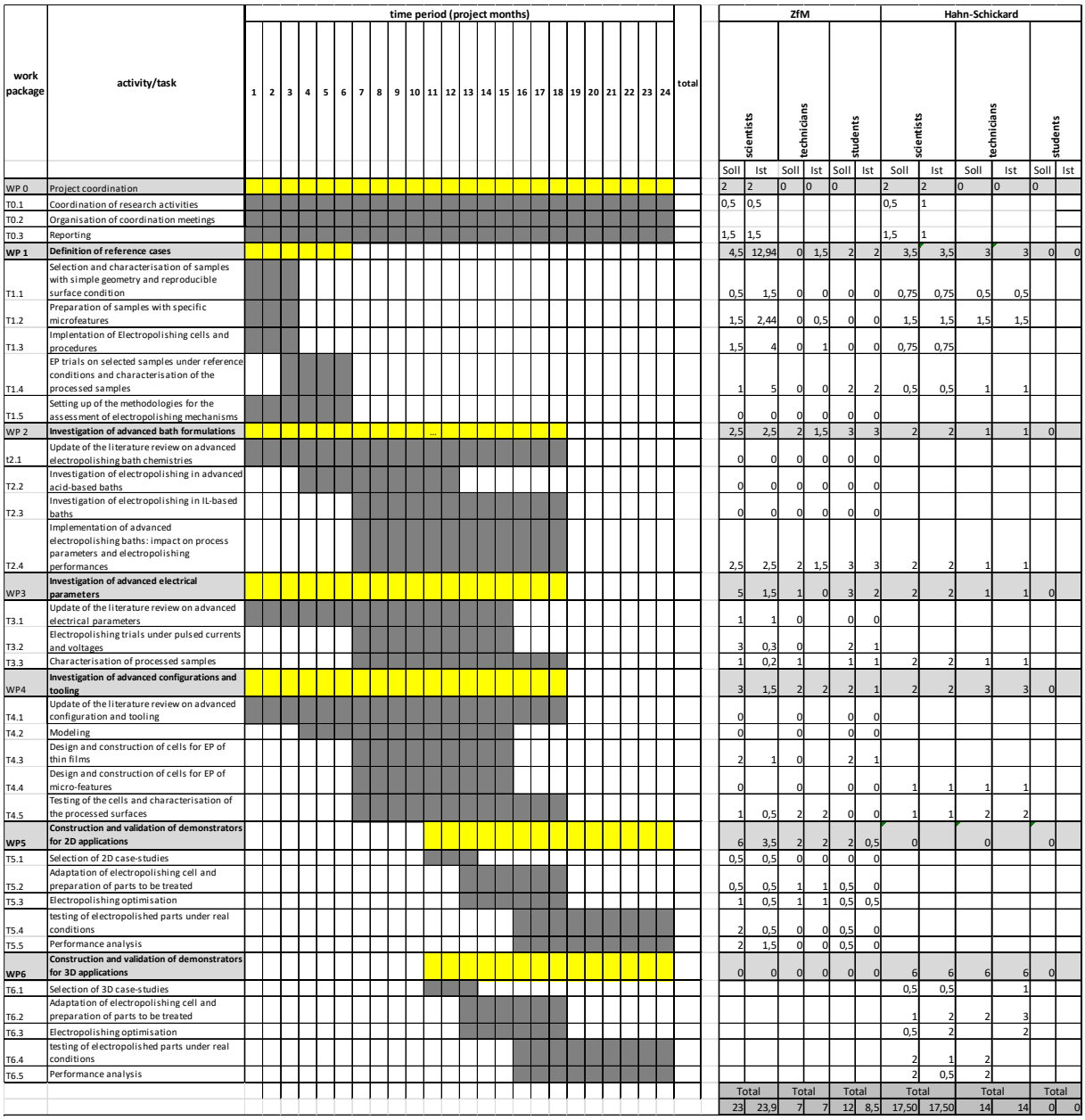

work package	activity/task	time period (project months)																								total	ZfM						Hahn-Schickard					
		1	2	3	4	5	6	7	8	9	10	11	12	13	14	15	16	17	18	19	20	21	22	23	24		scientists		technicians		students		scientists		technicians		students	
																											Soll	Ist	Soll	Ist	Soll	Ist	Soll	Ist	Soll	Ist	Soll	Ist
WP 0	Project coordination																										2	2	0	0	0		2	2	0	0	0	
T0.1	Coordination of research activities																										0,5	0,5					0,5	1				
T0.2	Organisation of coordination meetings																																					
T0.3	Reporting																										1,5	1,5					1,5	1				
WP 1	**Definition of reference cases**																										4,5	12,94	0	1,5	2	2	3,5	3,5	3	3	0	0
T1.1	Selection and characterisation of samples with simple geometry and reproducible surface condition																										0,5	1,5	0	0	0	0	0,75	0,75	0,5	0,5		
T1.2	Preparation of samples with specific microfeatures																										1,5	2,44	0	0,5	0	0	1,5	1,5	1,5	1,5		
T1.3	Implentation of Electropolishing cells and procedures																										1,5	4	0	1	0	0	0,75	0,75				
T1.4	EP trials on selected samples under reference conditions and characterisation of the processed samples																										1	5	0	0	2	2	0,5	0,5	1	1		
T1.5	Setting up of the methodologies for the assessment of electropolishing mechanisms																										0	0	0	0	0	0						
WP 2	**Investigation of advanced bath formulations**																										2,5	2,5	2	1,5	3	3	2	2	1	1	0	
t2.1	Update of the literature review on advanced electropolishing bath chemistries																										0	0	0	0	0	0						
T2.2	Investigation of electropolishing in advanced acid-based baths																										0	0	0	0	0	0						
T2.3	Investigation of electropolishing in IL-based baths																										0	0	0	0	0	0						
T2.4	Implementation of advanced electropolishing baths: impact on process parameters and electropolishing performances																										2,5	2,5	2	1,5	3	3	2	2	1	1		
WP3	**Investigation of advanced electrical parameters**																										5	1,5	1	0	3	2	2	2	1	1	0	
T3.1	Update of the literature review on advanced electrical parameters																										1	1	0		0	0						
T3.2	Electropolishing trials under pulsed currents and voltages																										3	0,3	0		2	1						
T3.3	Characterisation of processed samples																										1	0,2	1		1	1	2	2	1	1		
WP4	**Investigation of advanced configurations and tooling**																										3	1,5	2	2	2	1	2	2	3	3	0	
T4.1	Update of the literature review on advanced configuration and tooling																										0		0		0	0						
T4.2	Modeling																										0		0		0	0						
T4.3	Design and construction of cells for EP of thin films																										2	1	0		2	1						
T4.4	Design and construction of cells for EP of micro-features																										0		0		0	0	1	1	1	1		
T4.5	Testing of the cells and characterisation of the processed surfaces																										1	0,5	2	2	0	0	1	1	2	2		
WP5	**Construction and validation of demonstrators for 2D applications**																										6	3,5	2	2	2	0,5	0		0		0	
T5.1	Selection of 2D case-studies																										0,5	0,5	0	0	0	0						
T5.2	Adaptation of electropolishing cell and preparation of parts to be treated																										0,5	0,5	1	1	0,5	0						
T5.3	Electropolishing optimisation																										1	0,5	1	1	0,5	0,5						
T5.4	testing of electropolished parts under real conditions																										2	0,5	0	0	0,5	0						
T5.5	Performance analysis																										2	1,5	0	0	0,5	0						
WP6	**Construction and validation of demonstrators for 3D applications**																										0	0	0	0	0	0	6	6	6	6	0	
T6.1	Selection of 3D case-studies																																0,5	0,5		1		
T6.2	Adaptation of electropolishing cell and preparation of parts to be treated																																1	2	2	3		
T6.3	Electropolishing optimisation																																0,5	2		2		
T6.4	testing of electropolished parts under real conditions																																2	1	2			
T6.5	Performance analysis																																2	0,5	2			
																											Total		Total		Total		Total		Total		Total	
																											23	23,9	7	7	12	8,5	17,50	17,50	14	14	0	0

ZFM:

Die galvanische Abscheidung von Al für den Einsatz in der Mikrosystemtechnik hat aufgrund der Prozessführung und der Rauigkeit noch keine Industrierelevanz. Allerdings versprechen verhältnismäßig dicke Al-Schichten ein enormes Potential in der Aufbau- und Verbindungstechnik. Die durchgeführten Arbeiten vereinen den Charakter von Grundlagenuntersuchungen und anwendungsnahen Prozessen und Analysen zum Elektropolieren von galvanischen Aluminiumschichten. Aufgrund der Probenherstellung und deren Charakterisierung in der Forschungsstelle mussten einige Arbeitspakete intensiver bearbeitet werden als ursprünglich geplant (Siehe Verwendung der Zuwendungen). Innerhalb des Projektes war die Forschungsstelle eher exotisch, da sich die Projektpartner hauptsächlich mit verschiedenen Stählen befasst haben. Dadurch konnte nicht auf Erfahrungen der anderen Partner zurückgegriffen werden.

Die geleisteten Arbeiten zeigen, dass die galvanischen Al-Schichten mit einfachen Mitteln gut eingeebnet werden können. Zur Adaption für Waferlevel-Prozesse sind allerdings weitere Arbeiten und Optimierungen notwendig, da der Prozess sensibel auf kleinste Veränderungen bei der Anströmung reagiert.

Hahn-Schickard:

Das Elektropolieren von Werkzeugeinsätzen hat eine hohe industrielle Relevanz um Bauteile mit einer hohen Oberflächengüte und einer geringen Oberflächenrauheit herzustellen. Daher war es sehr wichtig in einem Vorwettbewerblichen Projekt, diese Themenfeld mit einem relativ hohen Risiko, zu erforschen.

Die im Arbeitsplan dargestellten und in der Auflistung der Arbeiten und Ergebnisse aufgeführten Aufwände waren für die Erreichung der Forschungsziele angemessen und notwendig.

3. Plan zum Ergebnistransfer in die Wirtschaft

Die nachfolgenden Transfermaßnahmen wurden aus dem Projektantrag übernommen, jedoch innerhalb des Projektverlaufes angepasst. Somit wurde manche Maßnahmen nicht wie geplant durchgeführt, da dies der Projektverlauf und -fortschritt nicht zugelassen haben.

Durchgeführte spezifische Transfermaßnahmen während der Projektlaufzeit

	Ziel	Rahmen		Datum/Zeit-raum
Maßnahme A: **Projekt-begleitender Ausschuss (PA)**	Diskussion der Forschungsergebnisse im PA	A1	Vorstellung des Projektes und Diskussion der geplanten Arbeiten	21.11.2017; 20.06.2018; 12.12.2018
Maßnahme B: **Messen**	Multiplikation der Projektergebnisse	B1	Vorstellung der Technologie auf der COMPAMED 2017 u. 2018	13.-16.11.2017; 12.-15.11.2018
		B2	Vorstellung der Technologie auf der Sensor+Test 2019	24.-26.06.2019
		B3	Semicon Europe 2019	11.-15.11.2019
Maßnahme C: **Mitglieder-versammlung** **HS, S**	Multiplikation der Projektergebnisse und Information von potenziellen Industriepartnern außerhalb des PA.	C1	Vorstellung des Projektes	Q1/2018

Maßnahme D: **Fach-tagungen**	Multiplikation der Projektergebnisse und Information von potenziellen Industriepartnern außerhalb des PA.	D1	Vorstellung der Technologie auf dem “Chemnitzer Seminar” des Fraunhofer ENAS	12./13.06.2018

Geplante spezifische Transfermaßnahmen nach der Projektlaufzeit:

	Ziel	Rahmen		Datum/Zeit-raum
Maßnahme D: **Fach-tagungen/ Publikationen**	Multiplikation der Projektergebnisse und Information von potenziellen Industriepartnern außerhalb des PA.	D3	Innovationsmesse bei Hahn-Schickard Stuttgart	Q3 / 2020
		D4	Jahrbuch der Oberflächentechnik	2020/ 2021
Maßnahme F: **Publikation im Internet**	Bereitstellung des Abschlussberichtes zur Nutzbarmachung der Ergebnisse für interessierte KMU	F1	Bereitstellung des Abschlussberichtes auf der Internetpräsenz von Hahn-Schickard und ZfM	Q2/2020
Maßnahme G: **Akademische Lehre**	Übernahme der Ergebnisse in die akademische Lehre	G1	Lehrveranstaltung „Technologien der Aufbau- und Verbindungstechnik“ des Instituts für Mikrointegration	WS 2019/ 20
Maßnahme H: **Akquisition von Firmen**	Akquisition von Firmen für geeignete Kooperationen zur Produktentwicklung, z.B. Direktaufträge, Verbundprojekte, Applikationszentrum	H1	Marketing Nutzen bestehender Partner aus Einzelanfertigung	
		H2	Beantragung von Folgeprojekten zur Umsetzung von Waferlevel-Elektropolierprozesse	Bis 2022

Einschätzung zur Realisierbarkeit des vorgeschlagenen und aktualisierten Transferkonzepts

Die oben dargestellten Maßnahmen adressieren insbesondere kleine und mittlere Unternehmen (KMU) und stellen einen optimalen Transfer der im Projekt erzielten Ergebnisse in die Wirtschaft sicher. Des Weiteren plant das ZFM die Akquise von einem Nachfolgeprojekt um die Technologie der AI-ECD und AI-EP in die Wirtschaft zu transferieren.

Danksagung:

Das Cornet IGF-Vorhaben Nr. 200 EBG der Forschungsvereinigung Hahn-Schickard Gesellschaft für angewandte Forschung e.V. wurde über die AiF im Rahmen des Programms zur Förderung der industriellen Gemeinschaftsforschung und -entwicklung (IGF) vom Bundesministerium für Wirtschaft und Energie aufgrund eines Beschlusses des Deutschen Bundestages gefördert. Für diese Förderung sei gedankt. Dem projektbegleitenden Ausschuss sei für die Unterstützung und die wertvollen Hinweise und Anregungen im Rahmen der PBA-Sitzungen gedankt.